STUDY ON UPWELLING AND DOWNWELLING ALONG THE WEST COAST OF INDIA- RELATIVE ROLES OF LOCAL VERSUS REMOTE FORCING

Thesis submitted to the

Cochin University of Science and Technology

in partial fulfilment of the requirement for the degree of

Doctor of Philosophy

in

Physical Oceanography

Under the Faculty of Marine Sciences

By

Phiros Shah

Reg. No. 3648

DEPARTMENT OF PHYSICAL OCEANOGRAPHY

SCHOOL OF MARINE SCIENCES

COCHIN UNIVERSITY OF SCIENCE AND TECHNOLOGY

COCHIN 682 016

January 2016

Study on Upwelling and Downwelling along the west coast of India- Relative roles of local versus remote forcing

Ph.D. Thesis under the Faculty of Marine Sciences

By

Phiros Shah
Department of Physical Oceanography
School of Marine Sciences
Cochin University of Science and Technology
Cochin 682 016
Email: phirosshah85@gmail.com

Supervising Guide

Dr. R. Sajeev
Associate Professor
Department of Physical Oceanography
School of Marine Sciences
Cochin University of Science and Technology
Cochin 682 016
Email:rsajeev@yahoo.com

Department of Physical Oceanography
School of Marine Sciences
Cochin University of Science and Technology
Cochin 682 016

January 2016

DEPARTMENT OF PHYSICAL OCEANOGRAPHY
SCHOOL OF MARINE SCIENCES
COCHIN UNIVERSITY OF SCIENCE AND TECHNOLOGY
COCHIN 682 016

Dr. R. Sajeev
Associate Professor

Certificate

This is to certify that the thesis entitled **"Study on Upwelling and Downwelling along the west coast of India-Relative roles of local versus remote forcing"** is an authentic record of the research work carried out by **Mr. Phiros Shah** under my supervision and guidance at the Department of Physical Oceanography, Cochin University of Science and Technology, Cochin 682 016, in partial fulfilment of the requirements for Ph.D degree of Cochin University of Science and Technology and no part of this has been presented before for any degree in any university. All the relevant corrections and modifications suggested by the audience during the pre-synopsis seminar and recommended by the Doctoral committee have been incorporated in the thesis.

Kochi - 682016
January 14th 2016

Dr. R. Sajeev
(Supervising Guide)

Declaration

I hereby declare that the thesis entitled **"Study on Upwelling and Downwelling along the west coast of India-Relative roles of local versus remote forcing"** is an authentic record of research work carried out by me under the supervision and guidance of Dr. R. Sajeev, Associate Professor, Department of Physical Oceanography, Cochin University of Science and Technology towards the partial fulfillment of the requirements for the award of Ph.D. degree under the Faculty of Marine Sciences and no part thereof has been presented for the award of any other degree in any University/Institute.

Kochi-16 **Phiros Shah**

January14th 2016

Dedicated to my Vappachi & Ummachi……

Acknowledgement

I am deeply grateful to my supervising guide, Dr. R Sajeev, for patiently taking me through this difficult task of environmental research. I express my deep and sincere gratitude to my guide for conceptualisation and implementation of this research topic, in addition to his peerless guidance and motivation all the way through my doctoral research. He is not only my academic supervisor, but also a real mentor and friend who let me know how to treat life with patience and fair-mindedness.

Prof. (Dr). A. N. Balchand (Dean, School of Marine Sciences and Head, Department of Physical Oceanography) and Prof. (Dr) Chandramohankumar (Department of Chemical Oceanography) also deserve special thanks as my doctoral committee members and advisors.

I am greatly indebted to Professor Trevor Platt, FRS, Plymouth Marine Laboratory, UK for his kind attention to my thesis. He gave me invaluable suggestions and corrections during the finalization of my thesis. My sincere and heartfelt thanks to him for his unflattering support. I extend my sincere thanks to Dr. Subha Satheyndranath, Head of Remote Sensing and Marine Optics at Plymouth Marine Laboratory for her timely advice during the finalization of my thesis.

I wish to express my sincere thanks to Dr. K.M Santhosh and Mr. P K Saji, Department of Physical Oceanography, for their timely advice, suggestions and encouragement during the research period. My heartfelt thanks to Miss. Nisa Anil for her sincere effort and support during the period of my doctoral research. She spends lot of her time for the suggestions and corrections during the finalisation of my thesis. My sincere thanks goes to Mr. Vasudevan, Research Scholar of this department for his brotherly affection and encouragement.

I want to thank Dr. T. V. Sathianandan (Head, FRAD, CMFRI for giving me the encouragement for the finalization of my thesis. My sincere thanks to Dr. Grinson George for his persistent encouragement and emotional support during the final phase of my thesis. He gave me full support and confidence even at times when the thesis progress was lagging. I express my sincere thanks to all the staff members of Fishery Resource and Assessment Division, CMFRI.

I am grateful to Dr. Thara K.J and Gopika N for their sisterly affection and appreciate for their assistance in the initial phase of my research work. I extend my sincere thanks to Mr. Lix John. K and Dr. Jhonson Zachariah for their memorable scientific advises and mental support during my doctoral research.

I take this opportunity to thank the Library staff members of School of Marine Sciences and office staffs of Department of Physical Oceanography for their co-operation. I extend my sincere gratitude to all my teachers and special thanks owe to Dr. Rasheed K, Dr. Benny N. Peter and Dr. S. Muraleedharan Nair.

This study was funded by the INDOMOD programme of INCOIS, Ministry of Earth Sciences, Government of India. During my research period, I got financial support from INCOIS for five years. I greatly acknowledge this as it was my maiden entry to the ocean research. The research facilities provided by the Cochin University of Science and Technology is thankfully acknowledged.

I acknowledge the help and encouragement rendered by my friends Dr. Shaiju P, Dr. Gireesh Kumar, Dr. Jayesh P, Dr. Deepulal P.M., Dr. Krishnamohan, Dr. Prabhakaran, Dr. Shinod N.K, Muhammad Shafeque, Sajan Kottopadathu, Prasanth P., Nirmala J., Jophiya, Jabir T., Manu Mohan, Shameem, Siva Kumar, Shinto Roose, Sudeep, Asif Shah, P. Chandrasekharan, Vimal Kumar, Salini T.C, Maya L. Pai, Sabeer V, Mridul, Akhil P Soman, Arjun S. Puthezhath,, Sruthy Abraham, Neethu Anto, Akhil, Nidhin Gopan, Vinny Johny, Neeraja M. Nair, Anis Danial, Maria, Monalisa, Muhammad K.M, Pranav and Bitto. I extend my sincere thanks to all CUMS hostel inmates during the period of my research and to all my M.Sc. classmates for their support and encouragement.

I express my sincere gratitude to all people who have helped and inspired me during my doctoral study.

I am deeply indebted to my father, mother, brother- in- law, sister and my nieces for their unflagging love and support. This thesis is simply impossible without them. The support and encouragement from my family is the greatest strength for me and the backbone and origin of my happiness. Finally I would like to thank my would-be Sumi for her encouragement, patience and emotional support too.

Phiros Shah

Preface

The Arabian Sea, part of the Indian Ocean lies between the Arabian Peninsula and the Indian subcontinent. The peculiarity of Arabian Sea is the seasonal reversal of circulation with respect to monsoon and also the upwelling and downwelling characteristics of the sea during the monsoon season. Remote forcing including planetary waves trigger these peculiarities of the sea. Many rivers entering into the sea and topographic features of surrounding land area also play a very important role in dynamicity. The Arabian Sea is one of the most active dynamic regions of the Indian Ocean as it is one of the major land locked sea. The sea is also very responsive to coupled ocean atmosphere phenomena and climatic changes.

Eastern boundary currents are less spectacular than western boundary currents and have received less attention. Nevertheless, the upwelling which is often associated with them has biological implications of considerable ecological and economic importance. West India Coastal Current (WICC) is the major eastern boundary current in the north Indian Ocean and it is mainly driven by the remote effects of winds along the east coast of India in terms of coastally trapped waves and the winds along the west coast also contribute. Even though moderate to strong upwelling favourable winds are blowing along the west coast of India during a year, the winter monsoon is characterized by downwelling along the coast. During the summer monsoon the west coast of India is characterized by upwelling associated with WICC and it is changed to downwelling during the winter monsoon. Many studies on upwelling have been carried out for understanding the upwelling phenomenon along the west coast of India (Banse, 1958, 1968; Sharma, 1968; McCreary and Chao, 1985; Johannessen et al., 1987; Shetye et al., 1990; Shankar, 2005). The studies are limited to explaining the general phenomenon of upwelling along south-west coast and its interanual variability. Studies on upwelling along north-west coast and downwelling along west coast of India are practically overlooked. With an extensive use of satellite derived data sets the present study is aimed at

investigating the upwelling and downwelling along west coast of India from 8ºN to 20ºN and relative roles of local and remote forcing involved in it. The study also deals with the influence of Indian Ocean Dipole (IOD) on upwelling and downwelling along the west coast of India.

The thesis is organized in five chapters. The first chapter gives an overview of general hydrography of Arabian Sea and a brief description of climatic events. It provides information on upwelling and downwelling processes including the different types. Detailed review on previous studies are also covered in this chapter along with the scope and specific objectives of the study.

The observed signals of upwelling and downwelling along the west coast of India are explained in the second chapter. The source of data and methodology adopted and the analysis made to notice the coastal upwelling and downwelling along the west coast of India is explained in this chapter. The analysis of depth of 26º isotherms, Sea Surface Height Anomaly (SSHA), Local Temperature Anomaly (LTA), Sigma-t, vertical velocity and Chlorophyll-a concentration along the west coast of India have been performed.

Chapter three covers detailed description of both local and remote forcing involved in upwelling and downwelling processes along the west coast of India by analyzing wind, surface current, surface mass transport, horizontal divergence and SSHA.

The interannual variability and influence of IOD on upwelling and downwelling is explained in the fourth chapter by analyzing the Sea Surface Temperature (SST), surface Ekman mass transport, vertical velocity, cross shore and along shore wind and SSHA.

The fifth chapter summarises the entire work. The literature used for the present study is incorporated under bibliography section followed by the list of publications.

Contents

List of Figures

List of Tables

Acronyms and Abbreviations

APDRC	Asia Pacific Data Research Center
ASCAT	Advanced Scatterometer
AVISO	Archiving Validation and Interpretation of Satellite Oceanography
DOI	Digital Object Identifier
E	East
EICC	East India Coastal Current
ENSO	El-Niño Southern Oscillation
ERS	European Remote Sensing Satellite
et.al	And others
Fig.	Figure
IOD	Indian Ocean Dipole
ITCZ	Intertropical Convergence Zone
JAMSTEC	Japan Agency for Marine-Earth Science and Technology
LH	Laccadive High
LL	Laccadive Low
LTA	Local Temperature Anomaly
N	North
NIOA	North Indian Ocean Atlas
NOAA	National Oceanic and Atmospheric Administration
OGCM	Ocean General Circulation Model
OSCAR	Ocean Surface Current Analysis Real-time
PO.DAAC	Physical Oceanography Distributed Active Archive Center
QuikSCAT	Quick Scatterometer
S	South
SMC	Summer Monsoon Current
SODA	Simple Ocean Data Assimilation
SOI	Southern Oscillation Index
SSHA	Sea Surface Height Anomaly
SST	Sea Surface Temperature
WICC	West India Coastal Current

.....ൠ.....

Chapter 1

INTRODUCTION

Contents

In the Indian Ocean, the Arabian Sea lies between the Arabian Peninsula and the Indian subcontinent. The characteristic properties of the Arabian Sea are the seasonal reversal of circulation with respect to monsoon and also the upwelling and downwelling observed during the monsoon season. Remote forcing, including planetary waves, triggers these peculiarities of the sea. Many rivers entering the sea, and topographic features of surrounding land area, also play important roles in the dynamics. The Arabian Sea is one of the most active regions of the Indian Ocean, as it is one of the world's major land locked seas. The sea is also very responsive to coupled ocean atmosphere phenomena and to climatic changes.

Compared with other low latitudinal oceanic regimes, the Arabian Sea has some specific ecological and economic distinctions. During the summer monsoon, both eastern and western boundaries of Arabian Sea provide upwelling. All other low latitudinal oceanic regimes are characterized by upwelling along the eastern boundaries only. Economic importance of Arabian Sea relies on the fishery productivity associated with the major upwelling zones in the eastern and western boundaries. During the northeast monsoon and winter these upwelling zones become downwelling zones. Although the stronger upwelling regimes are located in the western boundary, some 70% of fishery production derives from the eastern Arabian Sea. Since the west coast of India is the principal eastern boundary of the Arabian Sea, the upwelling and downwelling along the west coast of India determine the major part of biological productivity over the eastern Arabian Sea.

Against this background, the present study is focused on the upwelling and downwelling along west coast of India. This chapter comprises a review of literature followed by a general introduction to upwelling, downwelling and major climatic events. The objectives, scope and relevance of the study are also provided.

1.1 Upwelling

Upwelling is an ascending motion, of some minimum duration and extent, by which water from sub surface layers is brought into the surface layer and is removed from the area of upwelling by horizontal flow (Smith 1964, Sharma 1978). Based on its spatial occurrence upwelling can be classified in to three;

1.2 Equatorial Upwelling

Upwelling along the equator is mainly determined by the position of the Inter Tropical Convergence zone (ITCZ). Depending on the season, ITCZ

oscillates between south and north. The South-East trade winds blow across the Equator, with the result that there is a divergence to the south of the Equator; this is known as equatorial divergence and the upwelling along the equator relies on this equatorial divergence.

1.3 Open Ocean Upwelling

Open ocean upwelling is associated with Ekman divergence due to the cyclonic wind over the northern hemisphere and anticyclonic wind over the southern hemisphere. Along with horizontal movement, wind stress at the sea surface can cause vertical motion of water. Rising of deeper water as a result of divergence of surface water due to wind stress is referred to as upwelling. In the northern hemisphere, away from the coastal boundaries, when cyclonic winds are blown over the ocean surface, the average movement of the wind driven layer is towards the right of the wind, causing divergence of surface water and upwelling.

1.4 Eastern Boundary Currents and Coastal Upwelling

Although the eastern boundary currents are less strong than western boundary currents, the coastal upwelling associated with eastern boundary currents has significant ecologic as well as economic importance. Most of the eastern boundaries located in the trade wind zone are well known for their coastal upwelling and this is usually referred to as costal upwelling associated with low latitudes. Coastal upwelling along most of the eastern boundaries is driven primarily by wind. Whenever the equatorward winds are blowing over the eastern boundaries, the Ekman transport is towards offshore and 90º clockwise from the wind direction (Ocean Circulation, Angela Colling (2001).

Due to this surface offshore mass transport, sea level is lowered towards the coast. The landward horizontal pressure gradient due to the lowering of sea level towards the coast results in an equatorward geostrophic current. The wind-driven offshore current combined with equatorward geostrophic current together determine the strength and time span of vertical circulation along the eastern boundaries. The coastal upwelling is also affected by local factors such as the topography of the sea-bed and the shape of the coastline. It can also occur on a local scale, as a result of deflection of subsurface currents by bottom topography (Ocean Circulation, Angela Colling (2001).

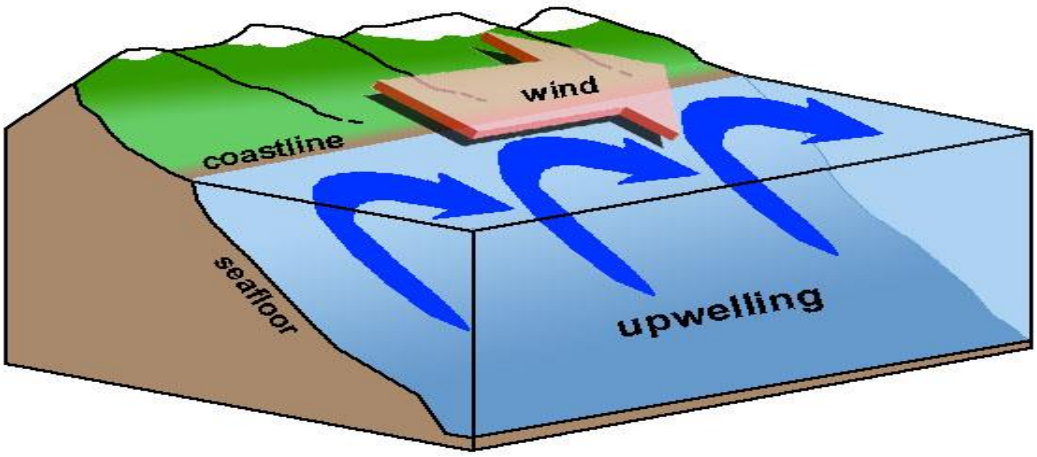

Fig. 1.1: Wind-induced coastal upwelling over the northern hemisphere. [Photo Courtesy: Geologycafe.com]

1.5 Downwelling

The descending motion of some minimum duration and extent by which oceanic surface water subsides to the deeper layers is usually referred to as downwelling. The surface water of the ocean subsides for various reasons related to density difference between the ocean layers and wind-induced convergence. The Sea Surface Temperature (SST) and biological productivity

can be significantly altered by downwelling. During downwelling the surface layer thickens with nutrient deficient warm water, resulting in a downward transport of oxygen-rich surface water.

1.6 Open Ocean Downwelling

Downwelling also occur in the open ocean. Downward movement of surface water as a result of convergence due to wind stress is referred to as wind-induced downwelling. As a result, dissolved materials, heat and surface oxygen are transferred to greater depths. Open-ocean downwelling is associated with convergence of surface water due to the anticyclonic wind over the northern hemisphere and cyclonic wind over the southern hemisphere. Along with horizontal movement, wind stress at the sea surface can cause vertical motion of water. In the northern hemisphere, away from the coastal boundaries, when anticyclonic winds blow over the ocean surface, the average movement of wind driven layer is towards the right of the wind, causing convergence of surface water and downwelling.

1.7 Coastal Downwelling

Whenever winds blowing over a coastline result in an onshore surface mass transport and convergence, then the particular coast is characterized by coastal downwelling. Due to these surface onshore mass transports, sea level rises towards the coast. The seaward horizontal pressure gradient due to the lowering of sea level towards offshore results a geostrophic current. Depending on the ocean boundary, the direction of the geostrophic current changes. When coastal downwelling happens on eastern boundaries, the direction of the geostrophic current is poleward. The wind-driven onshore current, combined with poleward geostrophic current, together determine the strength of downwelling.

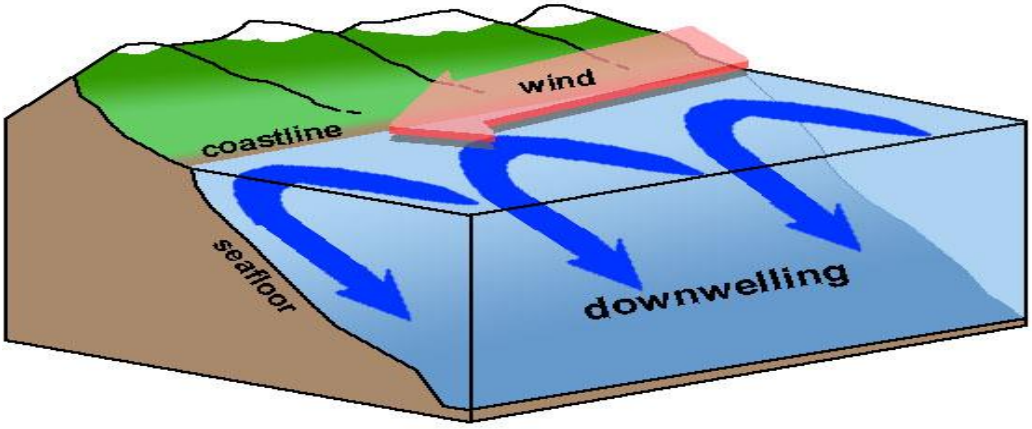

Fig. 1.2: Wind-induced coastal downwelling over the northern hemisphere. [Photo Courtesy: Geologycafe.com]

1.8 Indian Ocean Dipole (IOD)

An anomalous state of the ocean-atmosphere system, in which eastern equatorial Indian Ocean becomes unusually cold and western equatorial Indian Ocean becomes unusually warm (in contrast to normal years) is referred to as Indian Ocean Dipole (Saji et al., 1999; Webster et al., 1999; Vinayachandran et al., 2009). During normal years, the spatial distribution of Sea Surface Temperature (SST) in the Indian Ocean is characterized by warm water on the eastern side and cooler water on the west (Vinayachandran et al., 2009). The intensification of IOD happens during September-October and cold Sea Surface Temperature Anomalies (SSTA) suppress atmospheric convection in the east, whereas warm SSTA enhance convection in the west. Westerly winds over the equatorial Indian Ocean are replaced by easterlies during the positive IOD years. Weakening of equatorial jets during these years causes a reduction in the eastward transport of warm water as a result of an associated shallower-than-usual thermocline in the east. Sea level rises in the central equatorial Indian Ocean and it decreases in the eastern part. During the IOD years the temperature anomalies are also seen in the subsurface ocean (Vinayachandran et al., 2002)

and there is a strong coupling between the sub-surface and surface signals (Rao et al., 2002). Negative IOD can also occur and they have been considered as an intensification of the normal state. The negative IOD years are characterized by warmer sea surface temperature anomaly, enhanced convection, higher sea level, deeper thermocline in the east and cooler sea surface temperature anomaly, lower sea level, shallower thermocline and suppressed convection in the west (Vinayachandran et al., 2009).

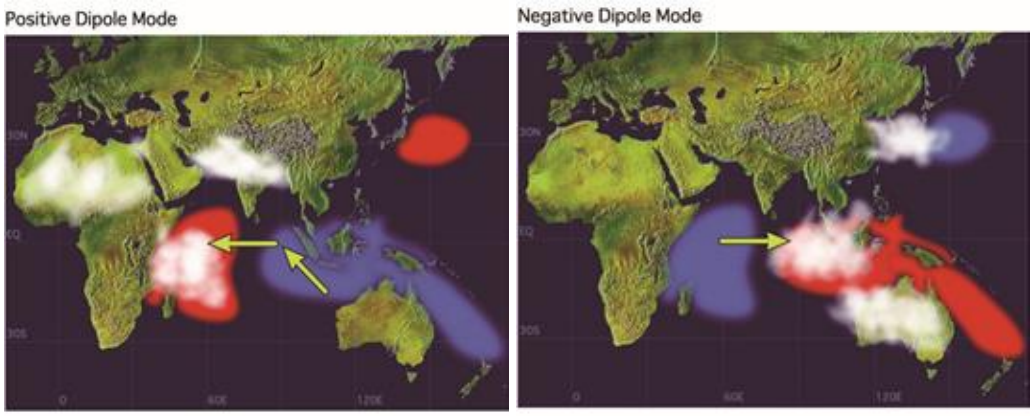

Fig. 1.3: Positive and negative phase of IOD. Red represents areas of warm water and blue represents areas of cold water. [Photo courtesy: www.jamstec.go.jp]

1.9 El Niño-Southern Oscillation (ENSO)

El Niño is an oscillation of the ocean-atmosphere system in the tropical Pacific having important consequences for weather around the globe (NOAA, 2006 http://www.elnino.noaa.gov/). This anomaly happens at irregular intervals of two to four years, and lasts from nine months to more than a year. The Southern Oscillation is the atmospheric component of El-Niño and it is called the El-Niño Southern Oscillation (ENSO). The strength of ENSO is measured by Southern Oscillation Index (SOI). The SOI is the surface air pressure difference between Tahiti and Darwin, Australia. El-Niño episodes are

associated with negative values of SOI, which means the pressure difference between Tahiti and Darwin is very small. El-Niño events begin by weakening of trade winds over the tropical Pacific, part of Walker circulation. A series of warm, subsurface water waves of a few centimeters amplitude and hundreds of kilometer width, crosses the Pacific along the Equator and creates a warm tongue of water near South America (Peruvian coast), where the ocean temperatures are normally cold due to upwelling. In such times, in contrast to normal years, the rainfall shifts from the western Pacific towards the east, while Indonesia and India become drier. The thermocline depth becomes greater during El-Niño over the eastern Pacific. The western side of the equatorial Pacific is characterized by warm, wet, low-pressure weather as the accumulated moisture is dumped by typhoons and thunderstorms.

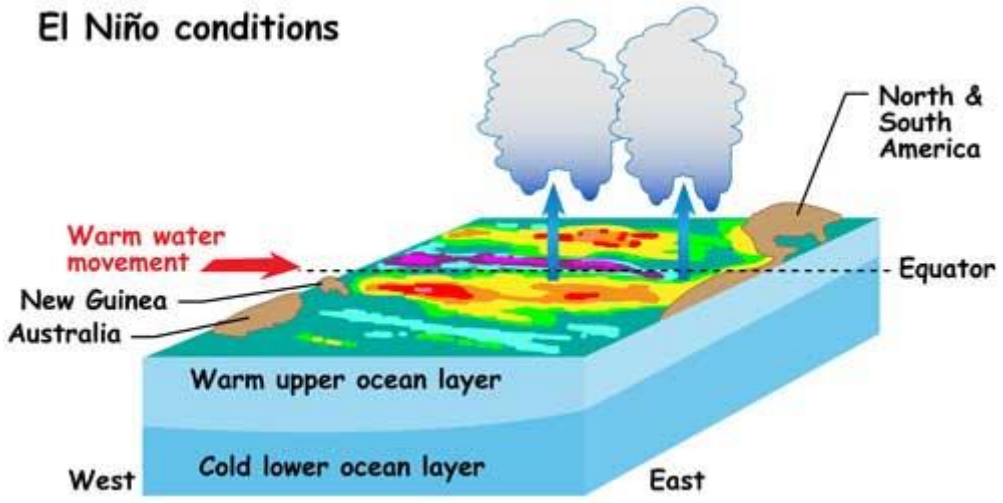

Fig. 1.4: El-Niño. [Photo Courtesy: climatekids.nasa.gov]

1.10 Review of Literature

Over the north Indian Ocean the winds are generally south-westerly during summer monsoons (May-September) and north-easterly during winter monsoons (November-February). The months March-April and October are

the spring and fall transition months characterized by weak winds. Compared with winter monsoon the winds are much stronger during the summer monsoon. In tune with the seasonally reversing winds, North Indian Ocean experiences a seasonally reversing surface circulation (Schott and McCreary, 2001; Shankar et al., 2002). These seasonally reversing winds are also unique to the North Indian Ocean; the Arabian Sea and Bay of Bengal are subjected to the similar reversing monsoon forcing as they are located in the same latitudinal belt. Arabian Sea is characterized by a clockwise circulation pattern during the summer monsoon and an anticlockwise circulation during winter monsoon. The Summer Monsoon Current (SMC) flows towards the east in the Arabian Sea and is fully developed during July and August (Cutler and Swallow, 1984). The SMC decreases its intensity during September. As October is the transition month, the current direction and intensity become variable over most of the Arabian Sea. Studies of Wyrtki (1973) revealed that during the summer monsoon, the water movement in the Arabian Sea is towards east and in the central Arabian Sea the surface current is found to be directed towards northeast during this time (Bauer et al., 1992). The major currents in Arabian Sea reverse their directions during boreal winter as a result of north-easterly winds (Varadachari and Sharma, 1967) and the direction of current in the open Arabian Sea is from east to west during this period (Wyrtki, 1973). Over the south-eastern Arabian Sea a large cyclonic and an anticyclonic eddy located at 10°N and 70°E are formed in the early summer and northeast monsoon respectively. Cyclonic eddy is referred as Laccadive Low (LL) and anticyclonic eddy is referred as Laccadive High (LH). Formation and dissipation of these eddies depend on the westward propagation of Rossby waves which are radiated by the poleward propagation of coastally trapped Kelvin waves along the west coast of India (Shankar and Shetye, 1997).

The West India Coastal Current (WICC) on the west and East India Coastal Current (EICC) on the east are the two dominant seasonally reversing coastal currents along the east and west coasts of India. During the summer monsoon the WICC flows towards equator along the coast and reverses its direction towards pole during the winter monsoon. The EICC is mainly driven by Ekman pumping due to local alongshore winds at the coast; remote effects of alongshore winds adjacent to the northern and eastern boundaries of the Bay of Bengal; and remote forcing from the Equator in terms of coastally-trapped waves. WICC is the major eastern boundary current in the north Indian Ocean. It is driven by the remote effects of winds along the east coast of India, and associated coastally-trapped waves. Winds along the west coast also contribute. The low-frequency circulation along the west coast consists primarily of these coastally-trapped Kelvin waves from the east coast (Shetye and Gouveia, 1998). In a detailed study, Shankar et al. (2002) showed that the circulation at any point in the north Indian Ocean is decided by both local forcing and remote forcing, whose signals are carried by equatorial and coastal waves. Numerical modeling studies using climatologically averaged winds have also established the importance of remote forcing on the surface circulation over the north Indian Ocean through propagating Kelvin and Rossby waves (Clarke, 1983; Potemra et al., 1991; Yu et al., 1991; McCreary et al., 1993, 1996).

Upwelling along the southwest coast of India is an annually recurring phenomenon during the southwest monsoon and is the dominant mechanism in the Arabian Sea for summer cooling (Jayaram et al., 2010). The slow and persistent rising of nutrient-rich subsurface water towards the ocean surface is referred as upwelling, that which is off the southwest coast of India is indicated by rapid upward movement of isotherms, surface cooling, and associated fall in sea level occurring during the southwest monsoon months of May to September

(Smitha et al., 2008). In southeastern Arabian Sea, the signatures of upwelling from the low sea level anomaly are noticeable from February/March itself (Jayaram et al., 2010, Johannessen et al., 1987), but the associated lowering of SST and an increase in productivity are noticeable only with the onset of southwest monsoon winds, which occurs by the end of May or early June. The west coast of India is one of the most biologically productive regions of the world oceans, contributing considerable fishery resources by virtue of well-known upwelling process during the summer monsoon season (Gopalakrishna et al., 2008; Madhupratap et al., 1994, 1996, 2001). The upwelling first appears in the southern latitudes along the southwest coast of India and progressively advances poleward during the summer monsoon. Along the southwest coast of India, the upwelling is modulated by both local and remote forcing (Gopalakrishna et al., 2008). Alongshore wind stress and wind stress curl have been identified as the two most important local forcing events responsible for the occurrence of upwelling through Ekman dynamics during the summer monsoon season (Shetye et al., 1985; Shetye and Shenoi, 1988; Pankajakshan et al., 1997; Jayaram et al., 2010). Remote forcing is characterized by coastally-trapped propagating Kelvin waves that reach south eastern Arabian Sea, triggered by both the equatorial zonal wind stress and the along shore wind stress off the west coast of India (Gopalakrishna et al., 2008). Seasonally, two pairs of upwelling and downwelling Kelvin waves propagate sequentially eastward along the Equator. After reaching the Sumatra coast, they bifurcate and propagate as two coastally-trapped Kelvin waves, one northward and the other southward. The northern branch propagates over varied distances along the coastal wave guide of Bay of Bengal as shown by Rao et al., 2009, who also revealed that between these two pairs of Kelvin waves only downwelling Kelvin wave generated during October to November reach the southwest coast of India. This substantiates the small influence of equatorial forcing on the

upwelling dynamics off southwest coast of India. Modeling studies by Shankar et al. (2002) and observational studies by Gopalakrishna et al. (2008) have clearly revealed that the alongshore wind stress at the southwest coast of India and remote forcing from the south of Sri Lanka are more significant forcing than the equatorial forcing that influences the upwelling signal in the Lakshadweep Sea during the summer monsoon.

From an analysis of sea surface temperature, surface salinity distribution, thermal structure and productivity Smitha et al. (2008) reported that various forcing mechanisms are involved in the generation of upwelling along the southwest coast of India. They classify different zones of upwelling along the west coast depending on the nature of forcing. Over the southern tip, off the Kanyakumari coast, the upwelling is strong and is mainly driven by the southwest monsoon winds that are tangential to the coast. Along the west coast area between 8ºN and 9ºN upwelling results exclusively from Ekman transport brought out by the long shore component of the wind stress. This area represents a shadow zone and here the role of remote forcing is minimal. The study also revealed that moderate to intense upwelling occurred along area north of this 9º N up to 13º N, due to the combined effect of the wind stress and remote forcing in the form of coastally-trapped Kelvin waves and the associated offshore penetration of Rossby waves. Within this area, the offshore extension of upwelling was maximum in the southern part and progressively weakened northwards, possibly due to the weakening of the offshore-radiating Rossby waves. Further north (13º N to 15º N), the process of upwelling is weak and confined very close to the coast, even though the winds are favorable for upwelling. Muraleedharan and Prasanna Kumar (1996) substantiate the finding that the upwelling-favorable conditions exist along the southern shelf, with a decreasingly conspicuous surface manifestation towards north.

By analyzing the density structure, thermal structure, mean sea level and divergence of surface current vectors, Sharma (1978) showed that upwelling starts during the early March at the southern tip of southwest coast of India and propagates pole wards as the southwest monsoon progresses. The cessation of upwelling along the coast starts during August and the sinking sets by September. Discussing forcing mechanisms involved in upwelling along the southwest coast he reported that the wind stress components of 1 dyne per cm^2 and above prevail through the coast only during southwest monsoon, and these components are obviously very weak during northeast monsoon. The wind components during northeast monsoon are insignificant in producing a vertical circulation except to supplement the motion when the current vector is favorable. He noticed that the upwelling-favorable offshore and equatorward wind stress components exist along the coast only during October to May and November to December respectively, when these components are too trivial to have an effect on vertical circulation. He also reported that from February to May the intense solar heating along the coast produces an offshore–onshore gradient of temperature generating a gradient current along the coast in southerly direction and that this is the causative mechanism of pre occurrence of current along the coast during spring, much in advance of wind reversal. This sets up an upward movement of water in the south of the coast during March. Even though the upwelling-favorable wind stress components do not exist along the coast during southwest monsoon, the magnitude of these components is very strong. The wind stress components again check any further upward movement from subsurface layers. Hence, he inferred that the upwelling along the southwest coast of India is due to the combined effect of wind and currents along the coast. The geostrophic balance of the southerly current is established along the coast during August, leading to the cessation of upwelling.

Studies of Darbyshire (1967) and Banse (1959, 1968) reported that upwelling along the west coast of India starts in March-April and is intensified by the southwest monsoon. Upwelling commences earlier in the southern latitudes and propagates northward as the monsoon progresses. Their studies also concluded that during the southwest monsoon, along the southwest coast of India, wind-induced upwelling was not favorable because prevailing winds are onshore from west or southwest during this season. Hence it was inferred that upwelling along the west coast of India was due not only to local winds but was also associated with large scale monsoonal conditions which drive the anticyclonic Arabian Sea monsoon gyre.

Antony et al. (2002) revealed the offshore extent of upwelling and downwelling over the eastern Arabian Sea. By analyzing the vertical as well as horizontal thermal structure over the eastern Arabian Sea during both the southwest and northeast monsoon season he inferred that the upward and downward oscillation of thermocline due to the process of upwelling and downwelling probably have an offshore extension of 350-400 km away from the coast. The study also concluded that even though the upwelling and downwelling processes are generally encountered in the shelf region along the west coast of India the horizontal scale of 350–400km indicates the offshore propagation of these coastal features.

In a detailed study by Hickey and Banas (2008) over the California current system, challenged the long-held belief that the upwelling of deep nutrients and associated phytoplankton along the eastern boundary depends only on alongshore wind stress. With a multidisciplinary biogeochemical approach over the California current system the authors concluded that the upwelling and phytoplankton blooms along the coast are not well correlated with alongshore wind stress and that high productivity is due not only to the

alongshore wind stress but also other driving forces. They listed the forcing mechanism involved in the process of high biological productivity as riverine input and tidal dynamics along the coast, upwelling induced by submarine canyons with high topographic resolution, and wind-induced remote forcing.

Studies of Sanilkumar et al. (2004) analyzing the thermal and salinity structure along the southwest coast of India during July 2003 indicated intense upwelling in the upper 60m water column along the coast. The offshore extent of upwelling was reduced significantly from south to north. A detailed modeling study by Rao et al. (2008) suggested that coastal upwelling off Cochin is at its peak during July and its intensity reduces towards north. While describing the downwelling process he concluded that temperature inversion along the coast is mainly dependent on downwelling over the south eastern Arabian Sea during the winter monsoon.

Explaining the buoyancy-forced downwelling associated with boundary currents using a high resolution, non-hydrostatic numerical model, Michael (2008) described the dependence of downwelling on thermohaline circulation associated with surface cooling. He also suggested that if the geostrophic velocity associated with the pressure gradient is oriented to the boundary at the surface, then there will be net downwelling and if it is oriented away from the boundary, it leads to a net upwelling. The study also revealed that the net downwelling depends on the surface heat loss, but also on the strength of boundary currents, the vertical stratification below the mixed layer, the mixed layer depth and the Coriolis parameter.

In the past, several studies were carried out on the coastal upwelling and downwelling process in the California current system, one of the major eastern boundary currents in the Pacific Ocean. All these studies revealed the influence

of vertical oscillations on the biological productivity and associated fisheries (Ware and Thompson, 1991; Thompson and Ware, 1996; Mackas, 2006; Hickey and Banas, 2008). Studies on the northeast Pacific also showed the influence of strong downwelling on the reduction of nutrient inventories and productivity over the shelf areas (Ianson et al., 2009). The timing and intensity of vertical circulation heavily influence the composition and vitality of the marine biota (Ware and Thompson., 1991; Mackas et al., 2001; Botsford et al., 2006; Barth et al., 2007).

1.11 Objectives of the Study

- To select and locate the areas and months of upwelling and downwelling along west coast of India.
- To study the different forcing mechanisms involved in upwelling and downwelling along the west coast of India and seek out the relative importance of local versus remote forcing.
- To study interannual variability and impact of Indian Ocean Dipole (IOD) on upwelling and downwelling along west coast of India.

1.12 Scope of the Study

Many studies on vertical circulation have been carried out for understanding the upwelling phenomenon along west coast of India (Banse, 1959, 1968; Sharma, 1978; McCreary and Chao, 1985; Johannessen et al., 1987; Shetye et al., 1990; Shankar et al., 2005). These studies were limited to explaining general phenomenon of upwelling along southwest coast and it's inter annual variability. Studies on upwelling along the northwest coast and downwelling along the west coast were minimal. The present study is aimed at investigating the upwelling and downwelling along the west coast of India from

8ºN to 20ºN and explains the governing forcing involved in vertical motion. This information may provide baseline data useful for any future upwelling and downwelling studies along this region.

1.13 Relevance and Purpose of the Study

In general, vertical circulation can influence weather as well as climate. Upwelling and downwelling have significant influence on global energy balance of the ocean. In tropical latitudes, they have profound influence on accumulation of heat and its transport to higher latitudes by major currents.

Even though the strength and velocity of vertical motions are small in scale compared with horizontal water movement, vertical motions have significant ecological as well as economic importance. The ecological importance of coastal upwelling lies in that, wherever they occur, they replace the surface water with nutrient-rich, sub-surface water and thus enhance the biological productivity. This increase in primary productivity benefits the entire food chain and hence supports higher trophic levels. Since downwelling maintains the transport of dissolved oxygen-rich surface water to the deeper layers, in extreme cases the lack of downwelling causes to mass mortalities, because of the deficiency of oxygen, and presence of sulfide- and methane-rich water. Further, these waters can extend on to continental shelves and can kill large numbers of marine organisms.

Though the upwelling along west coast of India is less in intensity when compared to the other thoroughly studied upwelling regimes of the Arabian Sea, it has profound impacts on the coastal fisheries of India. The west coast of India accounts for 70% fish yield of the total Arabian Sea production and the southwest coast alone accounts for 53% (Jayaram et al., 2010; Luis and Kawamura, 2004; Sanjeevan et al., 2009).

This background provides the motivation for the present work. The fundamental goal of this study is to describe the dynamics and inter annual variability of upwelling and downwelling along west coast of India and the relative importance of local versus remote forcing played on upwelling and downwelling.

.....ൟ.....

Chapter 2

OBSERVED SIGNALS OF UPWELLING AND DOWNWELLING ALONG THE WEST COAST OF INDIA

Contents

2.1 Introduction

Even though the velocities of vertical motions are small in scale compared with horizontal water displacement, vertical motions are an integral part of the oceanic circulation. They can be classified either as normal vertical advection or as forced vertical motions. Upwelling and downwelling are the ascending and descending vertical motions belonging to the forced vertical motions. Strength and duration of upwelling and downwelling are greatly dependent on the combination of driving forces involved. Explanation of forcing mechanism involved in vertical motions is beyond the scope of this chapter: it is described in Chapter 3. Identifying the location of upwelling and downwelling zones along the coastal waters is important because these vertical motions have significant influence on the environmental conditions in which the pelagic fishes live. The vertical motions are a strong determinant of the biological productivity over an oceanic region. Though upwelling enhances and downwelling reduces the nutrient concentration in the photic layer, both these

motions together determine the total biological productivity over a year. Population dynamics of fish depend on food supply, therefore coastal upwelling and downwelling zones determine annual fishery production. This is the basis of the economic importance of upwelling and downwelling. From the previous literature it was evident that the west coast of India contributes 70% of total fishery production over the Arabian Sea. Hence, improved understanding of the period and areas of upwelling and downwelling along the west coast of India is required for the design of fishing strategies for maximum sustainable yields.

Several proxies are used in the study of upwelling and downwelling in coastal areas. Many studies in the past used wind-induced surface Ekman mass transport as an indicator of upwelling and downwelling given its role in driving a substantial vertical circulation at any coast. But recent modeling and observational studies point out the relative importance of coastally-trapped waves, rather than wind, on coastal circulation. Hence, in this chapter, instead of wind-induced surface mass transports, some other physical properties, which are changed significantly by the vertical circulation at the coast, are used as proxy for the study of upwelling and downwelling. Ekman mass transport is explained in detail in Chapter 3. Even though the distribution of chemical properties is also significantly altered by forced vertical motion, these chemical parameters are not used as an index for the study of upwelling and downwelling because the chemical properties are rapidly modified by biochemical process in coastal waters.

2.2 Materials and Methods

From earlier studies it was evident that upwelling and downwelling areas are characterized by upward and downward movement of isotherms, hence the depth of 26º isotherm (D26) was used as a proxy for this study. For the temperature climatology over the north Indian Ocean D26 is considered as the core

of the thermocline. Sharma (1978) concluded that even though the vertical distribution of temperature is monotonic, it is largely altered by the other localized factors such as insolation, clouds and evaporation in the surface layers. Hence the vertical distribution of density is a preferred proxy for the study of vertical motion because density determines the stratification of the water column and the water movement is along isopycnals. Therefore the vertical section of sigma-t is used in this chapter for the identification of upwelling and downwelling. The upward and downward tilt of isopycnals represents upwelling and downwelling respectively. Sigma-t and D26 are derived from the North Indian Ocean Atlas (NIOA) by Chatterjee et al. (2012).

Due to the process of upwelling, surface water moves offshore by horizontal advection and relatively cooler subsurface water replaces the surface water. Consequently, to maintain isostatic balance upwelling areas are characterized by lowering of sea surface height compared with the surrounding waters. Convergence occurs in the surface during downwelling and water from surface subsides to deeper level. Thus downwelling areas are distinguished by sea surface elevation compared with nearby areas. The Archiving, Validation, and Interpretation of Satellite Oceanographic (AVISO) – merged and blended SSHA of $0.33^{o} \times 0.33^{o}$ from Asia-Pacific Data-Research Center (APDRC) data sets were used to characterize the variability of upwelling and downwelling along the coast.

Studies of Sharma (1978) reveal that along the southwest coast of India upwelling starts from 90m depth. Our observations on vertical distribution of sigma-t also show a vertical extension of upwelling and downwelling greater than 90 m depth. Following his approach, vertical velocity calculated with respect to the 100m depth level is used in this chapter for the identification of upwelling and downwelling zones. For the calculation of vertical velocity, horizontal divergence derived from the climatology of 20 years of SODA

currents from 1990 to 2010 is used. Calculation of horizontal divergence and vertical velocity is explained as follows

Horizontal divergence, $\nabla h.V = \frac{\partial u}{\partial x} + \frac{\partial v}{\partial y} + \frac{v tan\emptyset}{R}$ ..... (2.1)

where u is the zonal component of current velocity, v is the meridional component of current velocity, $\emptyset$ is the latitude. Here the term $\frac{v tan\emptyset}{R}$ represents the divergence due to the convergence of meridians at higher latitudes and usually neglected for the low latitudes. Hence, for the west coast of India the equation of horizontal divergence will become

$\nabla h.V = \frac{\partial u}{\partial x} + \frac{\partial v}{\partial y}$ ..... (2.2).

Vertical velocity, w = $-\int_0^h (\frac{\partial u}{\partial x} + \frac{\partial v}{\partial y})\, dz = -\int_0^h (\nabla h.V)\, dz$ ..... (2.3)

where w represents the mean vertical velocity from surface to the depth h and z is taken as positive downward. Here we can assume h =100m and mean vertical velocity between the levels z=0 and z=100m is calculated. The vertical velocity at 100m depth level was also calculated for the better knowledge of vertical motion at the subsurface level.

Because upwelling regions are characterized by relatively cooler waters than the surrounding areas, a difference in the temperature of the area of interest compared with that of an adjacent region along the same latitude, can be considered as an indicator of upwelling (Jayaram et al., 2010). Following the approach of Wooster et al. (1976), Naidu et al. (1999) and Smitha et al. (2008), the Local Temperature Anomalies (LTAs) were calculated along the west coast of India by comparing the temperature between offshore and coastal stations in the same latitude. LTA was calculated for different layers from surface to 30m depth. Because the influence of upwelling and downwelling is known to extend

200– 400 km from the coast in the southwest direction (Antony et al., 2002), offshore stations chosen were 3º off from the coastal stations for the calculation of LTA (Smitha et al., 2008). Positive LTA values suggest coastal upwelling processes and are calculated as

$$LTA = T_{off} - T_{coast} \quad \text{.....(2.4)}$$

Following previous studies the present work also used LTA as a proxy for the study of upwelling but not for the study of downwelling. Hence we calculate the LTA values only for the well-known upwelling periods (summer monsoon months). The grids selected for this study along west coast are given in Fig 2.1. Henceforth, the region between the limits of 8° N and 15° N along the coastal belt is referred to as the southwest coast and that from 15° N to 20° N as the northwest coast. Offshore and coastal grids selected for the calculation of LTA are given in the Fig. 2.1.

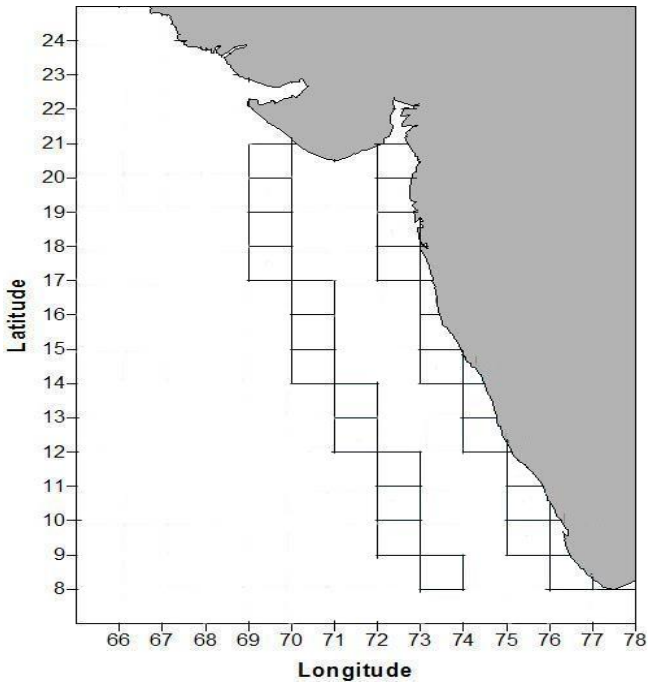

Fig. 2.1: Location map and the 1º × 1º squares used to derive LTA.

Since primary productivity along any coast is greatly dependent on the vertical circulation, the chlorophyll-a concentration (www.oceancolour.org) along the west coast of India is used as a proxy for the study of upwelling and downwelling along the west coast of India). Since upwelling and downwelling are annually recurrent phenomena along the west coast of India, climatologies of the above mentioned data sets were used in this study.

2.3 Results and Discussions

2.3.1 Depth of 26º Isotherm (D26)

Since the upwelling areas are characterized by ascending motion of isotherms, the distance between the surface and 26º isotherms decreases during upwelling periods and increases during downwelling. Hence lower values of depth of 26º isotherms represent upwelling and the higher values of D26 represent downwelling. The annual march of the D26 for different latitudes along the coastal belt showed uplifting (lower values) of the 26º isotherms during the southwest monsoon months and downward movement of 26º isotherms (higher values) during the northeast monsoon and winter along the west coast from 8º N to 20º N (Fig. 2.2), a clear indication that upwelling and downwelling along the west coast are not limited to the southwest coast. The most intense uplifting was observed from 8ºN to 15º N, and there was a lag from 8º N to 20º N observed in the D26. During the peak summer monsoon months from June to September the D26 values range between 10m and 40m along the west coast of India while the values range between 85m and 105m during northeast monsoon and winter from November to February.

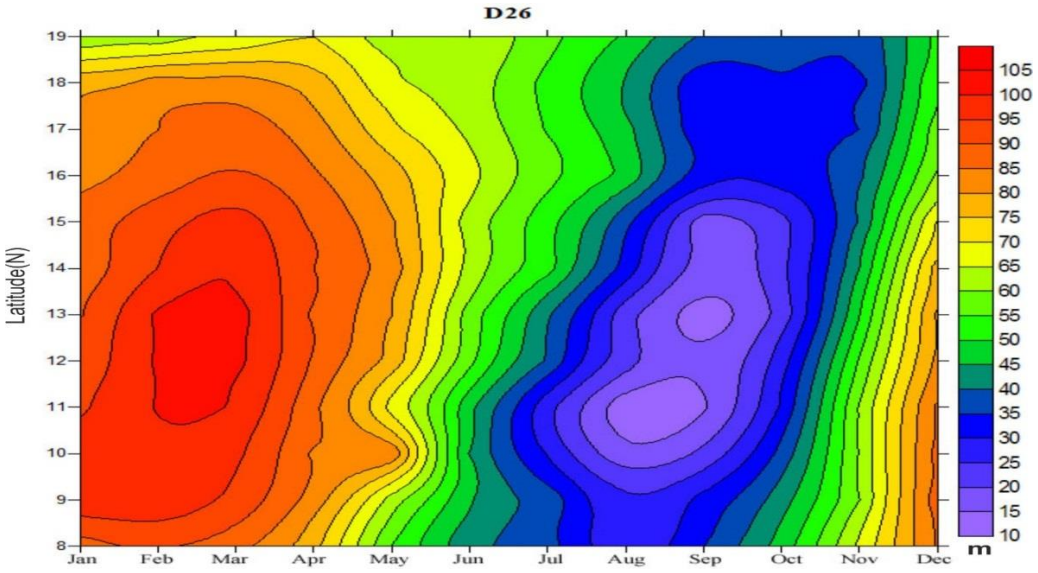

Fig. 2.2: Annual March of D26 (m) along the west coast of India from 8ºN to 20ºN.

From Fig. 2.2 it was also evident that along the west coast of India the ascending motion sets up by April (D26 values are markedly lowered compared with February and March) and intensify during the peak summer monsoon months. Along the northwest coast, the upwelling intensified by August and continued to October. From 17ºN to 19ºN, lower values of D26 were observed during November also. Sinking along the southwest coast starts by October (D26 values are noticeably increased compared with August and September) and intensified from December to February. Along the northern latitudes, intense downwelling was observed from January only. Table.2.1 shows the D26 values along the coast during a year. Analysis of Fig.2.2 and Table 2.1 reveals that even though the deepening and uplifting of isotherms are stronger on the southern latitudes from 8ºN to 15ºN, the northwest coast also shows significant upward and downward oscillation with a seasonal periodicity.

Table 2.1: Values of D26 (m) along the west coast of India.

Months	9°N	11°N	13°N	15°N	17°N	19°N
Jan	98.38	94.2	89.6	87.89	81.94	60.94
Feb	98.55	100.3	100.8	92.96	84.97	61.91
Mar	93.51	99.4	101.8	97.49	87.18	65.40
Apr	82.83	85.9	89.0	88.80	82.22	69.95
May	62.62	68.2	80.1	80.70	70.95	62.04
Jun	45.56	46.3	57.5	62.47	63.90	65.05
Jul	38.53	26.6	40.7	51.63	54.51	56.52
Aug	25.96	11.6	21.8	36.49	46.61	49.41
Sep	31.9	14.4	12.5	17.19	31.32	39.39
Oct	42.89	30.7	21.9	23.49	34.16	39.66
Nov	59.89	60.5	49.8	40.56	34.99	36.00
Dec	87.79	85.7	80.9	70.40	57.58	51.54

2.3.2 Sigma-t

Irrespective of previous studies which concentrated on upwelling along the southern latitudes and concluded that upwelling was less conspicuous towards north, the analysis of D26 in the present study revealed that even though strength of upwelling and downwelling were greater along the southwest coast, the northwest coast also experienced significant vertical oscillation with a seasonal periodicity. To check whether this finding is justified, I also analyzed spatial and vertical distribution of isopycnals at different latitudinal stations along the west coast of India. The isopycnals show clear upward movements during the summer monsoon months and clear downward tilt during the northeast monsoon and winter along the west coast of India (Fig. 2.3 to Fig. 2.10).

At the southern tip of west coast of India, upwelling starts by April, such that the downward tilt of isopycnals during March changes to upward (Fig. 2.3 and 2.7). The upwelling intensifies at this latitude as the monsoon progresses. The vertical sections of sigma-t at 13ºN indicate that the upwelling at these locations starts by May only (Fig.2.5). This suggests that there is a lag in the generation of upwelling from south to north. All the stations along the southwest coast show intensification of upwelling during the peak summer monsoon months of July and August.

Observations made on 17ºN indicate that over the northwest coast upwelling intensified during August and September. Vertical sigma-t structure during June and July does not show any significant upward and downward tilt and isopycnal are nearly parallel above 80m depth. Below this depth some upward tendencies are observed (Fig. 2.6). Along the southwest coast of India from 8ºN to 15ºN the downwelling sets by October and continues to March (Fig. 2.7 to Fig. 2.9).It is intensified during December to February. Along the northwest coast downwelling sets in by November and intensifies during January (Fig. 2.10).

In tune with the studies of Antony et al. 2002 , who observed an offshore extension of upwelling and downwelling up to 300km or 400km, the present investigation also revealed upwelling and downwelling extending 3º to 5º towards offshore over the west coast of India.(Fig. 2.3 to Fig. 2.10).

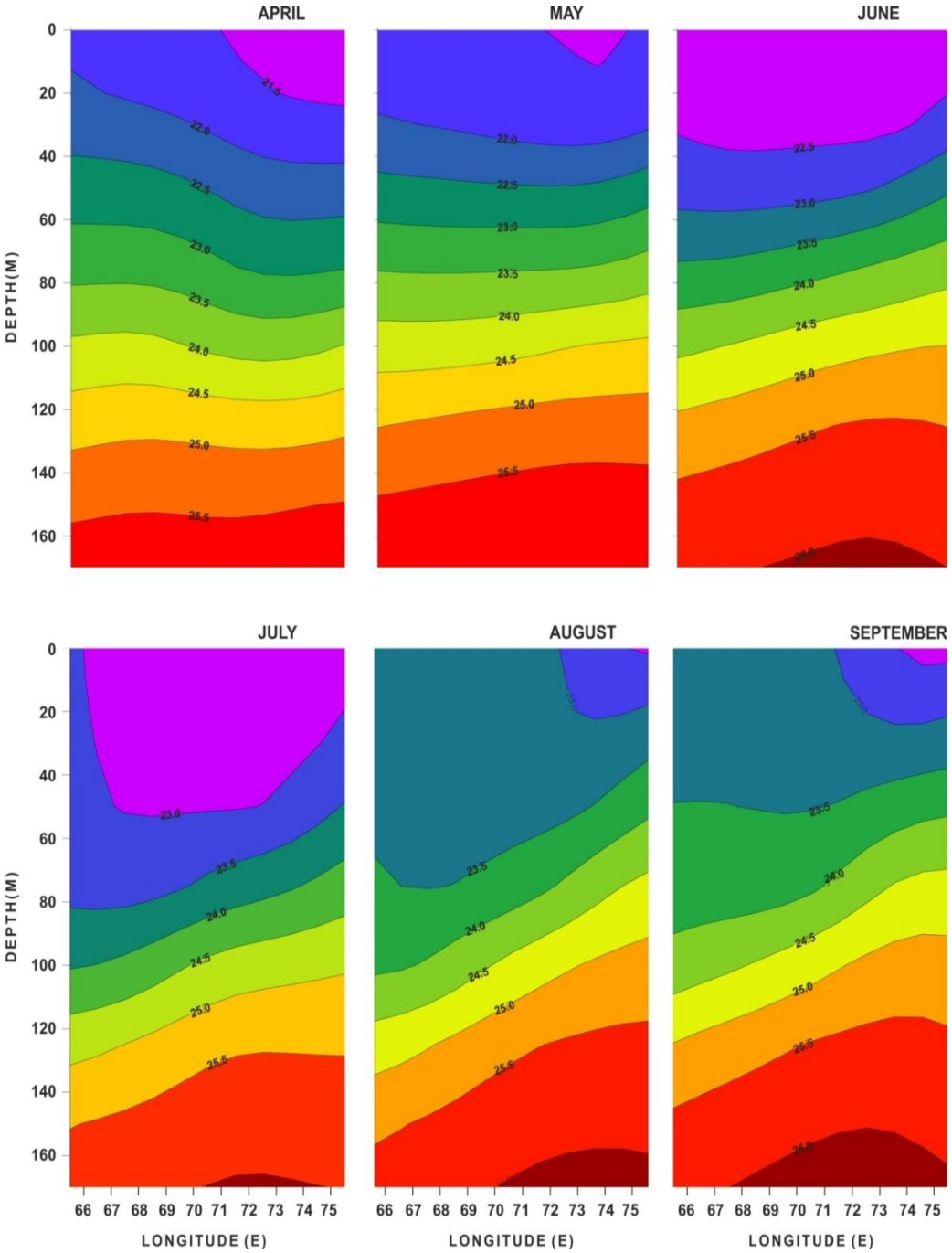

Fig. 2.3: Vertical distribution of sigma-t (Kg/m^3) at 9^{o}N along the west coast of India from April to September.

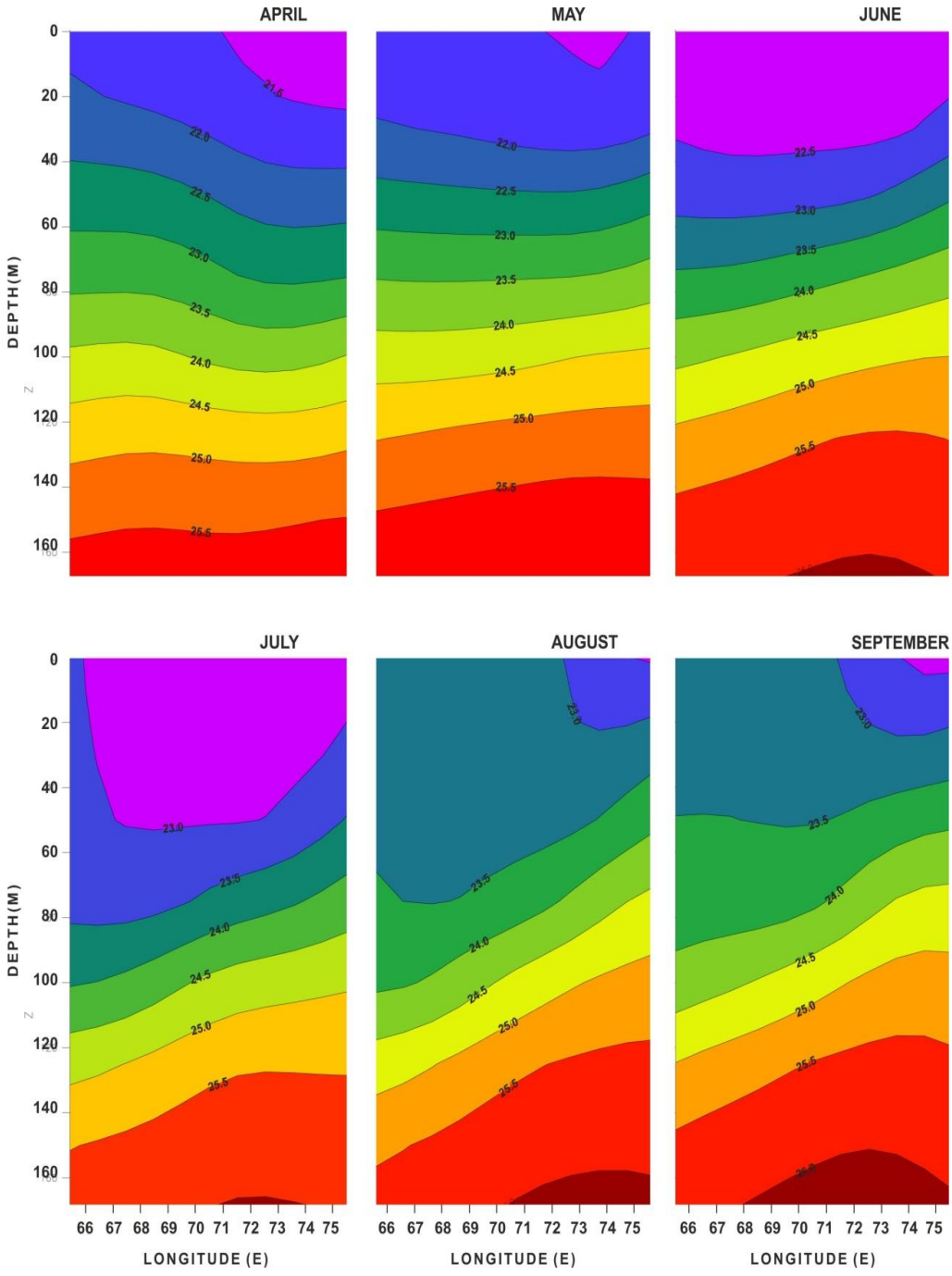

Fig. 2.4: Vertical distribution of Sigma-t (Kg/m^3) at 11ºN along the west coast of India from April to September.

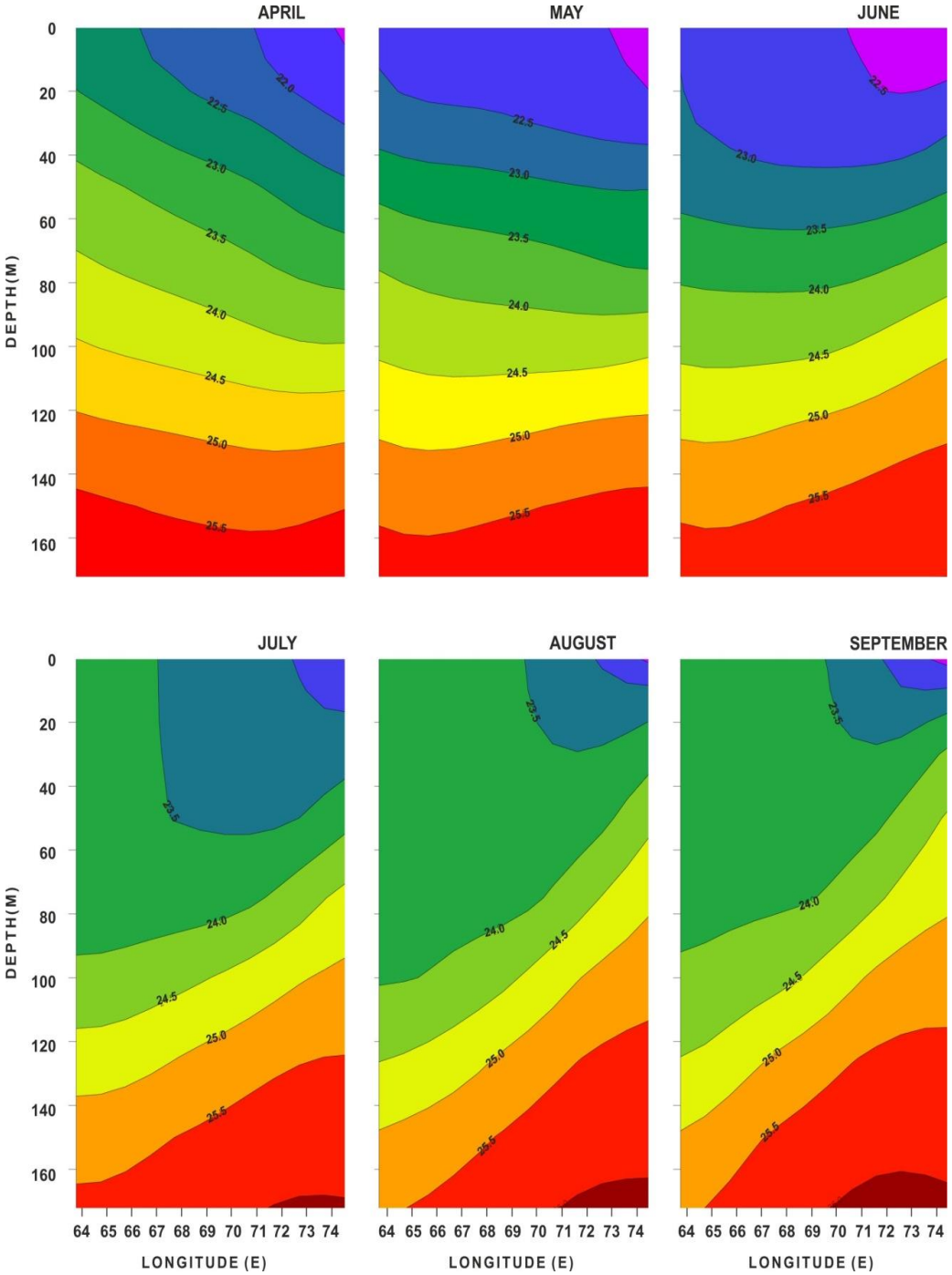

Fig. 2.5: Vertical distribution of sigma-t (Kg/m^3) at 13ºN along the west coast of India from April to September.

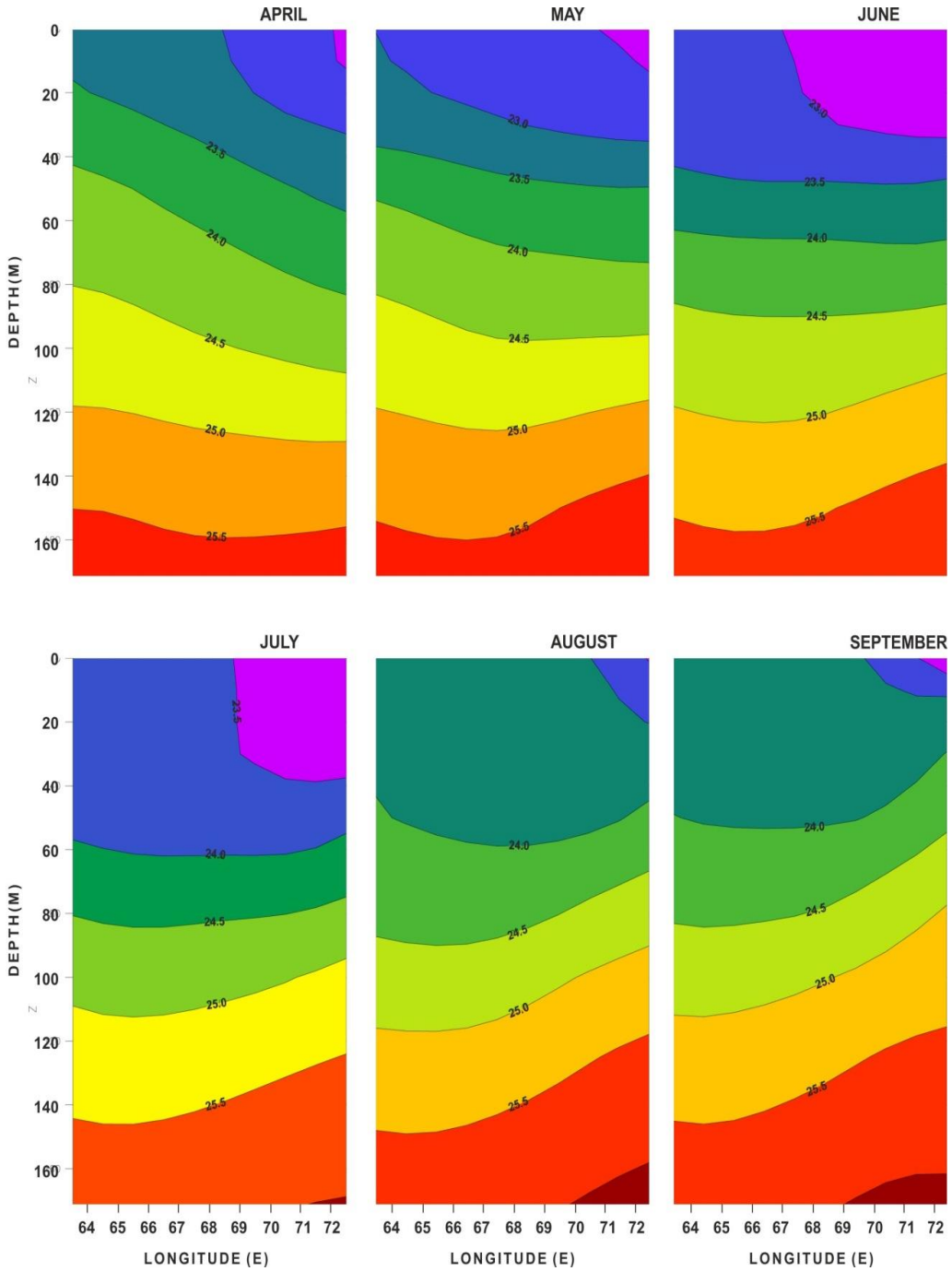

Fig. 2.6: Vertical distribution of sigma-t (Kg/m^3) at 17°N along the west coast of India from April to September.

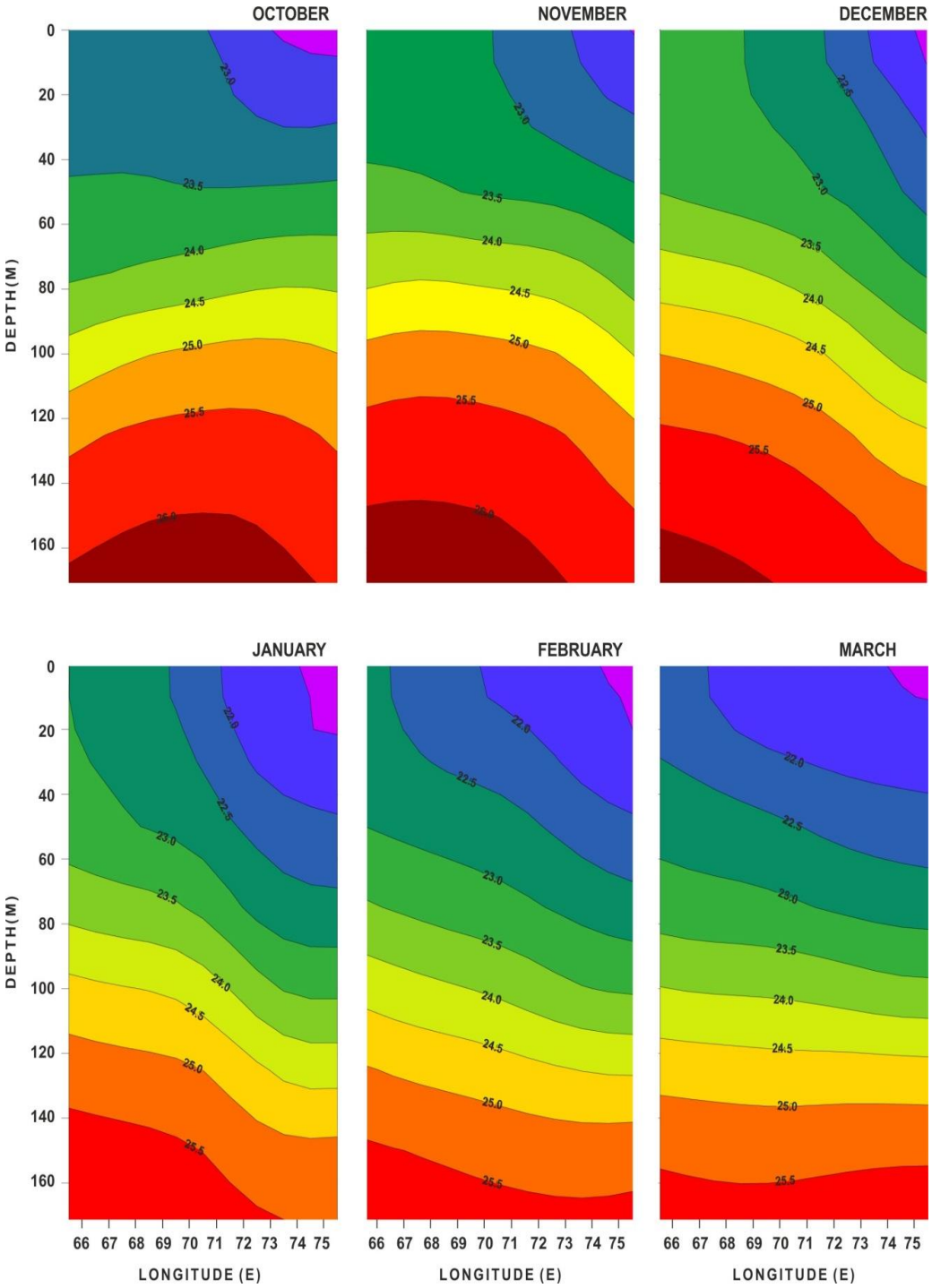

Fig. 2.7: Vertical distribution of sigma-t (Kg/m^3) at 9ºN along the west coast of India from October to March.

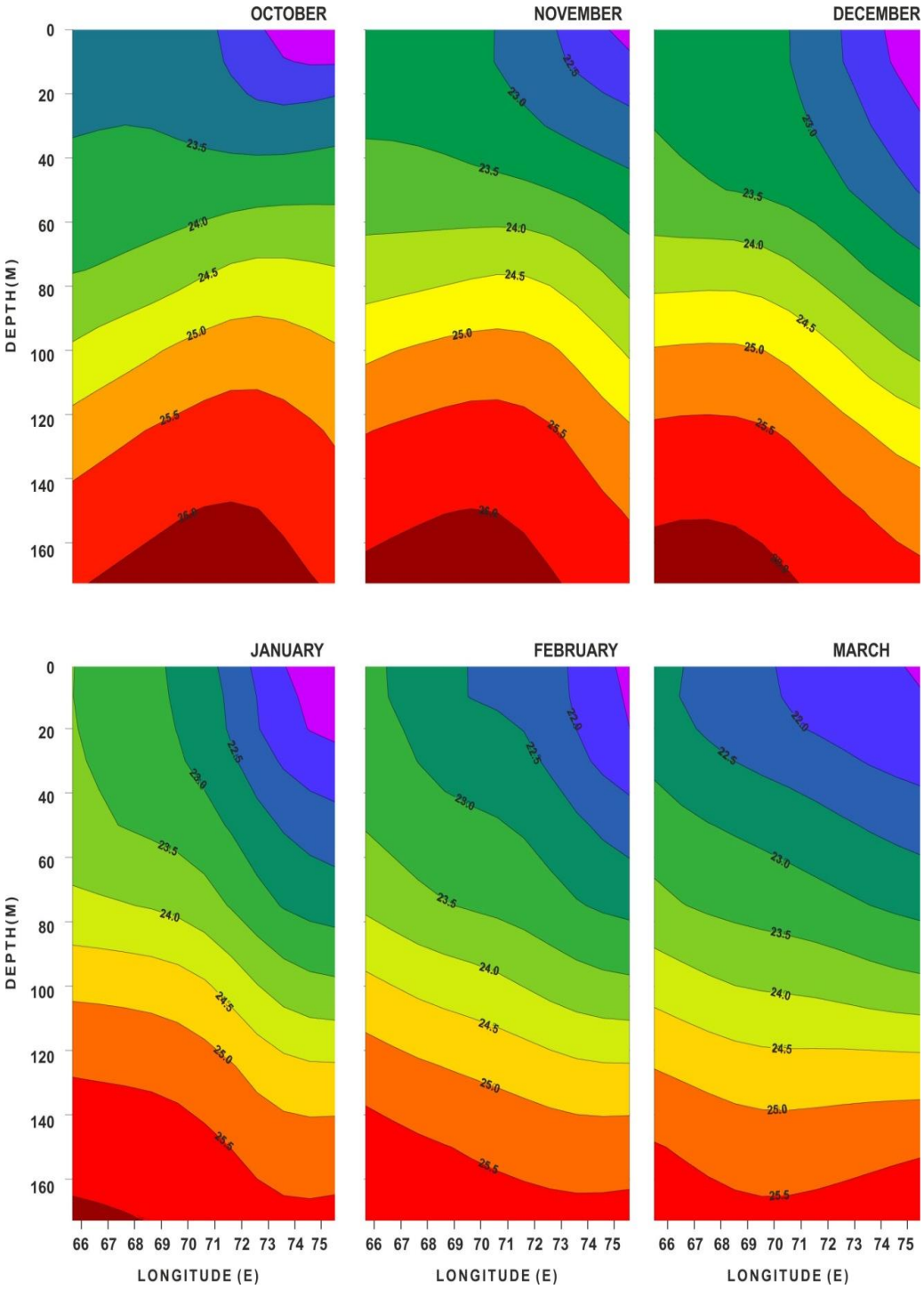

Fig. 2.8: Vertical distribution of sigma-t (Kg/m^3) at 11°N along the west coast of India from October to March.

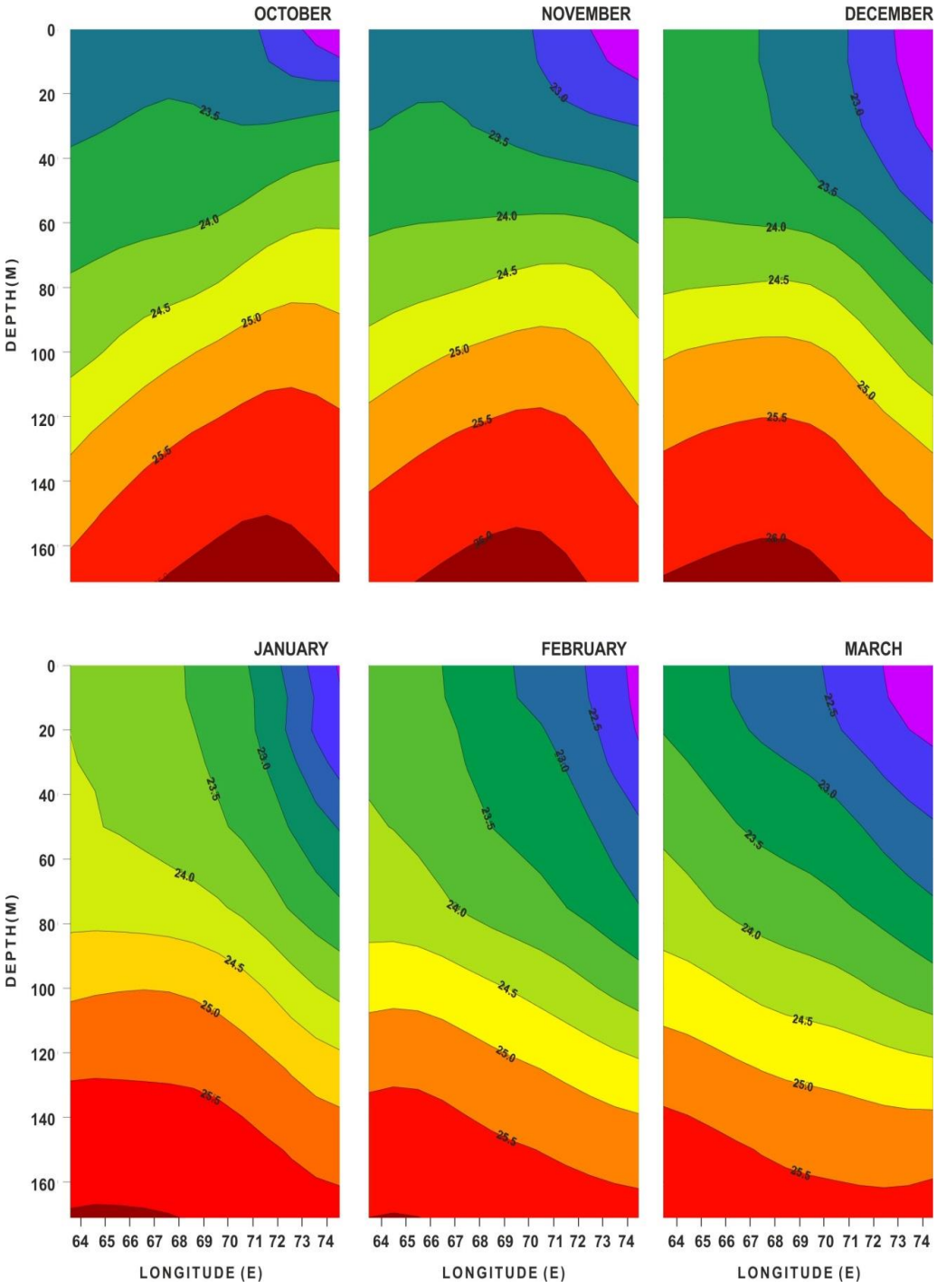

Fig. 2.9: Vertical distribution of sigma-t (Kg/m^3) at 13ºN along the west coast of India from October to March.

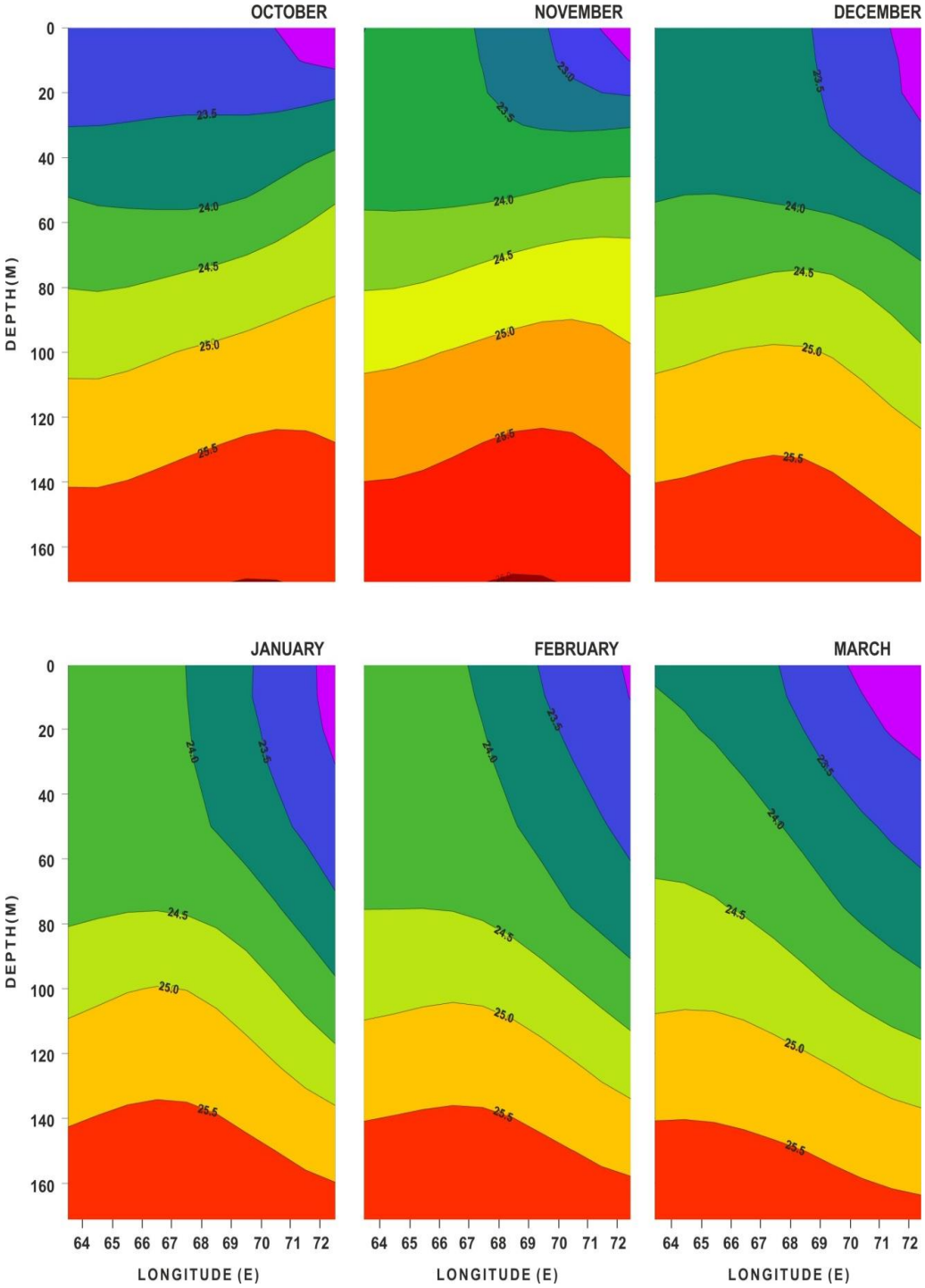

Fig. 2.10: Vertical distribution of sigma-t (Kg/m^3) at 17ºN along the west coast of India from October to March.

2.3.3 Sea Surface Height Anomaly (SSHA)

Analysis of monthly SSHA climatology along the west coast of India revealed that throughout the summer monsoon months the entire coastal belt was characterized by lowering in sea surface height. During the initial phase of summer monsoon, there were weak, negative SSHAs along the entire coast, whereas during June, weak, negative SSHA results were found from 8ºN to 19ºN; north of that latitude, weak, positive anomalies were observed. From July to September, intensification of the decline in SSHA was observed along the entire coastal belt of India, and the most intense negative SSHA was during August (Fig. 2.11). From the contours of the SSHA, it was evident that from May to September, the SSHA decline intensified and progressed, and during July, a strong decline in SSHA was observed, limited to southwest coast of India, but during August, it propagated to the entire coastal belt. Compared with September, SSHA was elevated along the west coast of India during October. During December and January, intensification of rise in sea level was observed along the west coast of India. These features diminished along the coast during March. These observations indicate that upwelling occurs along the coast during the southwest monsoon and downwelling during the northeast monsoon and winter.

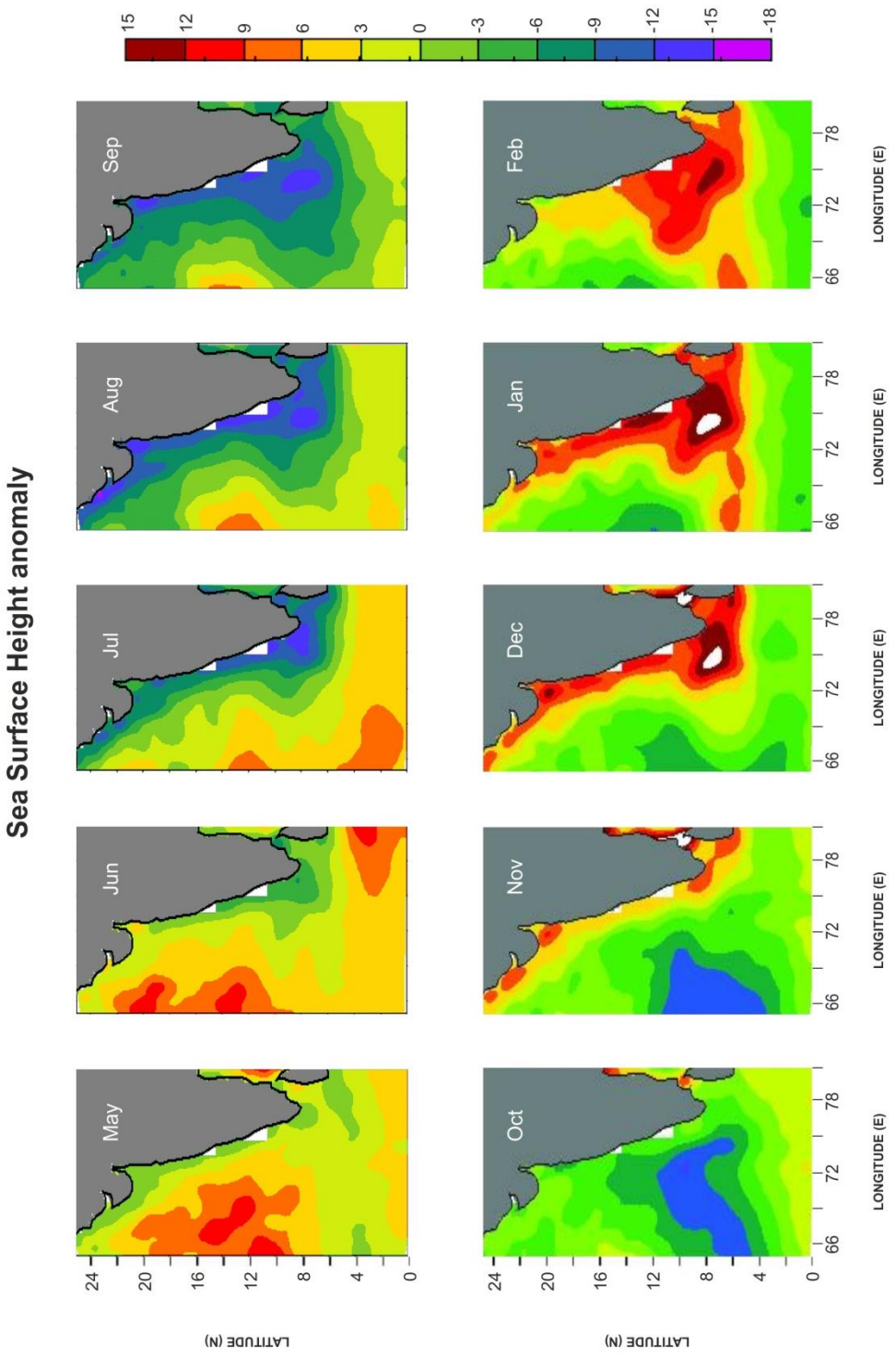

Fig. 2.11: Climatology of SSHA along the west coast of India during summer monsoon and winter.

2.3.4 Local Temperature Anomaly (LTA)

Analysis of Fig. 2.12(a) shows that the distribution of LTA over the surface waters with positive values (upwelling) was limited to southwest coast of India, whereas, along the northwest coast, the values were negative from16º N to 20º N during the summer monsoon except at 16º N during September. Strong positive anomalies of 0.8ºC were observed within a limited extent of southwest coast of India between 8ºN and 11ºN from July to September. This was a clear indication of strong upwelling along the southwest coast of India. From the surface LTA values, a lag was evident in the evolution of positive LTA (upwelling) from 8º N to 16º N. Even though the positive LTA were limited to the southwest coast at the surface waters, the observations at the 10m depth indicated positive temperature anomalies during May and September all along the west coast, except at 20ºN. The coastal belt from 16ºN to 20ºN was characterized by negative LTAs during June to August. After August, positive anomalies were observed from 16ºN to 20ºN (Fig. 2.12(b)). Similar features were also observed for LTA values at the 20m depth (Fig. 2.12(c)), but the LTAs at 30m were positive all along the west coast of India during May to September and along the southwest coast, the positive LTA strengthened after June. From 15ºN to 19ºN, the evolution of strong positive anomalies commenced after July (Fig. 2.12(d)). All the observations, from the surface to the 30m depth showed a lag in the evolution of positive anomalies from south to north, and it is also evident that the lag was greater at the surface than it was at depth. Observations from 10m to 30m showed that the zone between 15ºN to 19ºN was characterized by strong positive anomalies only after July. The gradient in temperature at 30m was three times greater than at the surface.

The results of the above mentioned parameters have been published in my paper (Shah et al., 2015)

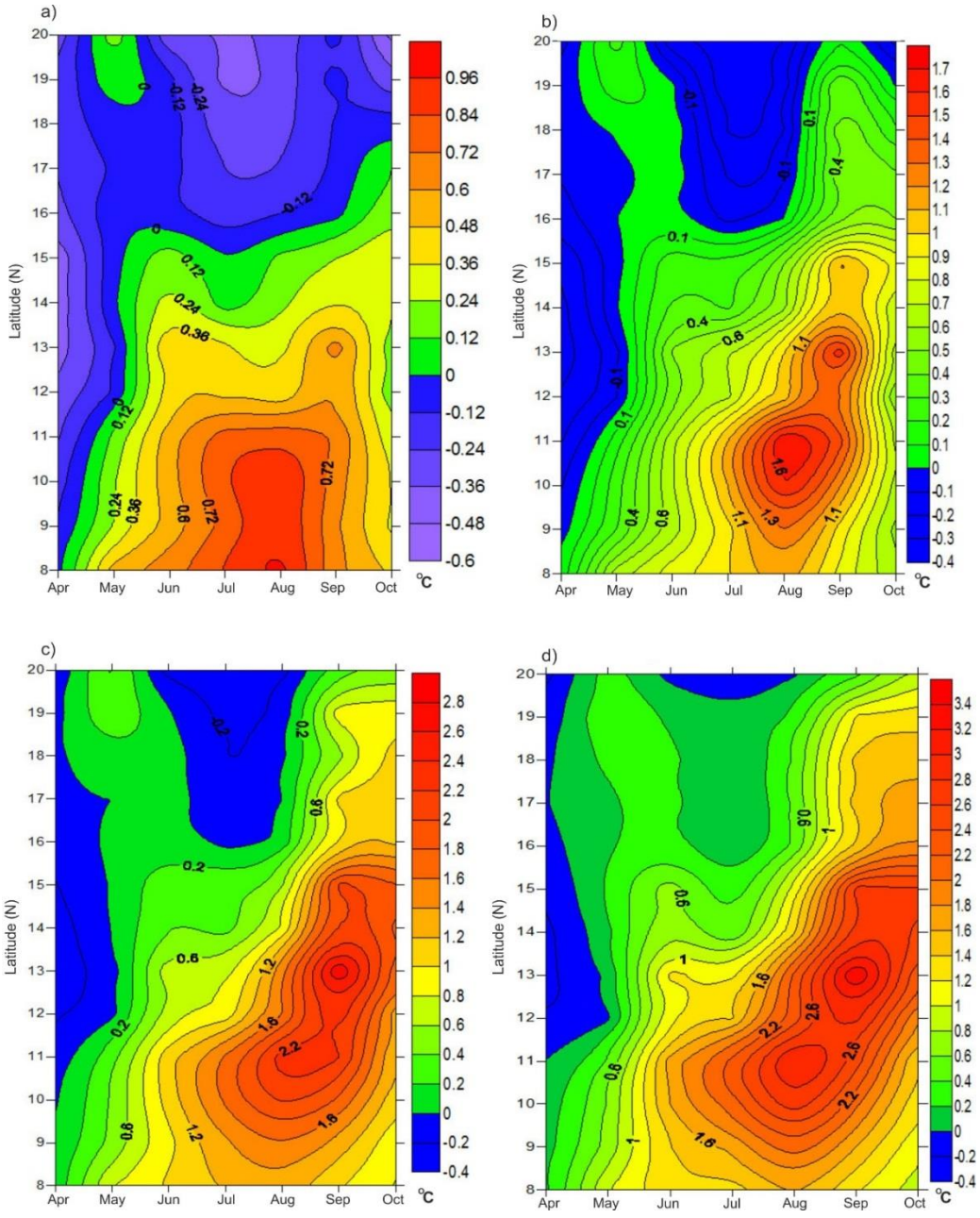

Fig. 2.12(a): Variation of LTA (°c) as a function of time (month) and space (latitude)along the west coast of India at (a): surface, (b): 10m, (c): 20m, (d): 30m.

2.3.5 Vertical Velocity

Fig. 2.13(a) & Fig. 2.13(b) represents the climatology of vertical velocity at 100m depth over eastern Arabian Sea from January to December. From April onwards positive vertical velocities (upward) are observed along the west coast of India (Fig. 2.13a). During May it intensified along the southern latitudes from 8ºN to 14ºN. During June intensification of upward vertical velocity is observed over the west coast from 8ºN to 18ºN, but the strength of upwelling was comparatively higher on the southern latitudes compared with the northern ones. During July, August and September, higher values of positive vertical velocity are observed over the southwest coast and moderate values of upward velocity are observed over the northwest coast. Even though strong upward vertical velocity is limited to southwest coast, northern latitudes also possess considerable upward vertical velocity during the peak summer monsoon.

During the northeast monsoon and winter the west coast of India was characterized by moderate-to-strong downward velocity. From October, the coast shows lower values of downwelling velocities except at 8ºN (Fig. 2.13b). This indicates the cessation of upwelling and evolution of sinking along the coast. During November, December and January, strong downward velocity is observed along the southwest coast from 8°N to 14°N and along the northwest coast, moderate velocity is observed. The month February shows moderate downwelling velocity along the west coast of India. Compared with the northwest coast, the magnitude of vertical velocity is stronger over the southwest coast.

Even though vertical velocity at 100m depth indicates higher magnitudes of 4×10^{-5} m/s along the southwest coast and 1.5×10^{-5} m/s along the northwest coast during the peak southwest and northeast monsoon, the mean vertical velocity between the surface to 100m depth indicates magnitudes of 2.15×10^{-5} m/s along the southwest coast and 0.76×10^{-5} m/s along the northwest coast.

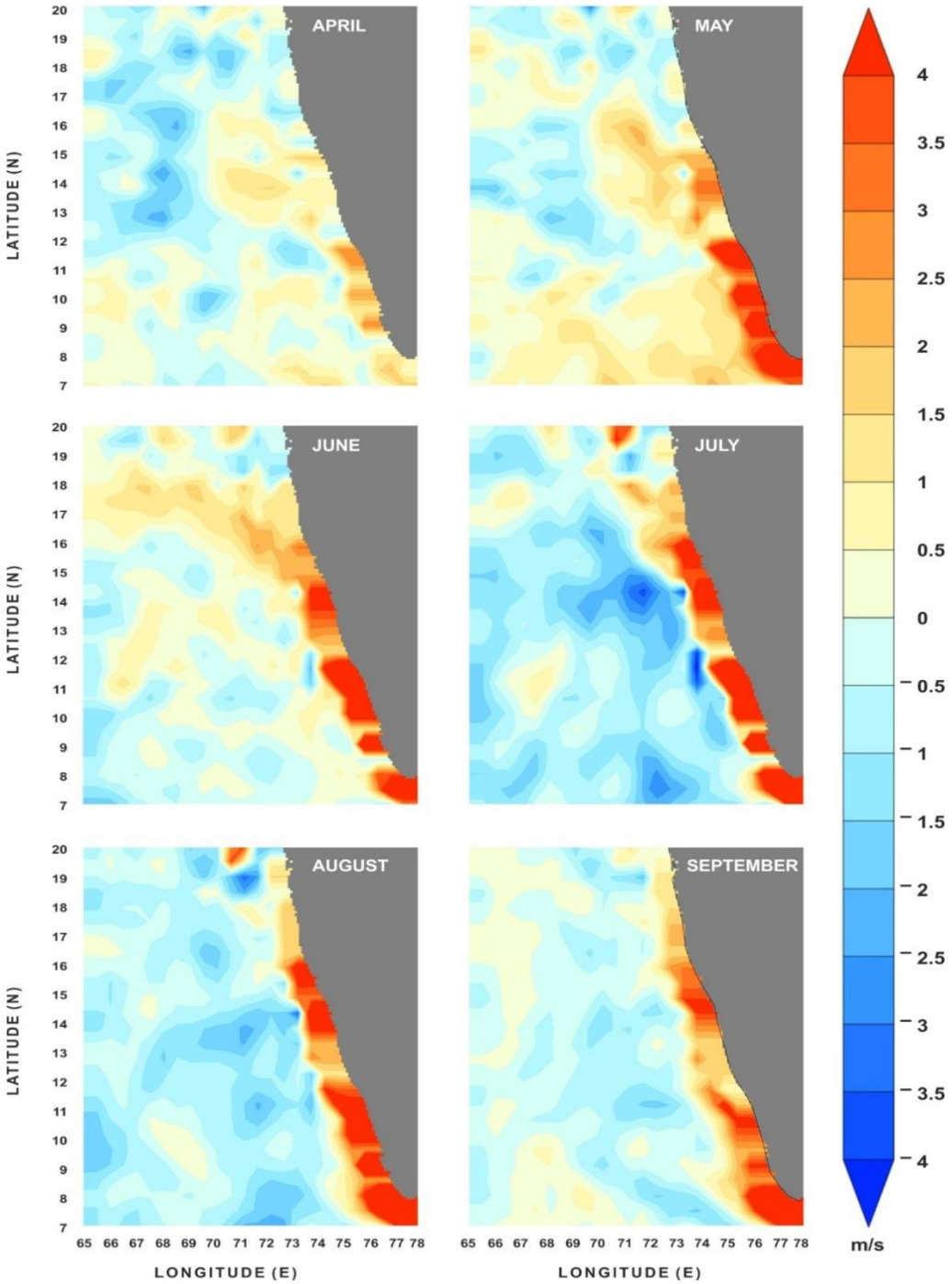

Fig. 2.13a: Climatology of vertical velocity ($\times 10^{-5}$ m/s) at 100m depth along the west coast of India from 8ºN to 20ºN during the summer monsoon.

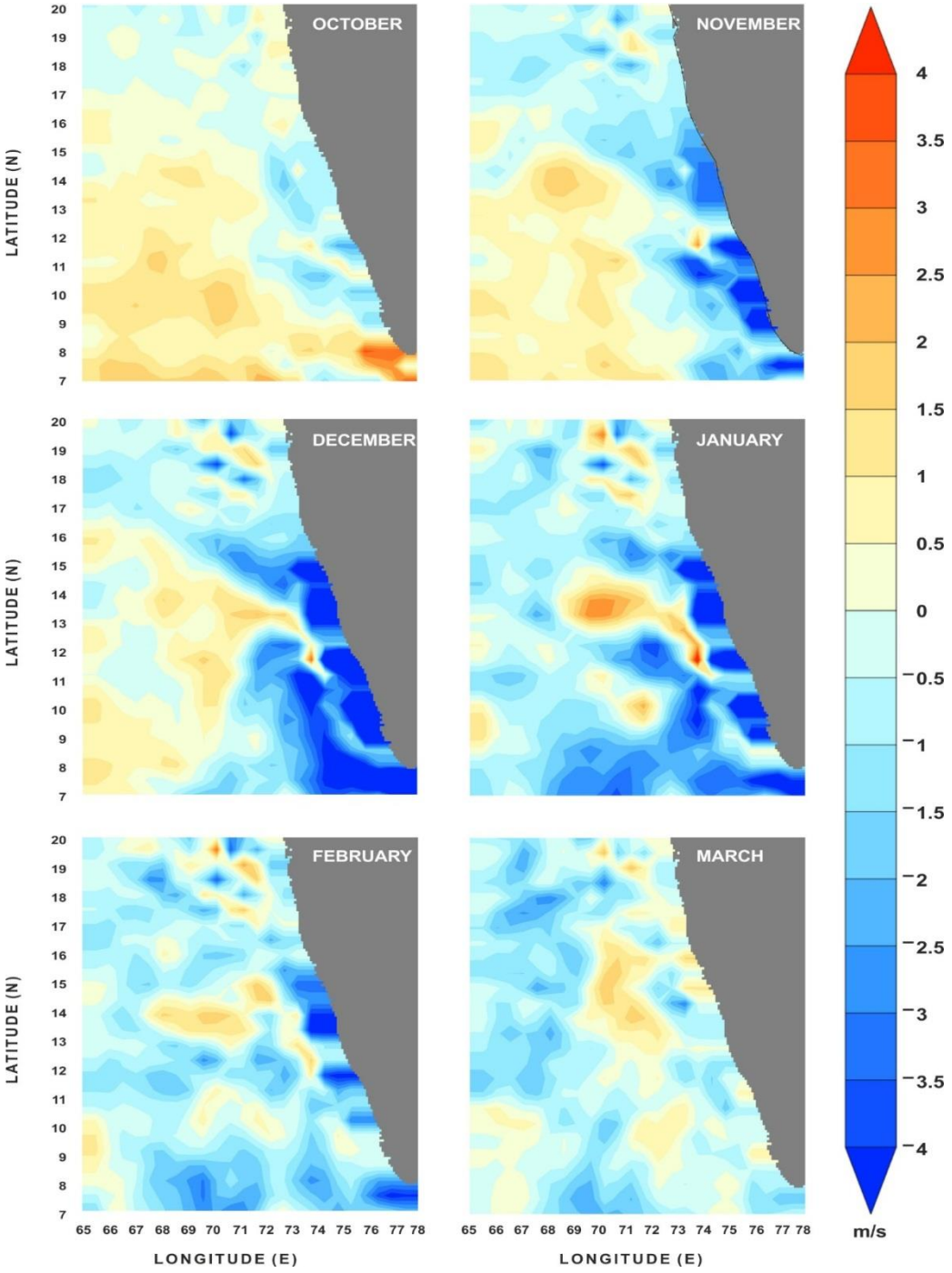

Fig. 2.13b: Climatology of vertical velocity ($\times 10^{-5}$ m/s) at 100m depth along the west coast of India from 8ºN to 20ºN during the northeast monsoon and winter.

2.3.6 Chlorophyll-a

The analysis of chlorophyll- a over the eastern Arabian Sea reveals that throughout the year northwest coast of India was characterized by higher concentrations of Chlorophyll-a compared with the southwest coast. Along the southwest coast, higher concentration of chlorophyll-a were observed only during the summer monsoon months. This was due to the ascending motion of nutrient rich subsurface water during this season. During the northeast monsoon and winter, chlorophyll-a concentration along the southwest coast of India was essentially very low (Fig.2.14a and Fig.2.14b). This was due to the impact of downwelling during this season. Along the northwest coast during both monsoons, significant chlorophyll-a concentration was observed. This indicates that rather than the vertical motions, chlorophyll-a concentration along the northwest coast of India was mainly determined by some other phenomena. But during July and August intensification of chlorophyll-a was observed along the northwest coast also. Fig. 2.15 clearly represents the intensification of chlorophyll-a during May to September along the southwest coast and during July to August along the northwest coast. This substantiates the results of findings on upwelling along the northwest coast during the peak summer monsoon.

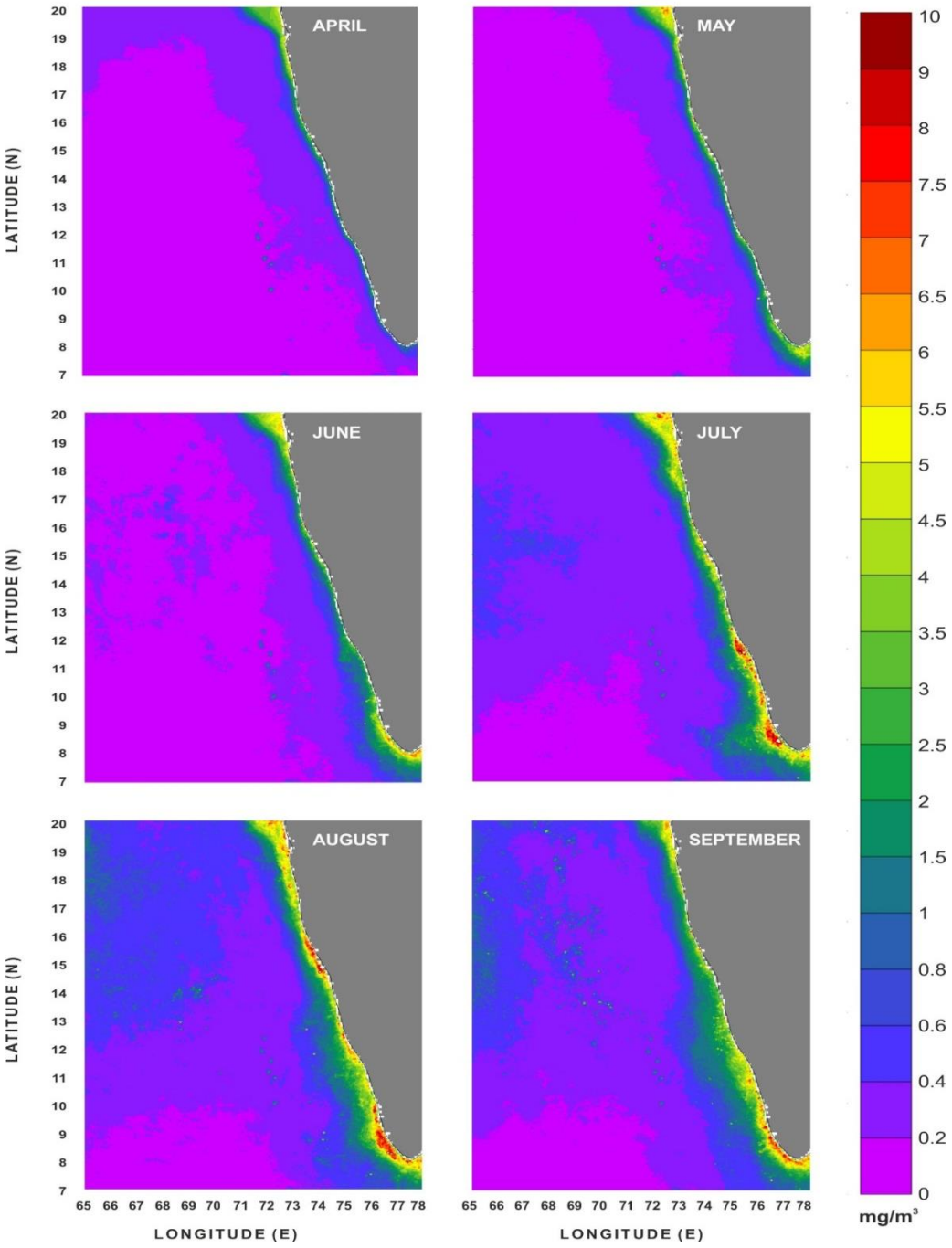

Fig. 2.14a: Climatology of Chlorophyll-a concentration (mg/m^3) along the west coast of India from 8ºN to 20ºN during the summer monsoon.

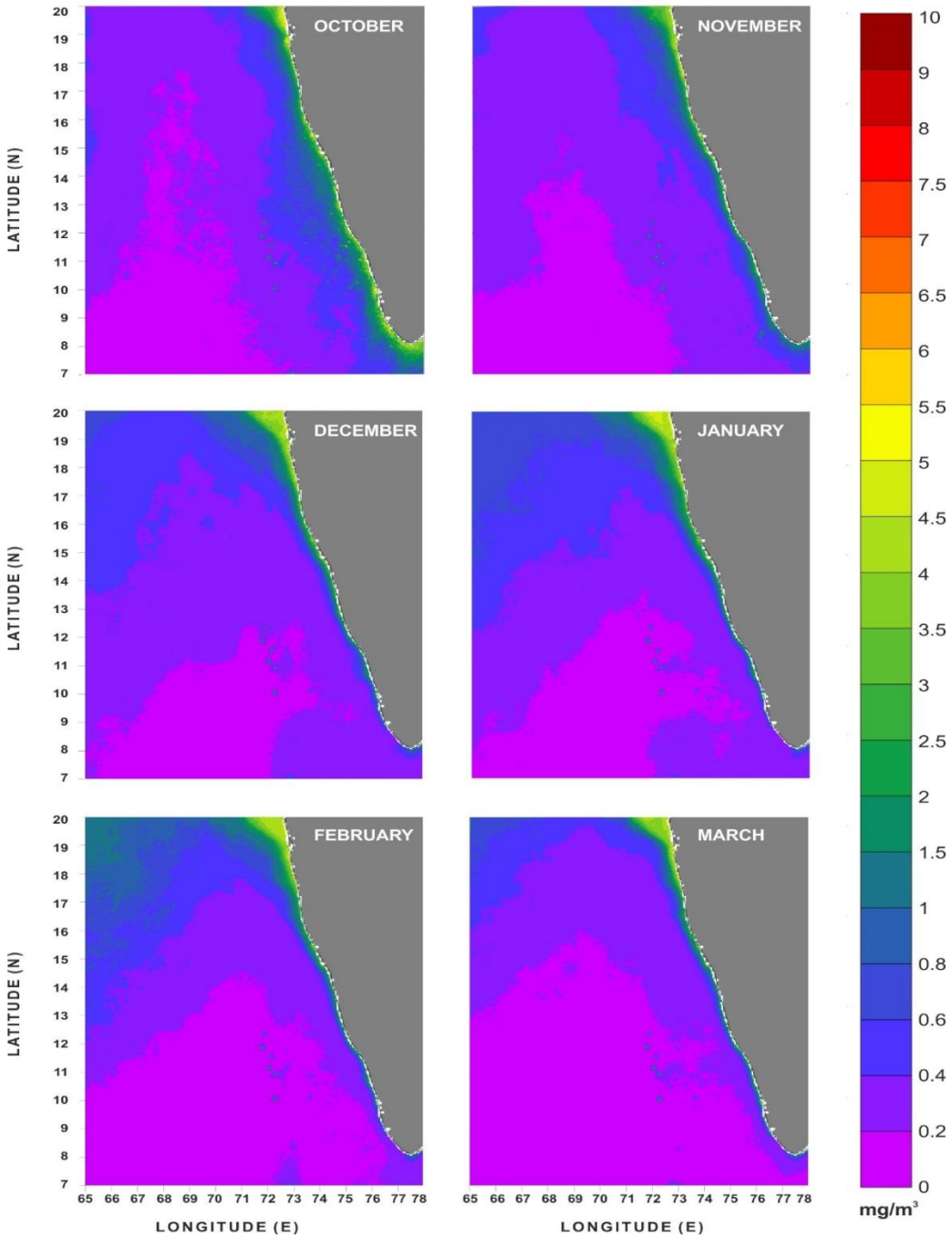

Fig. 2.14b: Climatology of Chlorophyll-a concentration (mg/m^3) along the west coast of India from 8ºN to 20ºN during the northeast monsoon and winter.

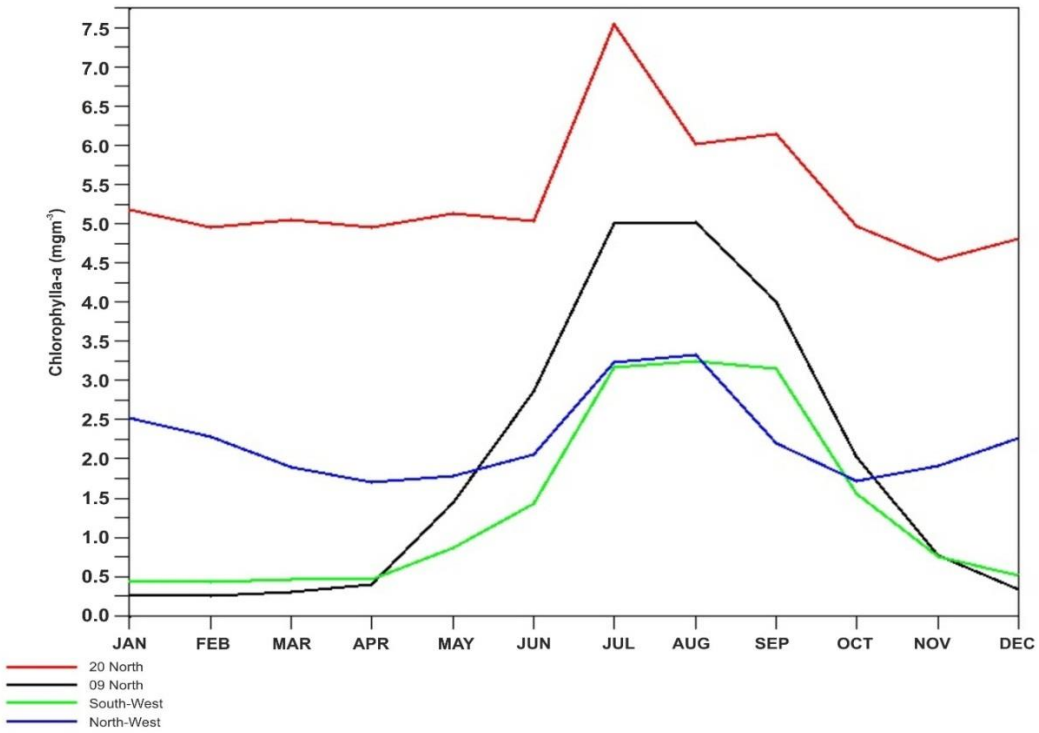

Fig. 2.15: Month wise variability of Chlorophyll-a concentration (mg/m^3) along the southwest and northwest coast of India (Climatology).

2.4 Conclusion

From the analysis of local temperature anomaly, depth of 26° isotherms, vertical velocity, SSHA, vertical profile of isopycnals, and chlorophyll-a concentration, it is concluded that the upwelling along the southwest coast of India starts at the southern tip (8°N) during April and propagates from south to north as the summer monsoon progresses, coming to an end during September. Unlike previous studies, I found that upwelling was not limited to the southwest (8°N to 15°N) coast but was also evident at the northwest (15°N to 20°N) coast. Upwelling features were clearly noticed at the near surface level along the northwest coast during the summer monsoon. One of the fundamental differences in the upwelling between southwest and northwest coast is that

upwelled water does not reach the surface along the northwest coast whereas upwelled water completely replaces the surface water along the southwest coast. During May and September the upwelled water reaches up to the 10m depth and from June to August it reaches up to the 30m depth along the northwest coast. The strength of upwelling was more on the southwest coast than on the northwest. The downwelling along the coast starts at the southern tip during October and continues until April. Downwelling also covers the entire west coast of India during the northeast monsoon and winter. Along the southwest coast the cessation of upwelling Starts during the end of September and downwelling sets during October. Whereas along the northwest coast the cessation of upwelling starts during October and the coast was characterized by sinking from November to March. Downwelling along the southwest intensified during December and February. The strength of downwelling was also more on the southwest coast than the northwest coast.

…..ꕥ…..

Chapter 3

LOCAL & REMOTE FORCING ON UPWELLING AND DOWNWELLING

Contents

3.1 Introduction

Concerning the driving forces of vertical motion along the west coast of India, almost all earlier observational studies gave priority to wind-induced Ekman mass transport. Only the work of Sharma, (1978) was an exception to this case. While discussing the vertical circulation, Sharma pointed out the importance of horizontal divergence as a driving force, and he considered that a current-induced upwelling would exist until the geostrophic balance was established. However, true geostrophic balance is never attained. But his studies were limited to a narrow transect from 8ºN to 12ºN along the south-west coast of India.

In this chapter, while describing the driving forces of vertical motion along the west coast of India, the following issues will be addressed.

1) What are the driving forces involved in upwelling and downwelling?

2) What is the relative role of local versus remote forcing in vertical circulation along the west coast of India?

3) What are the fundamental difference between the driving forces of upwelling and downwelling along the southwest and northwest coast?

The general approach to describe the driving forces of vertical circulation in this chapter are now explained.

In the previous chapter we have mentioned that depending on the strength and duration, the vertical motions can be classified as either normal vertical advection or as forced motions. Upwelling and downwelling are the ascending and descending vertical motions belonging to the class of forced vertical motions. Here we have to define what is meant by forced vertical motions as a basis for a good understanding of these upwelling and downwelling. To understand the vertical circulations we should first be familiar with the equation of continuity:

$$\frac{\partial u}{\partial x} + \frac{\partial v}{\partial y} + \frac{\partial w}{\partial z} = 0 \ldots\ldots\ldots\ldots\ldots\ldots\ldots\ldots\ldots\ldots\ldots\ldots\ldots\ldots \quad (3.1)$$

Horizontal divergence,

$$\nabla h \cdot V = \frac{\partial u}{\partial x} + \frac{\partial v}{\partial y} \quad \ldots\ldots\ldots\ldots\ldots\ldots\ldots\ldots\ldots\ldots\ldots\ldots\ldots\ldots\ldots\ldots \quad (3.2)$$

From these equations, the dependence of vertical velocity to the horizontal divergence can be understood: whenever there is a horizontal divergence of magnitude different from zero, there will be a vertical advection. Depending on the sign and magnitude of this horizontal divergence, the strength and direction of these vertical motions will differ. The horizontal divergence is

mainly dependent on the horizontal circulation. Hence, in the absence of any other triggering forces (local or remote), if there is strong horizontal circulation along any coast, the coast will also experience strong vertical circulation. This is the case globally for upwelling associated with strong eastern boundary currents. At particular latitude in the northern hemisphere, if the horizontal divergence values are positive (which indicates a convergence), a downward vertical motion will result and the strength of downward motion will depend on the strength of convergence. In the opposite case, if at a particular latitude the horizontal divergence is negative it indicates a surface divergence, and hence results an upward motion. If this horizontal divergence is triggered by external forces such as wind, remote forcing including planetary scale waves, Kelvin waves, or by a circulation associated with large-scale cyclonic and anticyclonic wind gyres rather than a normal density-gradient circulation, then the vertical motion will also be triggered. This type of triggered vertical motion belongs to the class of forced vertical motions. Upwelling and downwelling are examples of such forced vertical motions.

This chapter deals mainly with two types of forcing, one is local forcing and the other is remote forcing. Here local winds, surface currents and local surface divergence belong to the local forcing. In two parts, this study explains in detail the driving forces involved in vertical circulation. In first part, we try to understand the upwelling and downwelling by elucidating the local forcing. Whenever the local forcing fails to explain the vertical motions thoroughly and completely, then we proceed to the second part, in which we address the remote. Hence the methods used to identify the origin and propagation of remote forcing will be explained later in this chapter, as and when required. The data and methodology adopted for the two parts are explained separately as materials and methods (1) & (2).

3.2 Materials and Methods -1

Comprehensive use of satellite real time data for wind, Sea Surface Height Anomaly (SSHA), surface currents and horizontal divergence was made to explain the possible local forces involved in upwelling and downwelling along the west coast of India. Monthly wind data from the QuikSCAT satellite at $0.25^{o} \times 0.25^{o}$ resolution were obtained from the Ocean Watch Live Access Server and were used to derive the surface Ekman mass transport. The Archiving, Validation, and Interpretation of Satellite Oceanographic (AVISO) – merged and blended SSHA at $0.33^{o} \times 0.33^{o}$ resolution from Asia-Pacific Data-Research Center (APDRC) data sets were used to characterize the variability of upwelling along the coast. The grids selected for this study along west coast are given in Fig 2.1 in the second chapter. Henceforth, the region between the limits of 8^{o}N and 15^{o}N along the coastal belt is referred to as the southwest coast and that from 15^{o} N to 20^{o} N as the northwest coast. Ocean Surface Current Analysis Real-time (OSCAR) (1^{o}x1^{o}) data sets from National Oceanic and Atmospheric Administration (NOAA) were used to study the monthly and seasonal variability of surface currents over the eastern Arabian Sea. Simple Ocean Data Assimilation SODA ($0.5^{o} \times 0.5^{o}$) - assimilated model output from Asia Pacific Data Research Center (APDRC) were used to derive the horizontal divergence using equation (3.2). Since upwelling and downwelling are annually recurrent phenomena along the west coast of India, climatologies of the above mentioned data sets were used in this study.

The classical explanation of coastal upwelling and downwelling favors wind-induced surface mass transport away from and towards the coast respectively. Because the offshore and onshore mass transport across the coastal belt were greatly dependent on both the alongshore and cross shore component of the wind, the Ekman mass transport derived from both

components of wind stress was taken as an index of coastal upwelling. Along the west coast of India, these two components of wind were obtained with reference to the inclination of the coastline and can be computed as follows:

$$v = V\cos\phi - U\sin\phi \quad \ldots\ldots\ldots\ldots\ldots\ldots\ldots\ldots\ldots\ldots\ldots\ldots\ldots\ldots \quad (3.3)$$

$$u = U\cos\phi + V\sin\phi \quad \ldots\ldots\ldots\ldots\ldots\ldots\ldots\ldots\ldots\ldots\ldots\ldots\ldots\ldots\ldots\ldots\ldots\ldots \quad (3.4)$$

Where *v, u, U,* and *V* are alongshore, cross-shore, zonal, and meridional components of wind, respectively, and ø is the inclination of the coast. The inclinations of the coastline at different latitudes along the west coast of India are given in Table 3.1. Along the west coast of India the equatorward and offshore components of wind stress are favorable for upwelling, whereas the poleward and onshore components act against upwelling and favour downwelling. Equatorward and offshore components of the wind along west coast of India are represented by negative values and poleward and onshore components are represented by positive values. Hence negative values of the surface mass transport calculated with these components represent upwelling and positive values of surface mass transport represent downwelling. The bulk aerodynamic formula by Koracin, Dorman and Dever (2004) was used to find both the alongshore and cross shore components of the wind stress along the west coast of India.

$$\tau_y = \rho_a C_d \, w \, v \quad \ldots\ldots\ldots\ldots\ldots\ldots\ldots\ldots\ldots\ldots\ldots\ldots\ldots\ldots\ldots\ldots\ldots\ldots\ldots\ldots\ldots\ldots \quad (3.5)$$

$$\tau_x = \rho_a C_d \, w \, u \quad \ldots\ldots\ldots\ldots\ldots\ldots\ldots\ldots\ldots\ldots\ldots\ldots\ldots\ldots\ldots\ldots\ldots\ldots\ldots\ldots\ldots\ldots \quad (3.6)$$

where τ_y is the alongshore wind stress; τ_x is the cross shore wind stress; ρ_a is the density of the air, which was 1.2 kg/m^3; *w* is the magnitude of the wind speed; *v* is the alongshore component of wind speed; *u* is the cross shore component of wind speed, in meters per second; and *Cd* is the nonlinear drag coefficient

based on Large and Pond (1981) and on Trenberth et al. (1990) for low wind speeds. It can be computed as follows;

$$10^3 C_d = 2.18 \text{ ……...For } w \leq 1 \text{ m/s}$$

$$= 0.62+1.56w^{-1} \text{……... For 1 m/s} < w < 3 \text{ m/s} \quad \text{..... (3.7)}$$

$$= 1.14 \text{ …….For 3 m/s} \leq w < 10 \text{ m/s}$$

$$= 0.49 + 0.065w \text{….....For } w \geq 10 \text{ m/s}$$

Ekman mass transport can be calculated as follows:

$$M_{ev} = \tau_y / f \text{ ……..... (3.8)}$$

$$M_{eu} = \tau_x / f \text{……..... (3.9)}$$

where, M_{ev} is mass transport by the alongshore wind, M_{eu} is the mass transport by the cross shore wind, f is the Coriolis parameter ($2\Omega\sin\varphi$), Ω is the angular frequency of earth and φ is the latitude.

Table 3.1: Coastal angle (with respect to true north) along the west coast of India.

Latitude(°N)	Inclination(°)
8	35
9	18
10	24
11	30
12	22
13	14
14	28
15	30
16	7
17	15
18	3
19	3
20	3

3.3 Results and Discussion -1

3.3.1 Surface mass transport due to alongshore component of wind

As stated earlier, most of the previous studies on vertical circulation along the west coast of India treated the offshore transport due to the along shore component of wind as the primary driving force. Here I have attempted to check whether this assumption is consistent with the facts relating to the vertical circulation along the west coast of India. The advent of satellite oceanography helps us to resolve these problems by the rich availability of various physical oceanographic properties. Fig. 3.1 shows the surface mass transport due to the alongshore component of wind. From this figure we can deduce that along the west coast of India, throughout the year except the summer monsoon months, the coast was characterized by weak to moderate upwelling-favorable offshore transport. But during the summer monsoon, moderate onshore transport (positive values) was observed along the northwest coast and strong offshore transport was observed along the southwest coast (negative values). Tables 3.2 and 3.3 also show the values of surface mass transport along the coast throughout the year. The analysis of Table 3.2 shows that during May and September, the entire west coast of India was characterized by weak-to-moderate offshore surface mass transport, and compared with the northwest coast; offshore transport was strong along the southwest coast. From June to August, intense offshore mass transport occurred along the southwest coast of India, and the maximum and minimum values were observed as -1730 kg/m/s at 8ºN during July and -498 kg/m/s at 13ºN during June, whereas along the northwest coast of India, the zone between 16ºN and 20ºN was mainly characterized by very feeble offshore to moderate onshore transport increasing northwards during June to August. During July and August, weak offshore surface mass transport was observed at 16ºN and 17ºN. Offshore surface mass

transport values along 8ºN to 15ºN were five to six times larger than those observed at 16ºN and 17ºN during July. Along the west coast during July, the average value of surface transport is -1362.71kg/m/s (offshore) over the southwest coast and 309.63kg/m/s (onshore) over the northwest. The months June and August also follow the same demarcation between the southwest and northwest coasts (Shah et.al., 2015).

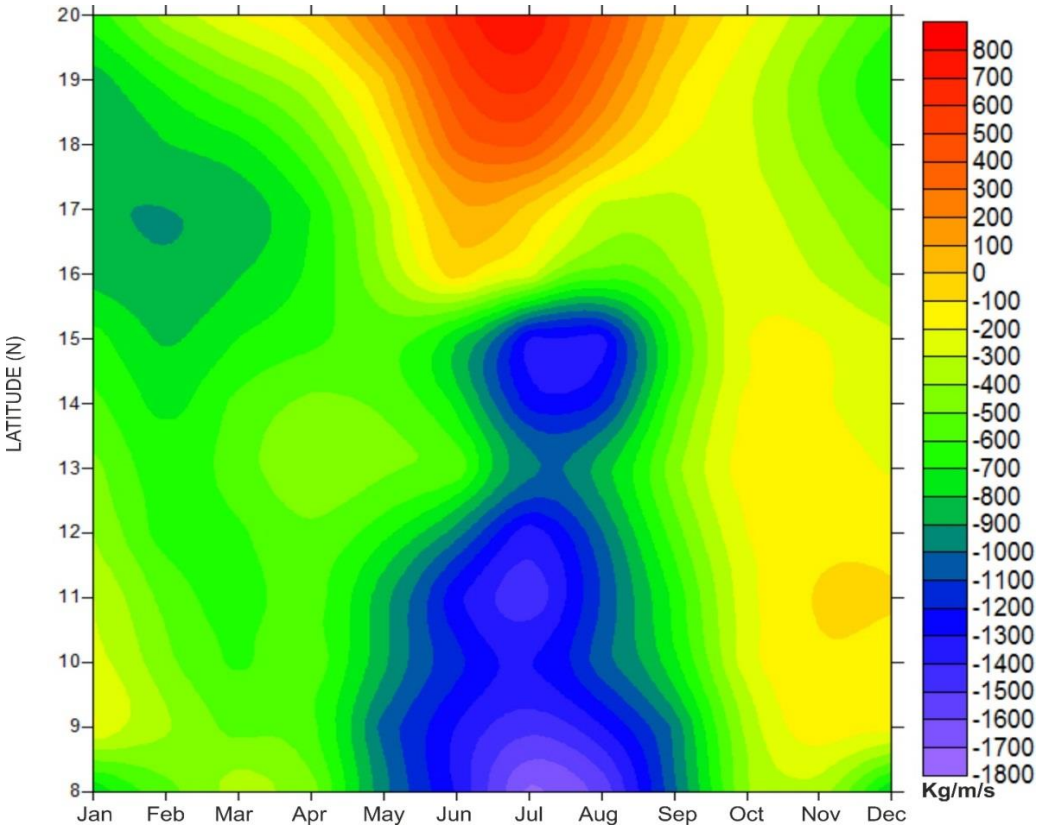

Fig. 3.1: Month wise variation of Surface Ekman mass transport (Kg/m/s) due to the alongshore component of Wind along the west coast of India (Climatology).

Table 3.2: Surface Ekman mass transport (Kg/m/s) due to the alongshore component of wind for the summer monsoon along west coast of India.

Months	8 °N	9 °N	10 °N	11 °N	12 °N	13 °N	14 °N	15 °N	16 °N	17 °N	18 °N	19 °N	20 °N
May	-964.8	-1048	-875	-866.6	-667.5	-486.1	-519.1	-570.2	-404.7	-348.4	-172	-6.355	298.3
Jun	-1304	-1303	-1156	-1279	-946.5	-498.1	-719	-785.3	-27.9	68.65	341.6	505.9	661.5
Jul	-1730	-1468	-1301	-1495	-1375	-966.7	-1236	-1330	-237.9	-40.54	412.4	647.5	766.7
Aug	-1576	-1308	-1033	-1093	-1012	-841.4	-1179	-1360	-529.8	-343.3	68.81	304.5	462.5
Sep	-1030	-985.9	-732.8	-680.9	-552.8	-436.7	-548.2	-643.8	-415.3	-344.3	-185.2	-76.97	59.73

Table 3.3: Surface Ekman mass transport (Kg/m/s) due to the alongshore component of wind for the northeast monsoon and winter along west coast of India.

Months	8°N	9 °N	10 °N	11 °N	12 °N	13 °N	14 °N	15 °N	16 °N	17 °N	18 °N	19 °N	20 °N
Nov	-341.2	-131	-116	-93	-127.1	-159.8	-191.9	-191.8	-309.4	-381.1	-465.5	-502.5	-374.2
Dec	-811.2	-149.3	-172.8	-80.96	-147.8	-209.9	-260.9	-271.8	-439.9	-503.4	-609.4	-694.2	-587.3
Jan	-791	-179.2	-265.5	-292.7	-401.2	-464.3	-567.7	-654.6	-831.9	-888.4	-900.7	-856.2	-654.8
Feb	-540.3	-383.6	-477.1	-535	-657.1	-674.9	-742.1	-820.8	-886.8	-901.8	-802.8	-659.2	-356.5

From Table 3.3 it was inferred that the entire west coast was characterized by weak-to-moderate offshore transport during the northeast monsoon months and winter. Compared with the peak winter months January and February, the coast experienced feeble offshore transport during November and December. Here, one of the interesting features noticed is that the offshore transport is stronger along the northwest coast than the southwest during the northeast monsoon and winter periods. Along the west coast during January, the average value of surface transport is -451.63kg/m/s over the southwest coast and -826kg/m/s over the northwest. All the other months clearly show the same southwest-northwest demarcation along the west coast of India.

The overall analysis of surface mass transport due to the alongshore wind (Fig. 3.1, Table 3.2 and Table 3.3) reveals that throughout the year, entire west coast of India was experienced weak-to-moderate offshore transport except during the peak summer monsoon months June, July and August. During the peak summer monsoon, moderate onshore transport was observed along the northwest coast and the strong offshore transport was noticed along the southwest coast.

If the assumption that the surface mass transport due to the alongshore wind stress is enough to explain upwelling and downwelling along west coast of India were correct, then from the above analysis we would expect weak-to-moderate upwelling along the entire west coast all over the northeast monsoon, winter and transition periods. Also, during May and September, moderate upwelling was expected over the entire west coast. During the peak summer monsoon months June, July and August, strong upwelling was expected over the southwest coast and along the northwest coast mass transport is towards onshore and anticipates downwelling. But our findings in Chapter 2 about the period and area of upwelling were completely contradictory to the above expectation.

The results of Chapter 2 reveal that upwelling occurred over the entire west coast of India during the summer monsoon and was not limited to the southwest coast. Upwelling, however, was clearly evident at the 10m depth along the northwest coast during May and September. The main difference in upwelling along the southwest and northwest coast during June to August was that vertical excursion of upwelled water along the northwest coast was limited to the 30m depth, whereas along the southwest coast the upwelled water reached the surface. From Local Temperature Anomaly (LTA) it was also evident that the intensity and south-to-north propagation speed of upwelling were greater at the deeper level than at the surface. The analysis also revealed that during the northeast monsoon and winter, the coast was characterized by downwelling.

On the basis of this discussion, we assert that the surface mass transport due to the alongshore wind stress alone is not enough to explain thoroughly and completely the upwelling and downwelling phenomena along the west coast of India.

The study of Sharma (1978) hints at the importance of both components of wind for a sustainable vertical oscillation. His studies revealed that, whenever the cross shore components of wind is towards offshore and alongshore component is equatorward, then the winds are favorable for upwelling along the west coast of India. The reverse is true in the case of downwelling. Following his study, in the present study both components of wind are analyzed for a better understanding of the phenomena. When the cross shore component of wind is towards offshore along the west coast of India, then the surface mass transport is away from the coast and will have negative values. If the cross shore component of wind is towards onshore, then the surface mass transport is towards the coast and will have positive values.

3.3.2 Surface mass transport due to the cross shore component of wind

Concerning the surface mass transport due to the cross shore component of wind (Fig.3.2) during November, December and January, the entire west coast was characterized by strong surface mass transport away from the coast. From February to April, moderate mass transport was observed towards the coast. During the summer monsoon from May to August, the coast was characterized by strong mass transport towards the coast and it was antagonistic to upwelling but favorable for downwelling. The surface mass transport due to the cross shore component of wind also followed the same trend of surface mass transports due to the alongshore component, except during the peak summer monsoon. During summer monsoon the mass transport due to the alongshore component of wind was upwelling-favorable along the southwest coast of India, whereas the mass transport due to the cross shore component was downwelling-favorable.

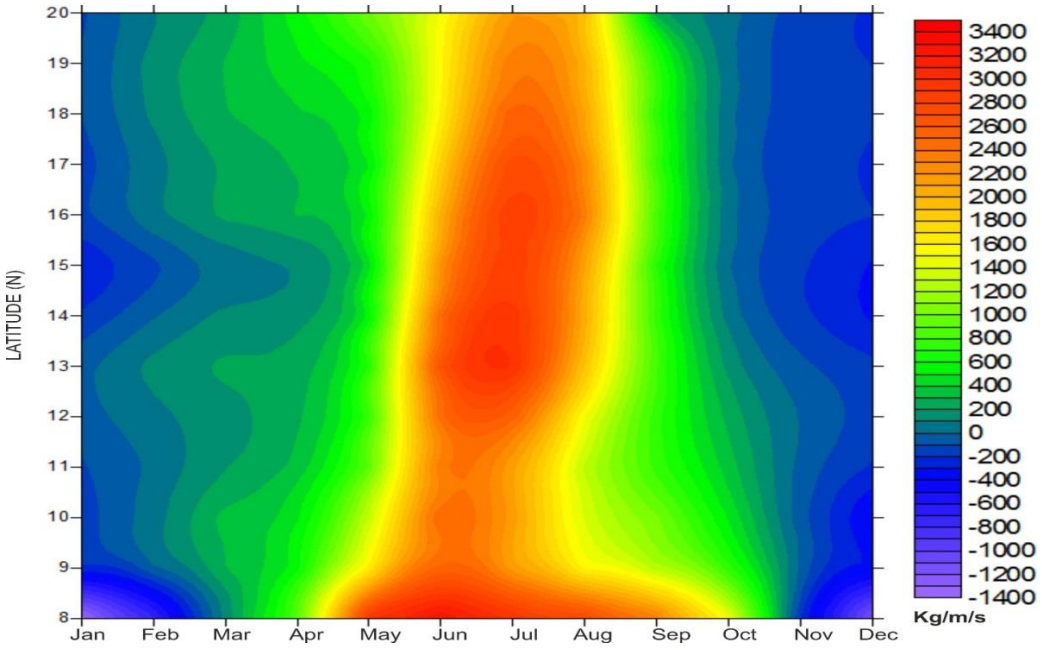

Fig. 3.2: Month wise variation of Surface Ekman mass transport (Kg/m/s) due to the cross-shore component of Wind along the west coast of India (Climatology).

3.3.3 Surface Ekman mass transport and Sea Surface Height Anomaly (SSHA)

Since the upwelling and downwelling areas are characterized by reduction and increase in sea surface height respectively, we can pool the findings of Chapter 2 and Chapter 3 in Fig. 3.3 and Fig 3.4. From Fig. 3.3 it is evident that even though the wind-induced offshore mass transport (negative values) was limited to the southwest coast during the peak summer monsoon months and onshore transport (positive values) was observed along the northwest coast, the reduced SSHA propagated all along the west coast of India rather remaining limited to the southwest coast. This was a clear indication of upwelling along the entire west coast of India during the summer monsoon, and it was not limited to the southwest coast.

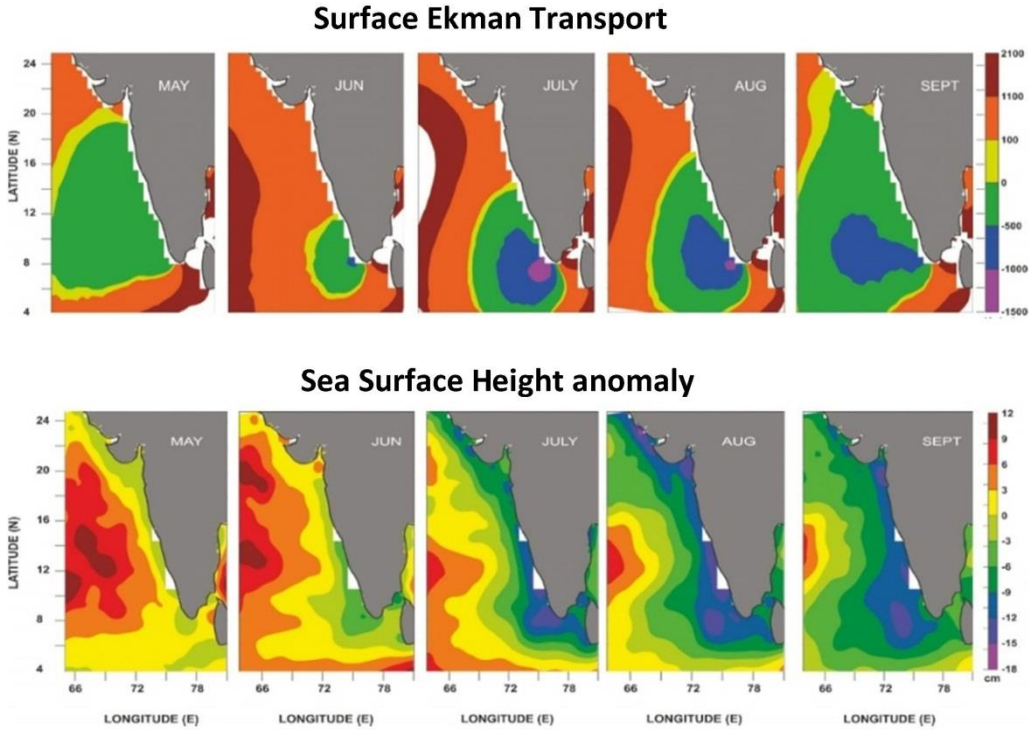

Fig. 3.3: Climatology of surface Ekman mass transport (kg/m/s) and SSHA (cm) along the west coast of India during the summer monsoon.

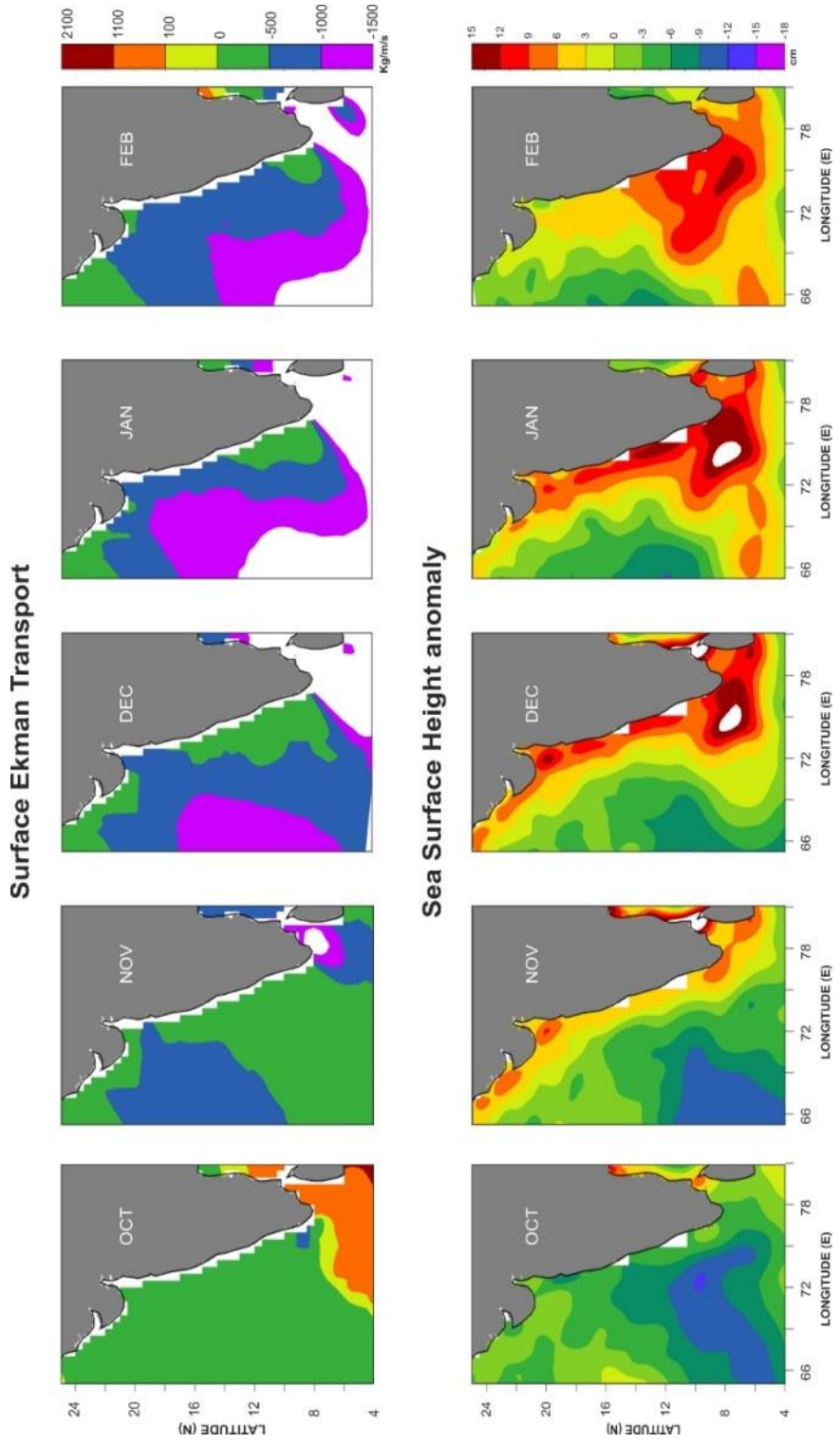

Fig. 3.4: Climatology of surface Ekman mass transport (k/m/s) and SSHA (cm) along the west coast of India during the northeast monsoon and winter.

Fig. 3.4 reveals that even though the surface mass transport due to the wind stress is towards offshore and it does not favors downwelling along the coast during the winter and northeast monsoon period, the entire west coast of India was characterized by increasing SSHA, and thus by downwelling.

Thus we can conclude that upwelling and downwelling along the west coast of India were driven not only by the wind-induced surface mass transport but that some other driving forces were also involved.

3.3.4 Surface currents and wind over the eastern Arabian Sea

Fig. 3.5 shows the magnitude and direction of surface currents over the eastern Arabian Sea. It is evident that along the west coast of India during the summer monsoon the currents were equatorward and the maximum strength was observed during July and August. During summer monsoon, the direction of these currents was in tune with the direction of wind along the southwest coast and over the northwest coast the direction of current was against the wind as shown in Fig. 3.6. During the transition months the current strength was very weak over the west coast. During the northeast monsoon and winter periods the current direction was poleward and the maximum strength was observed during December and January (Fig. 3.7). During this period the current direction along the entire west coast was against the wind as shown in Fig. 3.8. These findings about the surface currents are consistent with the studies of Shankar et al. (2002).

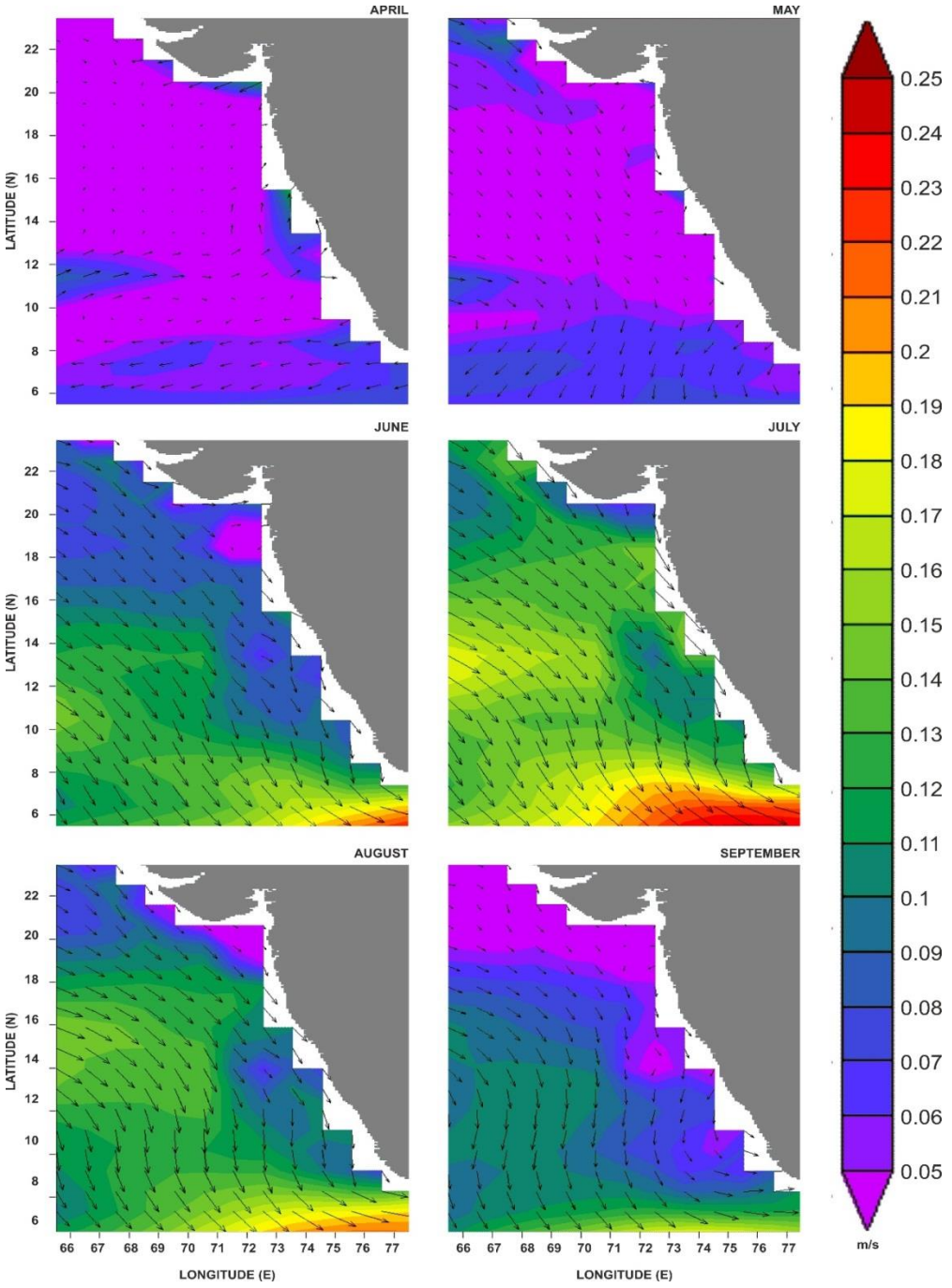

Fig. 3.5: Magnitude and direction of surface current (m/s) over the eastern Arabian Sea during the summer monsoon (Climatology).

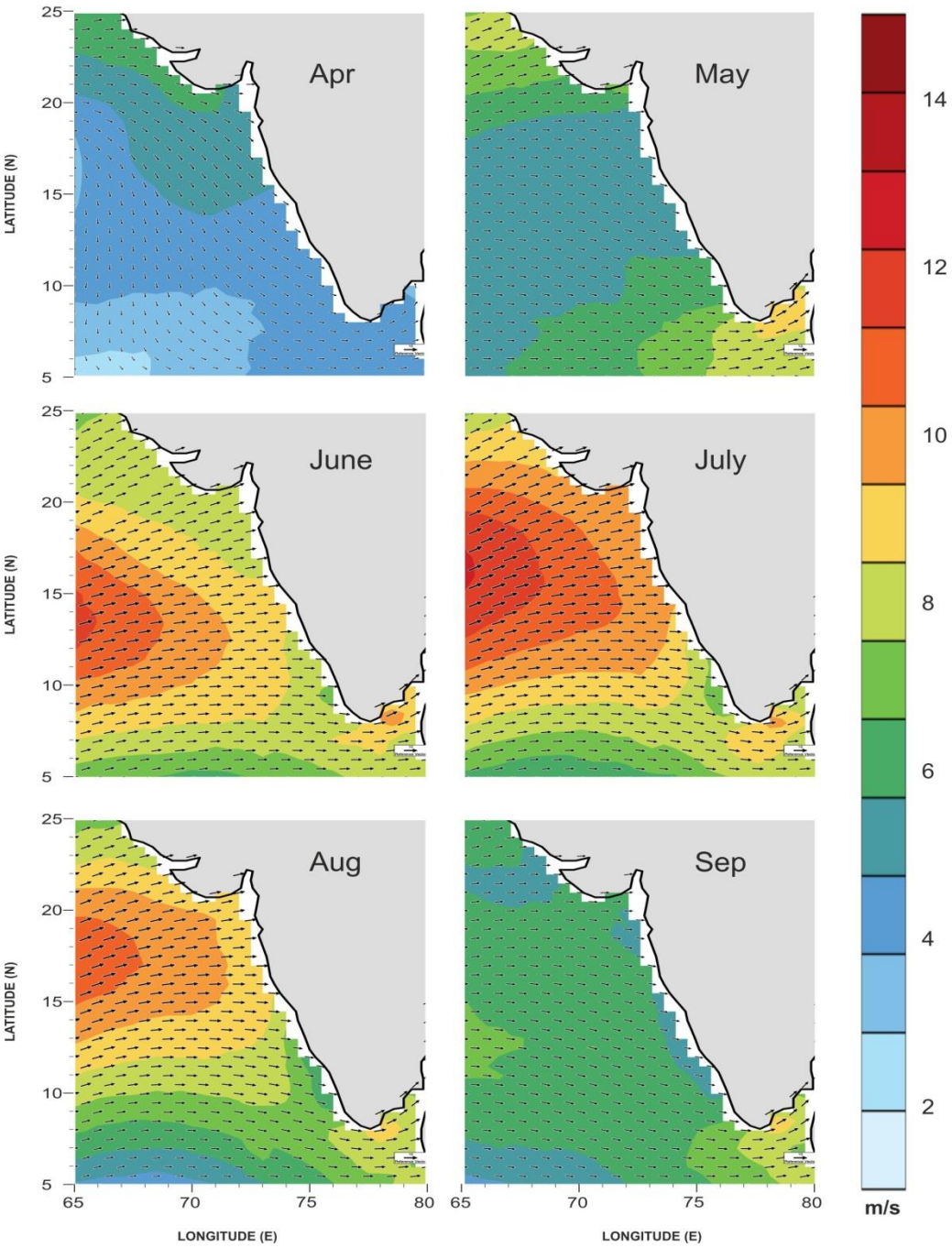

Fig. 3.6: Magnitude and direction of wind (m/s) over the eastern Arabian Sea during the summer monsoon (Climatology).

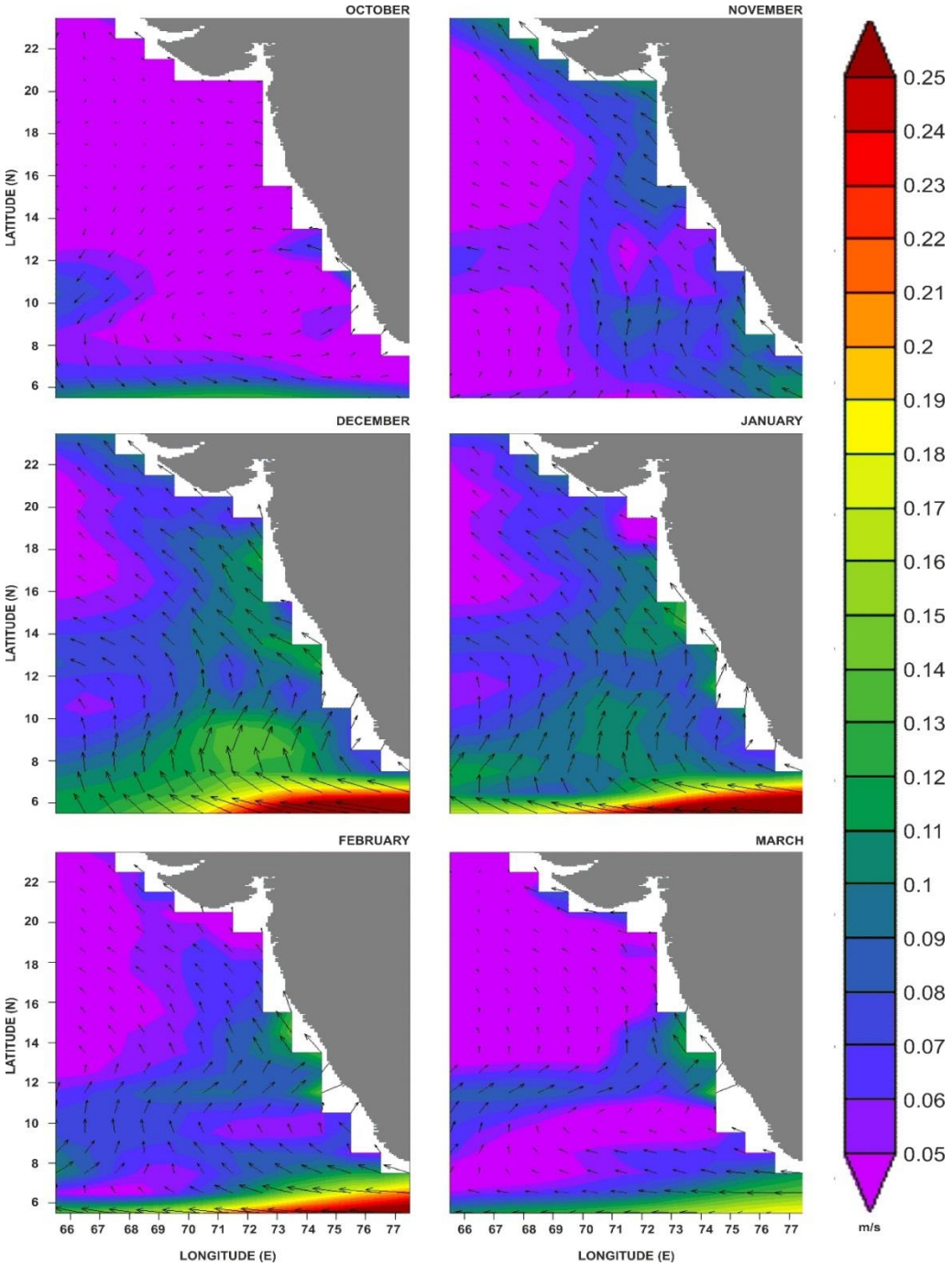

Fig. 3.7: Magnitude and direction of surface current (m/s) over the eastern Arabian Sea during the northeast monsoon and winter (Climatology).

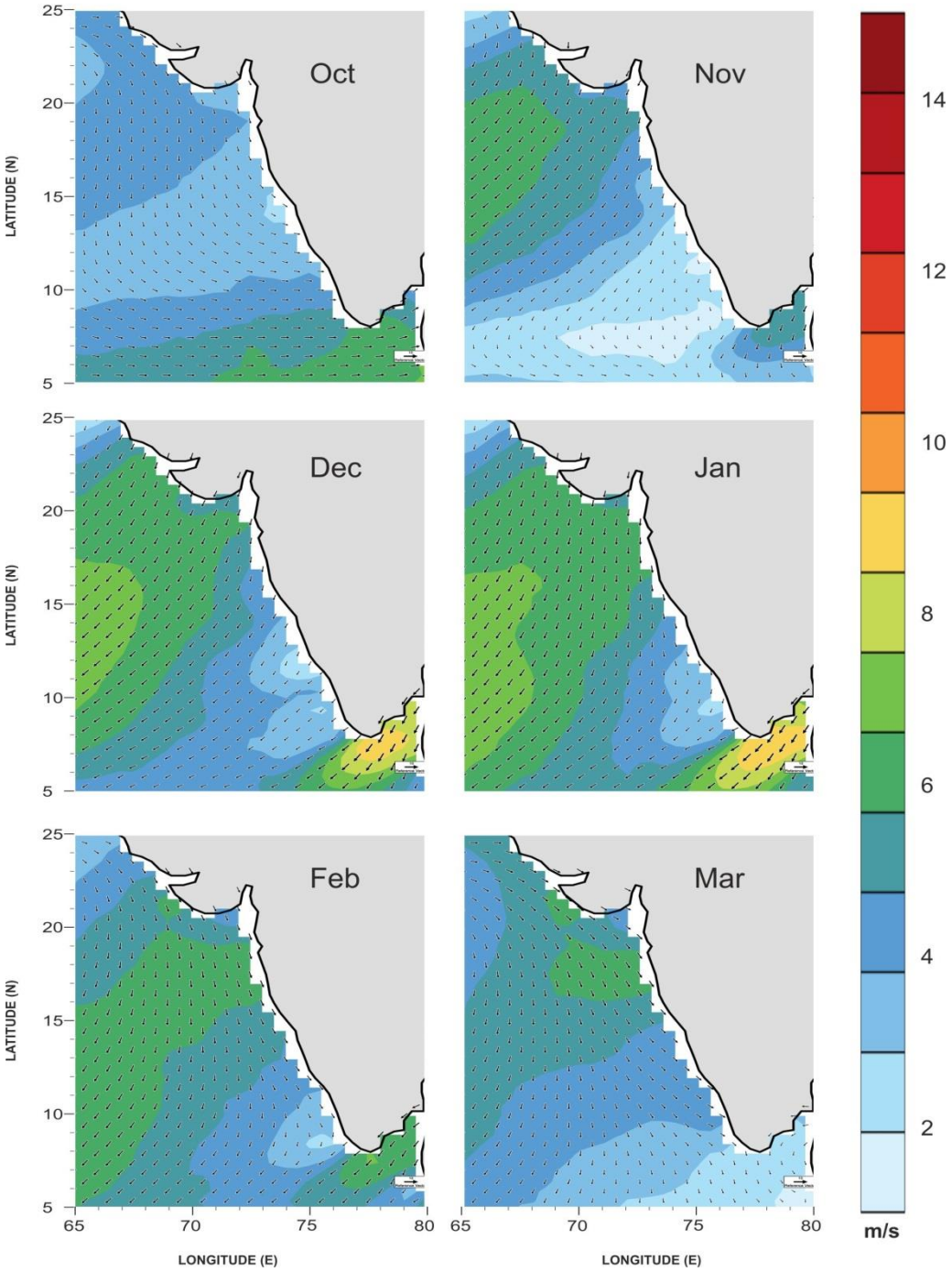

Fig. 3.8: Magnitude and direction of wind (m/s) over the eastern Arabian Sea during the northeast monsoon and winter (Climatology).

3.3.5 Horizontal divergence along the west coast of India

The analysis of Fig.3.9 reveals that during the summer monsoon the southwest coast of India was characterized by strong horizontal divergence from May to September. During June intensification of horizontal divergence was observed over the west coast from 8ºN to 18ºN, but the strength of divergence was comparatively higher on the southern latitudes compared with the northern ones. During July, August and September, higher values of horizontal divergence are observed over the southwest coast and moderate horizontal divergence are observed over the northwest coast. Even though strong horizontal divergence was limited to the southwest coast, northern latitudes also possess considerable horizontal divergence during the peak summer monsoon.

During May and September, upwelling along the entire west coast is due to the combined effect of this divergence and of wind. Here, we have to give particular attention to the northwest coast, because during the peak summer monsoon months (July and August), along the northwest coast of India, the surface mass transport due to the wind stress is not favorable for upwelling but the horizontal divergence due to the surface currents is conducive to upwelling. Hence, unless the wind changes, the horizontal divergence acts as the driving force for observed upwelling in the near surface level along the northwest coast during July and August. But the strong onshore surface mass transport due to the wind stress inhibits the excursion of upwelled water to the surface level during this period, along the northwest coast. This is the explanation for the vertical ceiling of upwelling along the northwest coast compared with the southwest.

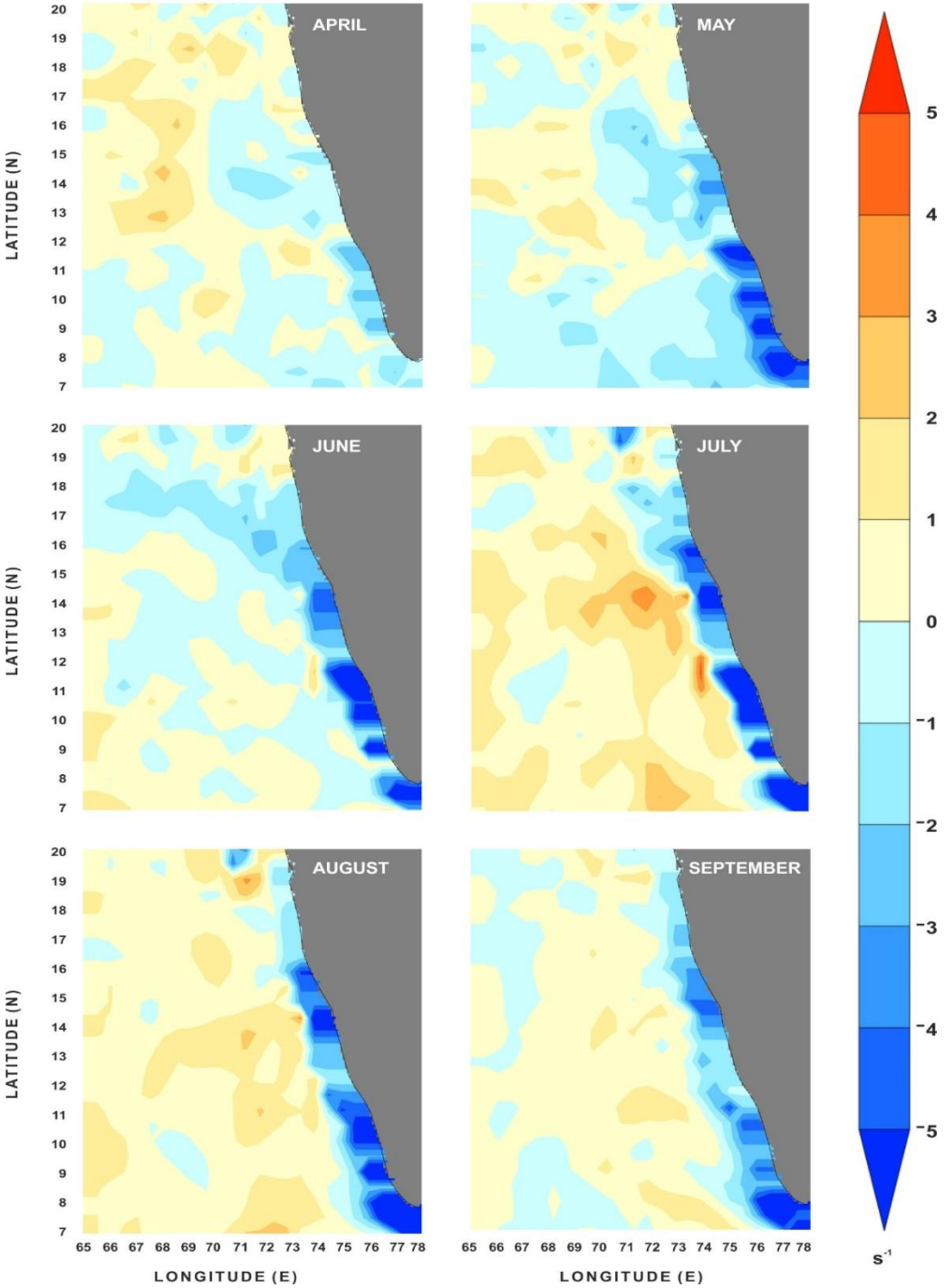

Fig. 3.9: Climatology of surface horizontal divergence ($\times 10^{-7}$ s^{-1}) along the west coast of India from 8ºN to 20ºN during the summer monsoon.

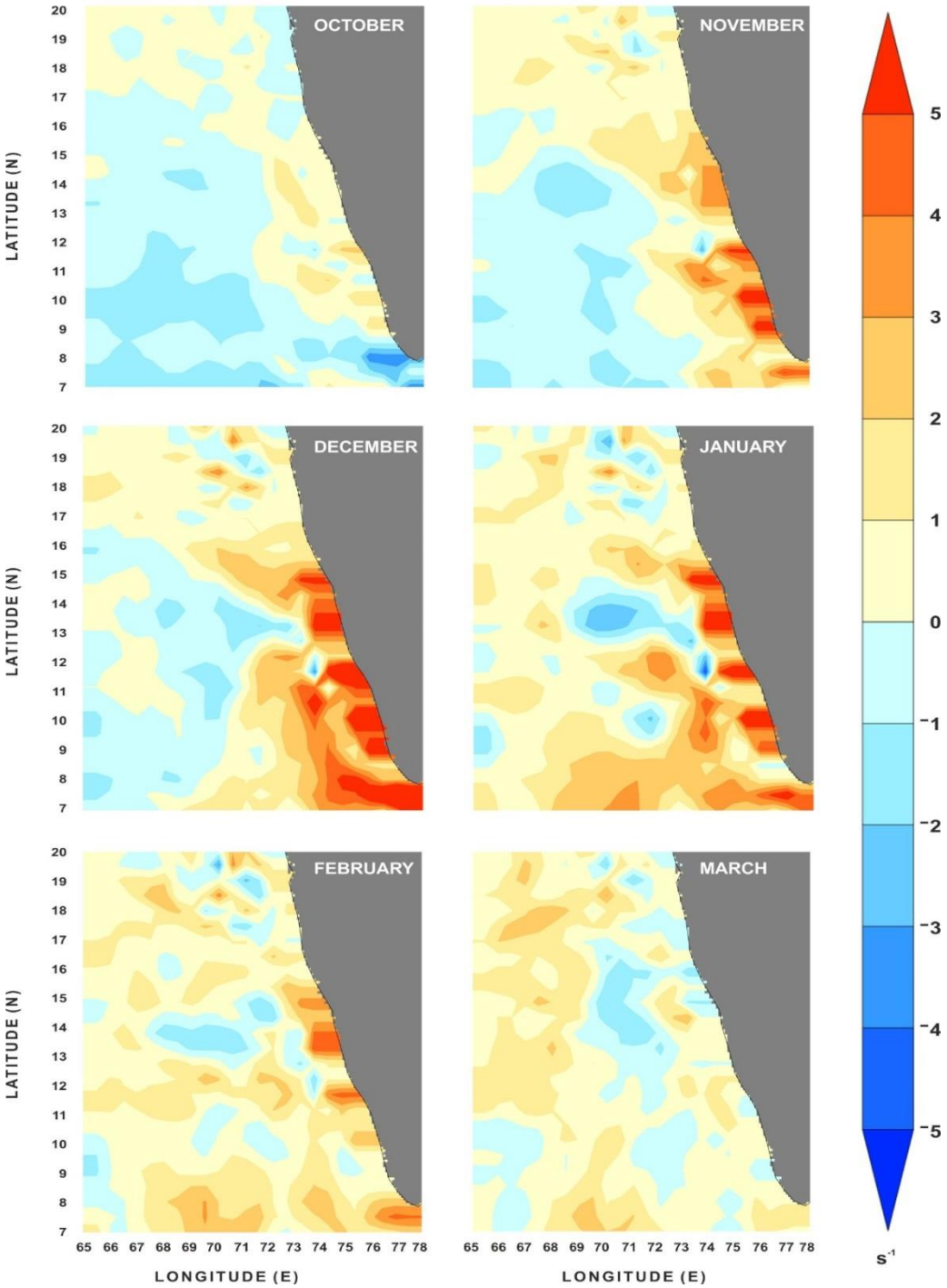

Fig.3.10: Climatology of surface horizontal divergence ($\times 10^{-7}$ s^{-1}) along the west coast of India from 8ºN to 20ºN during the northeast monsoon and winter.

The west coast of India experienced moderate-to-strong convergence during the northeast monsoon and winter (Fig.3.10). During November, December and January, strong convergence (positive values) is observed along the southwest coast from 8ºN to 14ºN and along the northwest coast, moderate convergence values are observed. The months February and March show moderate and weak convergence along the entire west coast of India. Compared with the northwest coast, the magnitude of convergence is stronger over the southwest coast. Even though the wind-induced surface mass transport does not favour downwelling along the west coast of India during the winter season, the convergence due to the surface currents does induce downwelling. This is the basis for downwelling along the west coast of India.

It can arise a question;

If the wind along the west coast of India does not support strong poleward currents and downwelling during northeast monsoon and winter, then what is the reason for strong poleward currents and convergence during this period?

The answer to this question involve remote forcing.

In Chapter 2, from the distribution of upward and downward tilt of isotherms, we have noted that upwelling and downwelling along the west coast of India have an offshore extension of 3º to 5º away from the coast. Antony et al. (2002) have similar observations on the offshore extension of upwelling. They argued that if upwelling and downwelling along the west coast of India were due only to the local forcing, then it would not have any offshore extension and must be limited to the shelf width. Their study also concluded that the offshore extension of upwelling was due to the penetration of Rossby waves by the coastally-trapped propagation of Kelvin waves. Several studies on the coastal circulation over the north Indian Ocean also reported the propagation of

coastally-trapped Kelvin waves along the east and west coasts of India (McCreary et al., 1993; Shankar et al., 2002, Vialard et al., 2009).

Here we introduce the second part of this chapter, explaining first the materials and methods adopted.

3.4 Materials and Methods – 2

In the present study, the lack of high temporal resolution oceanographic and atmospheric data sets creates some problems for describing the presence and propagation of coastally-trapped waves. We have to find novel methods for using the remote-sensing data sets. The first requirement is to become familiar with Kelvin waves.

Kelvin waves are a special type of gravity waves, constrained by Earth's rotation that may be trapped at the Equator or along vertical boundaries such as coastlines or mountain ranges. The existence of Kelvin waves depends on (a) gravity and stable stratification for sustaining a gravitational oscillation (b) significant Coriolis acceleration (c) presence of vertical boundaries ηor the Equator (Wang. 2002).

The basic dynamics of Kelvin waves are the same as for Poincare waves and are explained below. The special form of cross shore and alongshore momentum equations, without considering the viscous forces, over the west coast of India are given by equations (3.10) & (3.11)

$$\frac{\partial u}{\partial t} = -g\frac{\partial \eta}{\partial x} + fv \quad \text{..... (3.10)}$$

$$\frac{\partial v}{\partial t} = -g\frac{\partial \eta}{\partial y} - fu \quad \text{..... (3.11)}$$

where u is the cross shore component of velocity, v is the alongshore component of velocity, g is acceleration due to gravity, η is the sea surface elevation and f is the Coriolis parameter.

Rearranging the equation (3.10) & (3.11)

$$\frac{\partial u}{\partial t} - fv = -g\frac{\partial \eta}{\partial x} \quad \text{..... (3.12)}$$

$$\frac{\partial v}{\partial t} + fu = -g\frac{\partial \eta}{\partial y} \quad \text{..... (3.13)}$$

For the coastally-trapped Kelvin wave along the west coast of India, we need a solution such that velocity into the wall (cross shore component of velocity) is identically zero everywhere, such that $u=0$.

Then, equations (3.12) & (3.13) will become

$$-fv = -g\frac{\partial \eta}{\partial x} \quad \text{..... (3.14)}$$

$$\frac{\partial v}{\partial t} = -g\frac{\partial \eta}{\partial y} \quad \text{..... (3.15)}$$

From equations (3.14) & (3.15), it is clear that the cross-shore momentum balance is geostrophic, whereas the alongshore momentum balance is the same as that for shallow water gravity waves.

Then the solution to the sea surface elevation will become;

$$\eta = \eta o \exp(x/L)\cos(ky - \omega t) \quad \text{..... (3.16)}$$

where x the is distance in the offshore direction (between longitudes), L is the Rossby radius of deformation which determines the offshore limit of coastally-trapped Kelvin waves, k is the wave number and ω is the angular frequency of the propagating Kelvin wave. The equation (3.16) also indicates the unidirectional poleward propagation of Kelvin waves at the eastern boundaries of ocean in the northern hemisphere. These waves propagate cyclonically around the boundaries of the ocean in the northern hemisphere.

The wave amplitude decays offshore with scale equal to the Rossby radius of deformation (L) and it can be computed as,

$$L = \frac{c}{f} \quad \text{..... (3.17)}$$

Where c is the coastally-trapped wave velocity along the vertical boundary. Here we can calculate the first baroclinic velocity of the wave using the concept of baroclinic radius of deformation. The baroclinic radius of deformation is the length scale up to which the geostrophic balance exists in a flow. Considering the circulation in continental shelf waters, this baroclinic radius is limited in the vicinity of shelf width (Antony et.al., 2002). Since the cross shore momentum balance of a coastally-trapped Kelvin wave is geostrophic, we can assume that the Rossby radius of deformation of a coastally-trapped Kelvin wave is equal to the baroclinic radius of deformation on the shelf;

$$L = R_{bc} \quad \text{..... (3.18)}$$

Baroclinic radius of deformation can be calculated using,

$$R_{bc} = \frac{1}{f}\sqrt{\frac{g(\rho_2 - \rho_1)d}{\rho_2}} \quad \text{..... (3.19)}$$

where ρ_1 and ρ_2 are densities of upper and lower layers of water and d is the depth of water column.

We can also download the baroclinic radius of deformation along the west coast of India from the global atlas of first baroclinic Rossby radius of deformation and gravity wave phase speed published by Chelton et al. (1998). By applying equation (3.19) in (3.18) and substituting the values of baroclinic radius of deformation we can easily deduce the first baroclinic wave velocity along the west coast of India.

Describing the offshore penetration of Rossby waves at 15ºN along the west coast of India Vialard et al. (2009) explained the linear wave theory. According to this theory, every particular latitude has a critical period.

$$P_{cr} = \frac{4\pi y}{c}. \quad \text{..... (3.20)}$$

where c is the velocity of first baroclinic mode Kelvin wave and *y* is the latitude. Coastal Kelvin waves with period $P > P_{cr}$ radiate offshore as Rossby waves and those with $P < Pcr$ will remain coastally-trapped.

From equation (3.20), we can deduce the critical period for different latitudes along the west coast of India. The values of baroclinic radius, first baroclinic velocity and critical period along the west coast of India are represented in Table 3.4.

Table 3.4: Baroclinic radius, Baroclinic velocity and Critical period of Kelvin wave along the west coast of India.

Latitude (ºN)	Baroclinic radius(Km)	Baroclinic velocity(m/s)	Critical Period(days)
8	116.0	2.47	49
10	90.0	2.39	61
12	70.0	2.30	74
14	69.0	2.52	86
16	54.0	2.40	98
18	53.0	2.50	111
20	50.0	2.60	123

From Table 3.4 it is clear that the baroclinic radius of deformation along the west coast of India decreases from 116 km at 8ºN to 50 km at 20ºN, while

the critical period shows an increasing trend from south to north. The values of critical period range between 49 days at 8ºN to 123 days at 20ºN. Based on the above information on critical period we have tried to capture the characteristics of Kelvin waves along the west coast of India using Advanced Scatterometer (ASCAT) daily wind and daily SSHA data. To check the impact of wind blowing over the entire north Indian Ocean on the sea surface height variability along the west coast of India due to generation of boundary-trapped Kelvin waves, initially we band pass both data sets in 49 to 123 day band using a Lanczos filter. Then we make a lag correlation between zonal winds over the entire north Indian Ocean and selected box-averaged values of SSHA along the west coast of India as following the approach of Vialard et al. (2009) and Gopalakrishna et al. (2006).

3.5 Results and Discussion – 2

Fig. 3.11 represents the contour-filled plots of spatial correlation (95% confidence level) between box-averaged SSHA at the southern tip of west coast of India and zonal wind over the entire north Indian Ocean. The SSHA is averaged over 8ºN to 9ºN and 76ºE to 77ºE. From Fig. 3.11(a) to Fig. 3.11(f), it is evident that a significant positive correlation exists over the eastern equatorial Indian Ocean from 32 to 52 days lag. After 52 days this correlation diminished over the equatorial region. This indicate the impact of zonal winds blowing over the equatorial Indian Ocean on the SSHA along the west coast of India by the propagation of Kelvin waves.

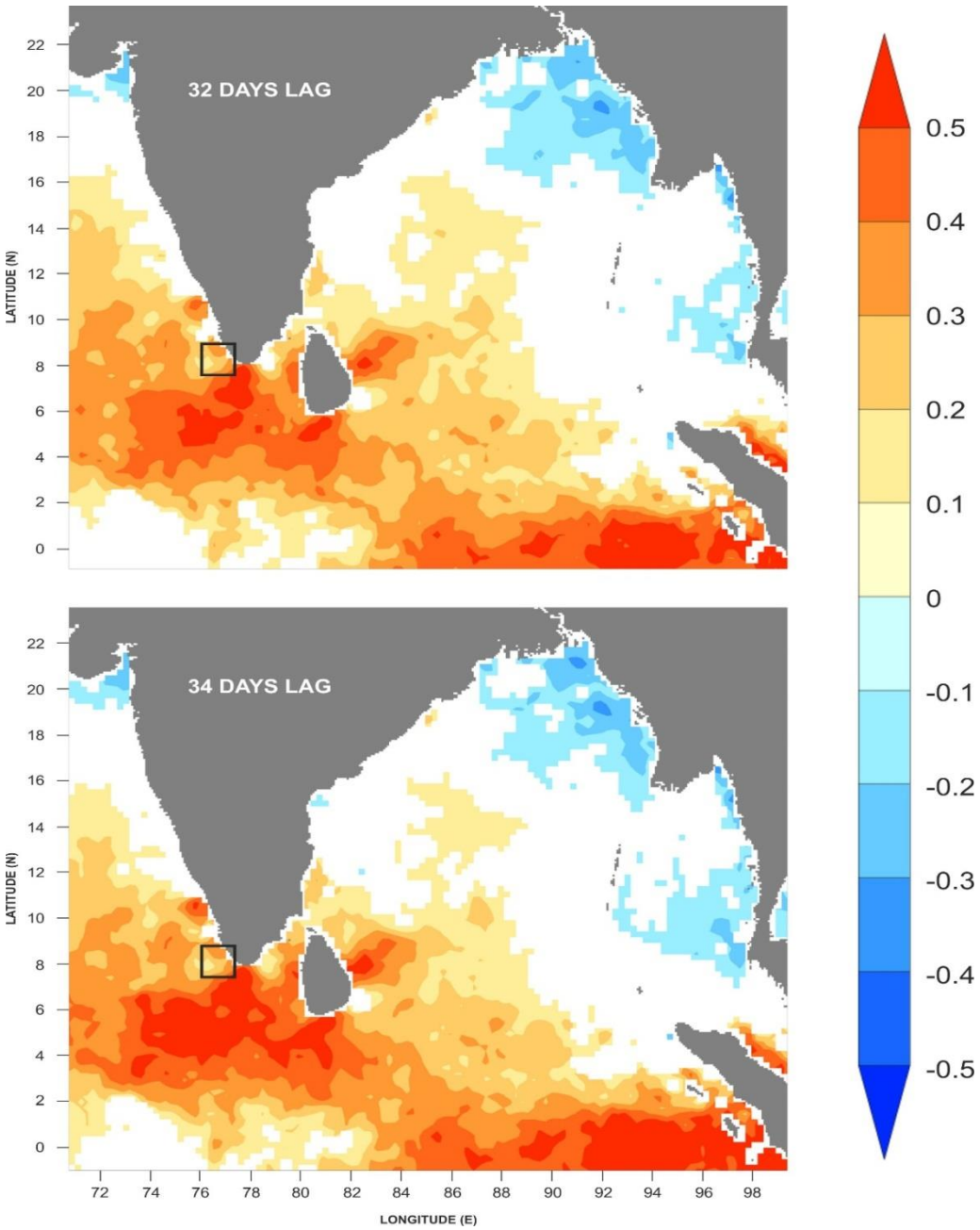

Fig. 3.11(a): Lag correlation (32-34) days between SSHA in the coastal box [7.5ºN: 8.5ºN and 76ºE: 77.5ºE] and zonal wind over the rest of the basin.

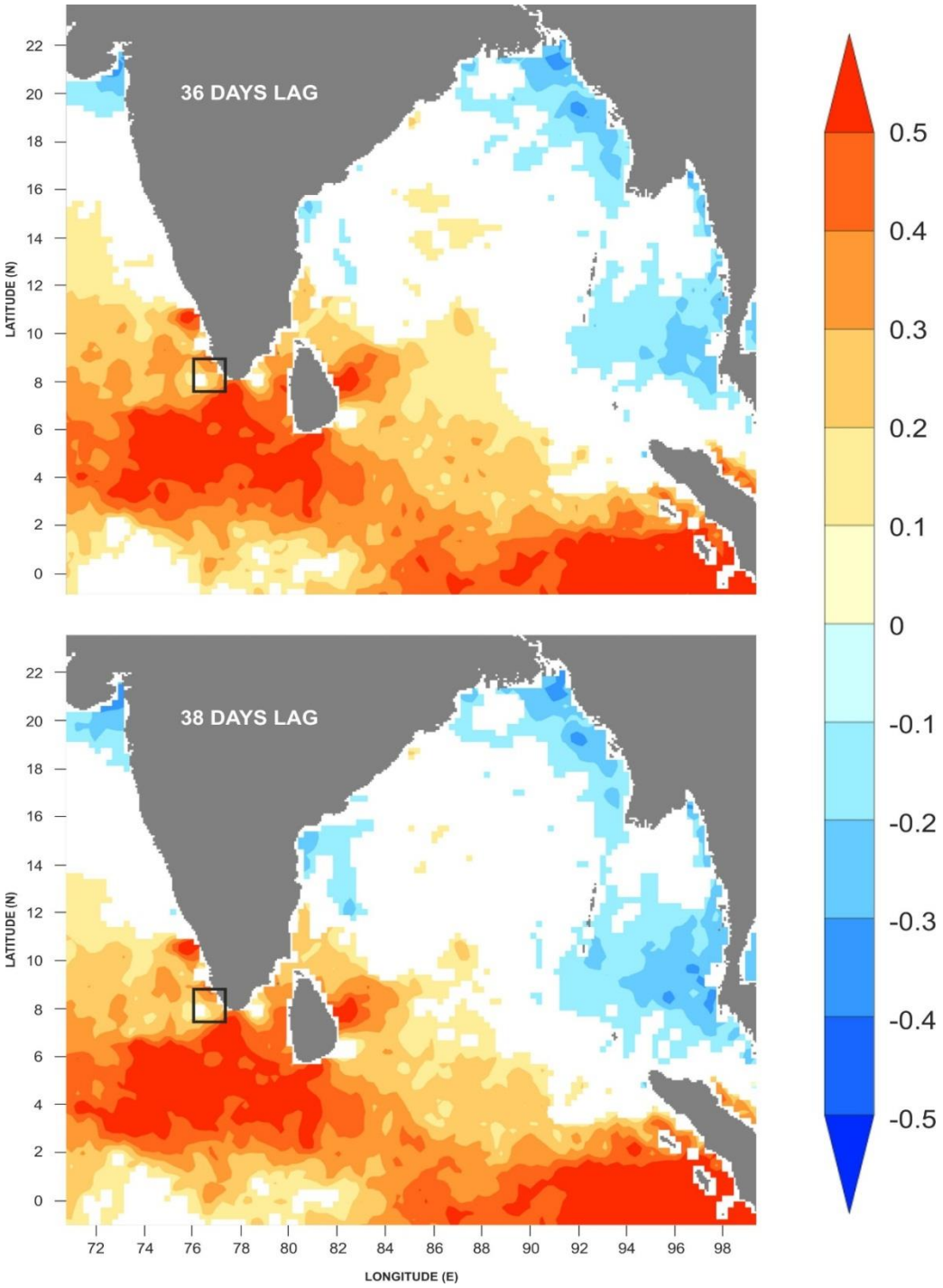

Fig. 3.11(b): Lag correlation (36-38) days between SSHA in the coastal box [7.5ºN: 8.5ºN and 76ºE: 77.5ºE] and zonal wind over the rest of the basin.

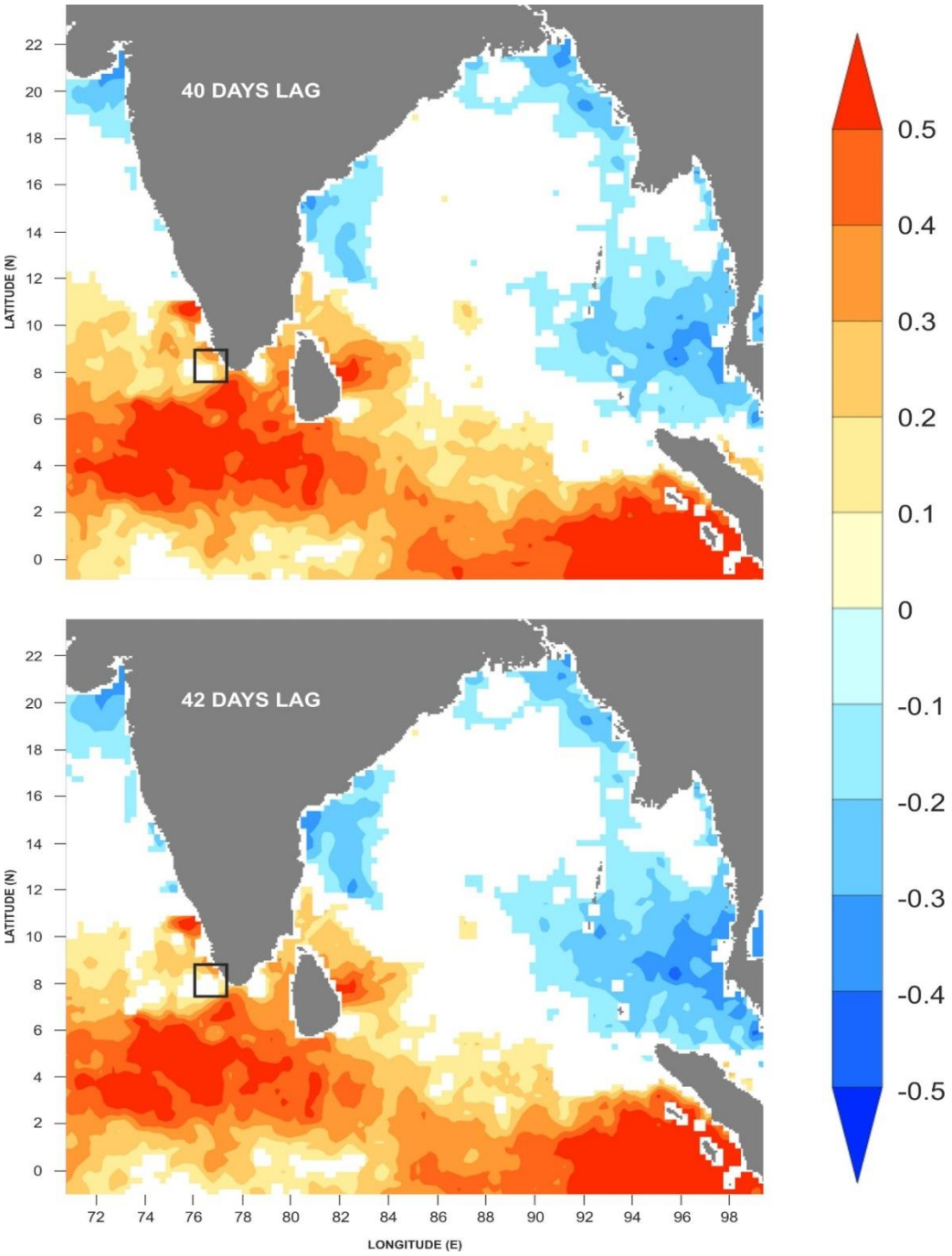

Fig. 3.11(c): Lag correlation (40-42) days between SSHA in the coastal box [7.5ºN: 8.5ºN and 76ºE: 77.5ºE] and zonal wind over the rest of the basin.

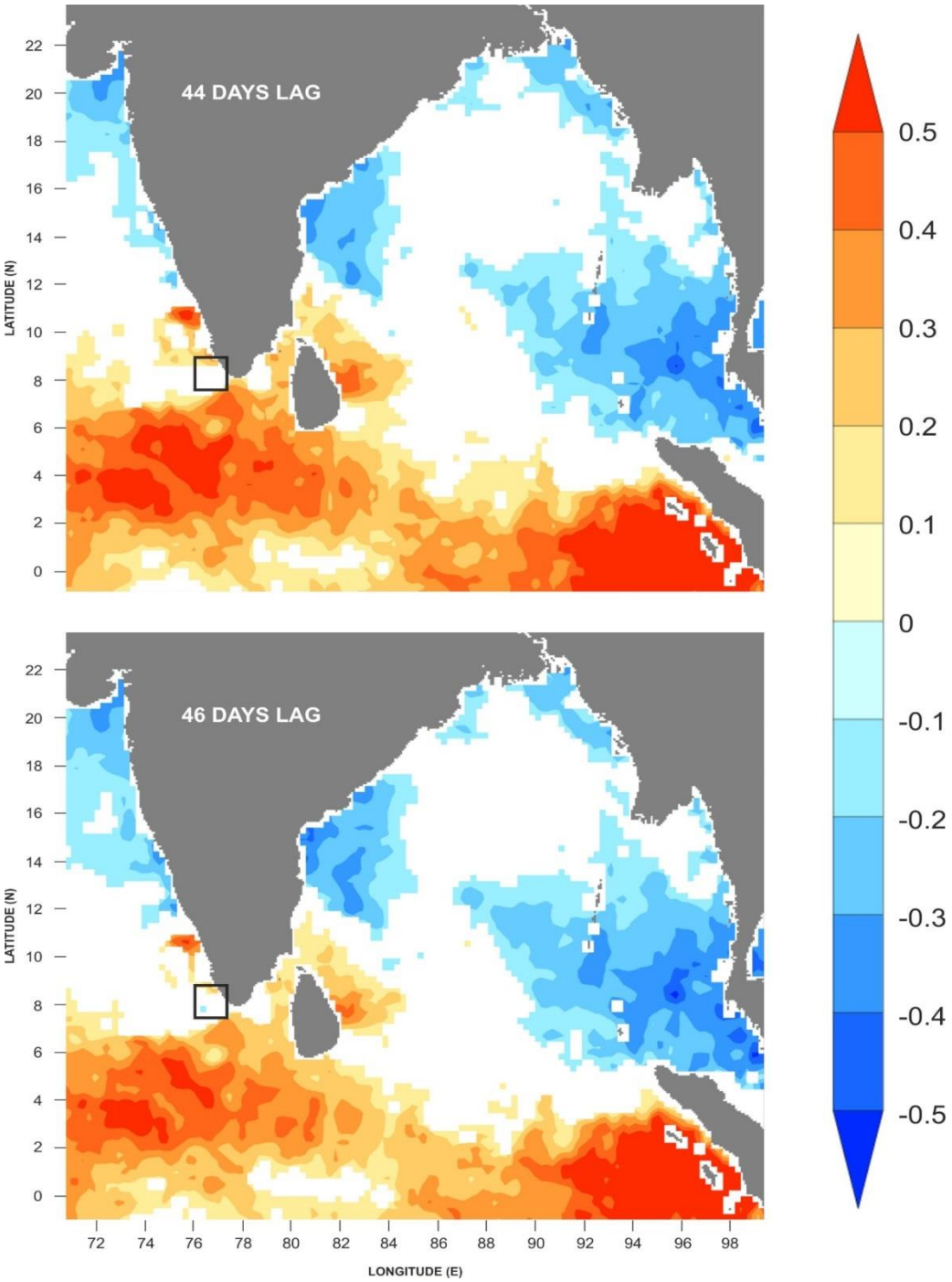

Fig. 3.11(d): Lag correlation (44-46) days between SSHA in the coastal box [7.5ºN: 8.5ºN and 76ºE: 77.5ºE] and zonal wind over the rest of the basin.

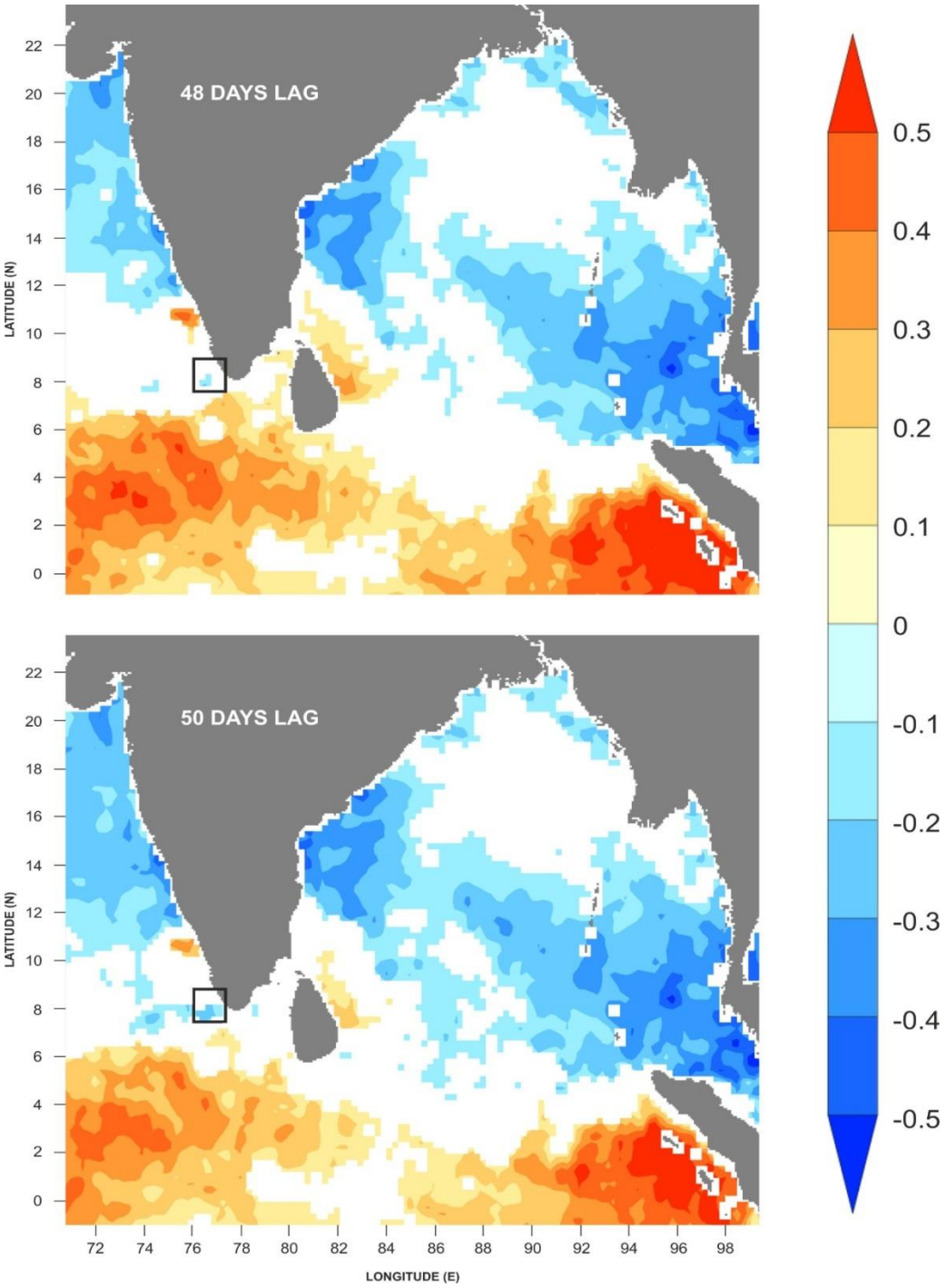

Fig. 3.11(e): Lag correlation (48-50) days between SSHA in the coastal box [7.5ºN: 8.5ºN and 76ºE: 77.5ºE] and zonal wind over the rest of the basin.

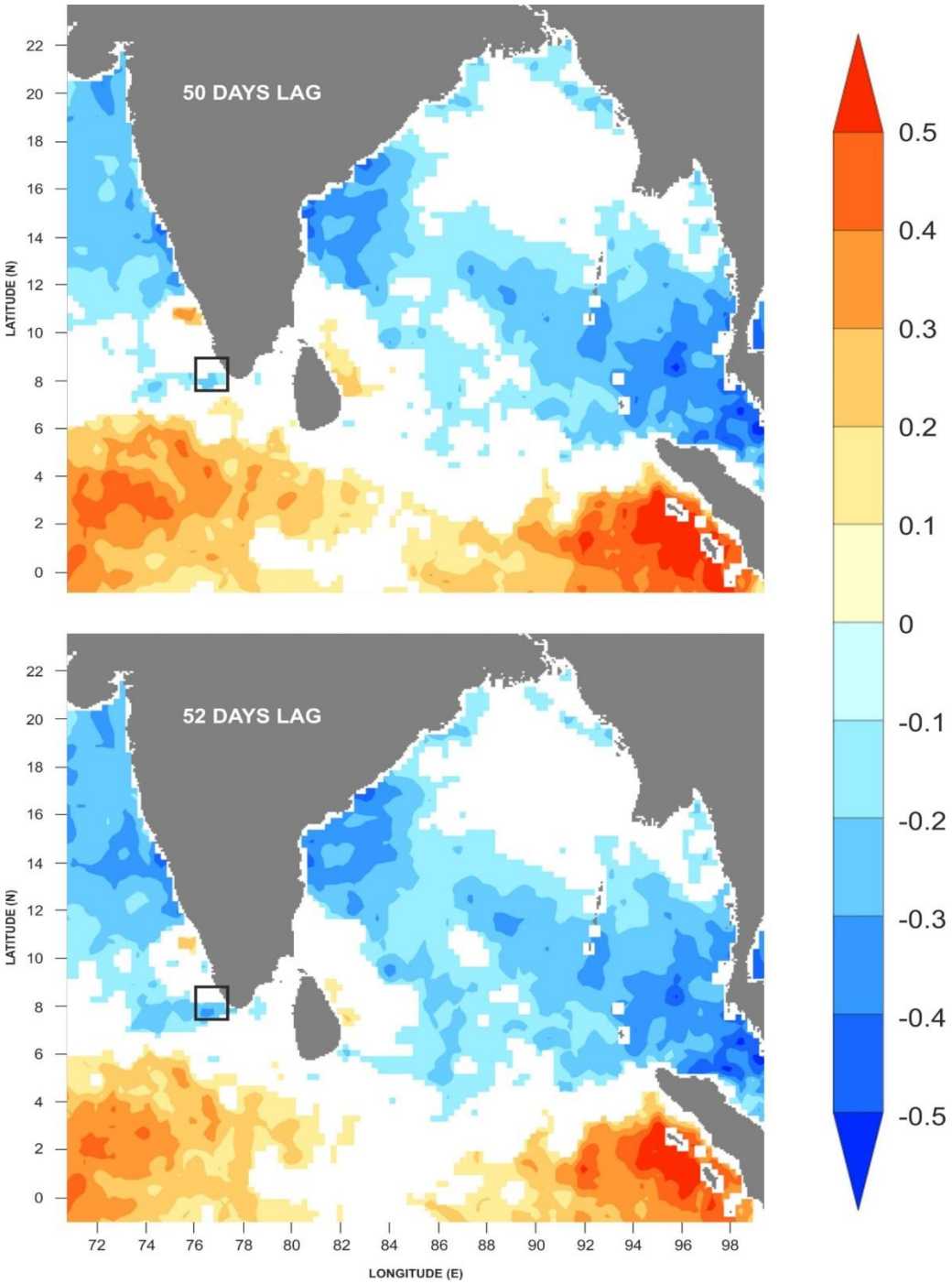

Fig. 3.11(f): Lag correlation (50-52) days between SSHA in the coastal box [7.5ºN: 8.5ºN and 76ºE: 77.5ºE] and zonal wind over the rest of the basin.

To know the periods of the westerlies (positive) and easterlies (negative), Hovmoller diagrams of zonal winds are generated over the equatorial Indian from 1ºS to 1ºN following Rao et al. (2009). From the Hovmoller diagram (Fig. 3.12), it is clear that westerly winds blow during October to December and April to May. Easterlies and weak westerlies are blowing July to September over the eastern rim of Equator. During January to March weak westerlies are prevailing over the equatorial Indian Ocean.

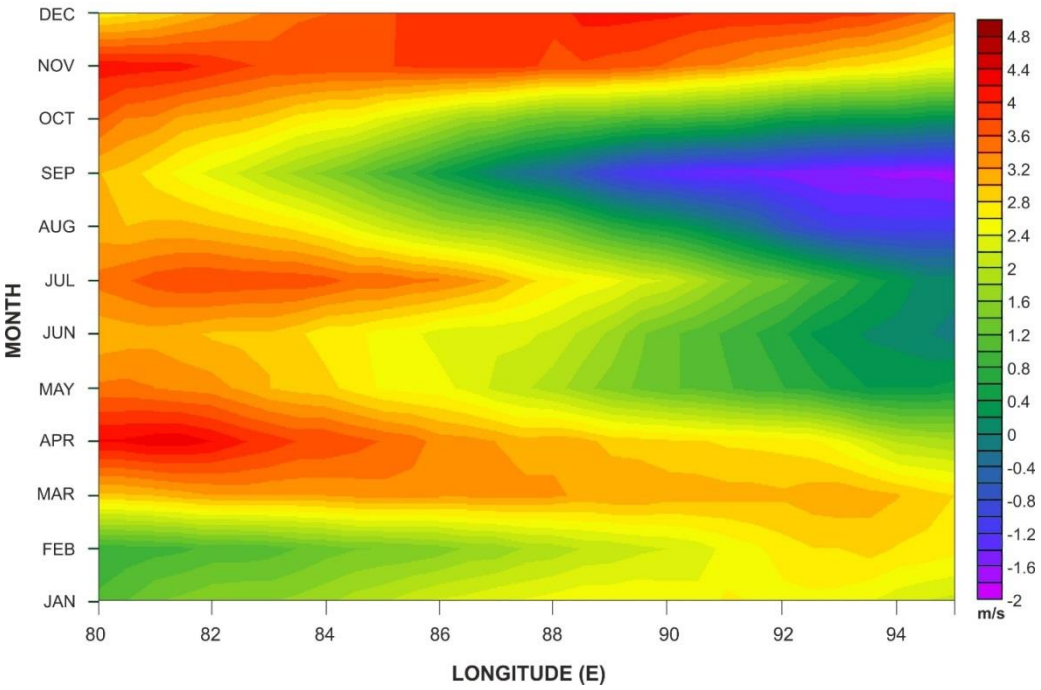

Fig. 3.12: Hovmoller diagram of zonal wind (m/s) over the eastern equatorial Indian Ocean (Climatology).

The correlation between SSHA and zonal wind is positive only when both parameters has same sign and strong correlation was observed if both has proportional change in magnitude. But it is also known that during January and February, SSHA has strong positive values over the west coast of India and wind has weak positive values over the equator (Fig. 2.11 and Fig. 3.12).

During April to June, wind has positive values over the Equator but SSHA has negative values over the west coast of India. From July to September, both wind over the equator and SSHA along the west coast of India have negative signs. During October to December both wind and SSHA have positive values. Hence we can assert that the significant positive correlation shown in Fig. 3.11(a) to Fig. 3.11(f) is possible only from July to December. To track the Kelvin wave signals carried over the coastal belt of north Indian Ocean from the Equator, sea surface height anomaly over the entire Indian Ocean from June to December was used. Fig. 3.13 shows the SSHA over the north Indian Ocean during June to September.

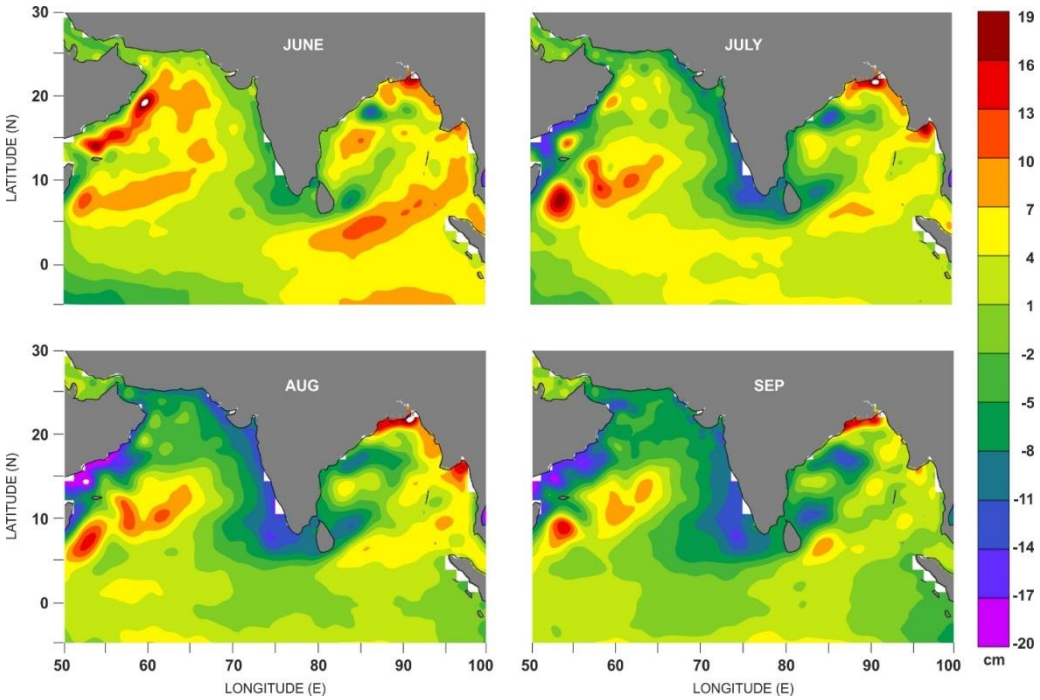

Fig. 3.13: Climatology SSHA (cm) over the north Indian Ocean during June to September.

In this figure we do not see any propagating signals of SSHA from the Equator and coastal wave guides of Bay of Bengal to the Arabian Sea. But from October to December we are see a propagation of positive SSHA from the wave guides of equator and Bay of Bengal to the west coast of India (Fig. 3.14(a) to Fig. 3.14(b). From this observation we can conclude that Kelvin waves from the Equator and Bay of Bengal reach Arabian Sea only during the northeast monsoon and winter. This downwelling Kelvin wave is the reason for downwelling along the west coast of India during winter and northeast monsoon, even when the wind is not supporting downwelling.

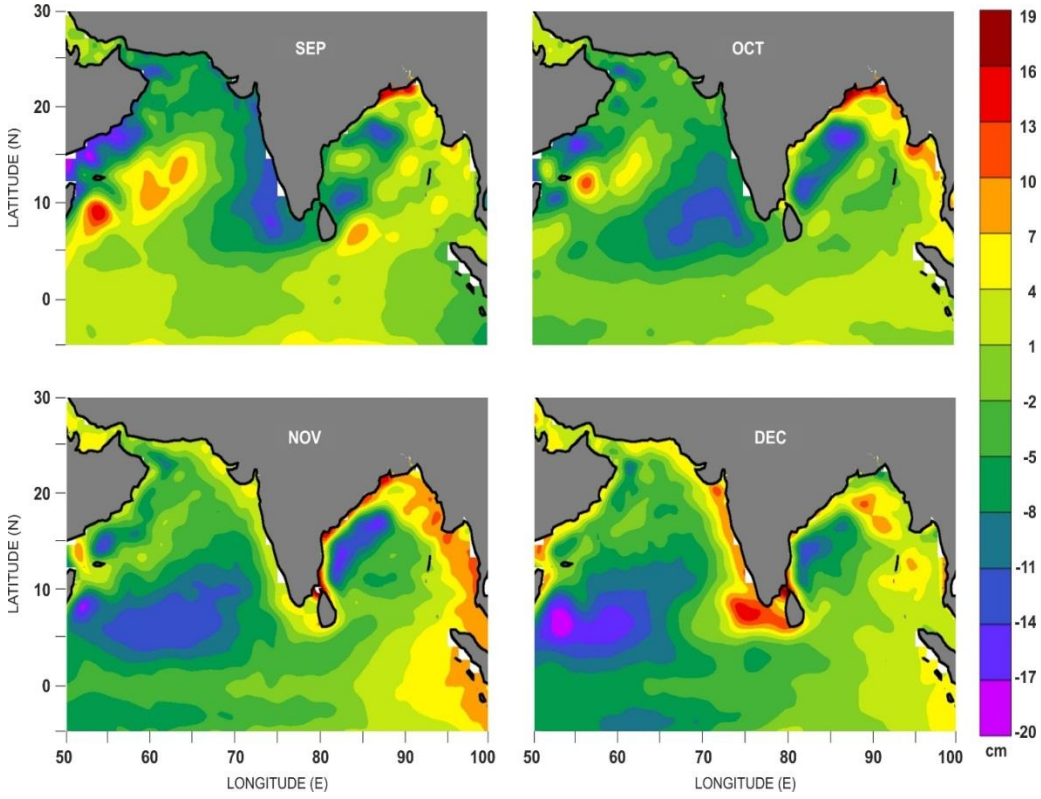

Fig. 3.14(a): Climatology of SSHA (cm) over the north Indian Ocean during September to December [propagation of Kelvin waves along the coastal wave guides of Bay of Bengal and reaches the west coast of India during December].

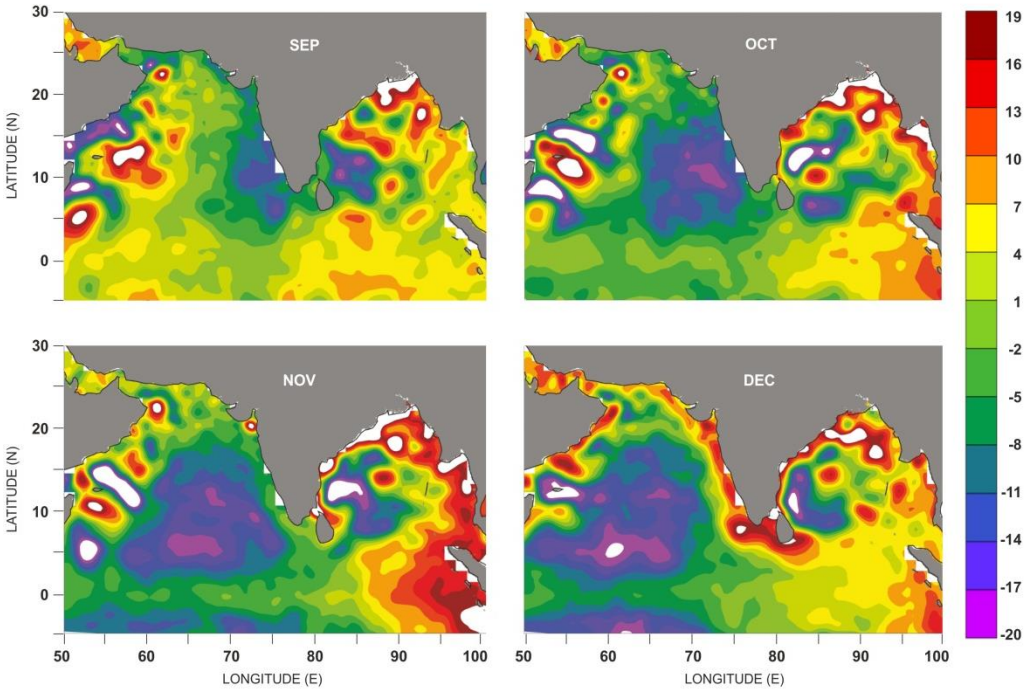

Fig. 3.14(b): SSHA (cm) over the north Indian Ocean during December to January for the year 1998 [characterized by propagation of Kelvin waves along the coastal wave guides of Bay of Bengal and reaches the west coast of India during December].

From Fig. 3.15(a) to Fig. 3.15(d), a significant negative correlation was also observed at the southern tip of India and over the Gulf of Mannar region with 8 to 12 days lag. Here the SSHA is averaged over 14ºN to 15ºN and 73.5ºE to 74.5ºE. From the Fig.3.16, it was also clear that a negative SSHA (upwelling mode of Kelvin wave) propagated from the southern tip to the entire west coast of India during July and August. This upwelling Kelvin wave is the reason for mild upwelling on the northwest coast of India during July and August even though wind is not favorable.

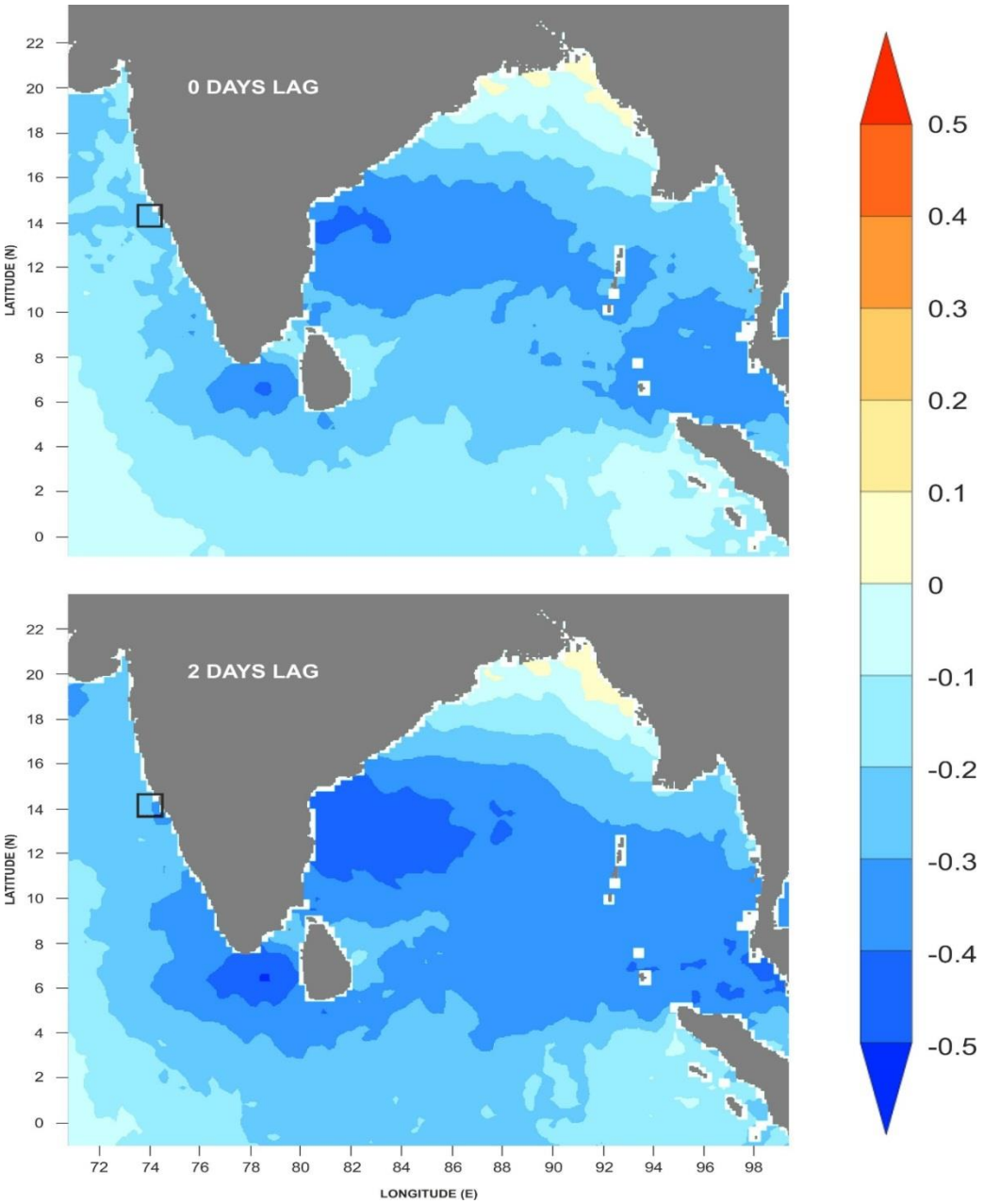

Fig. 3.15(a): Lag correlation (0-2) days between SSHA in the coastal box [14ºN: 15ºN and 73.5ºE: 74.5ºE] and zonal wind over the rest of the basin.

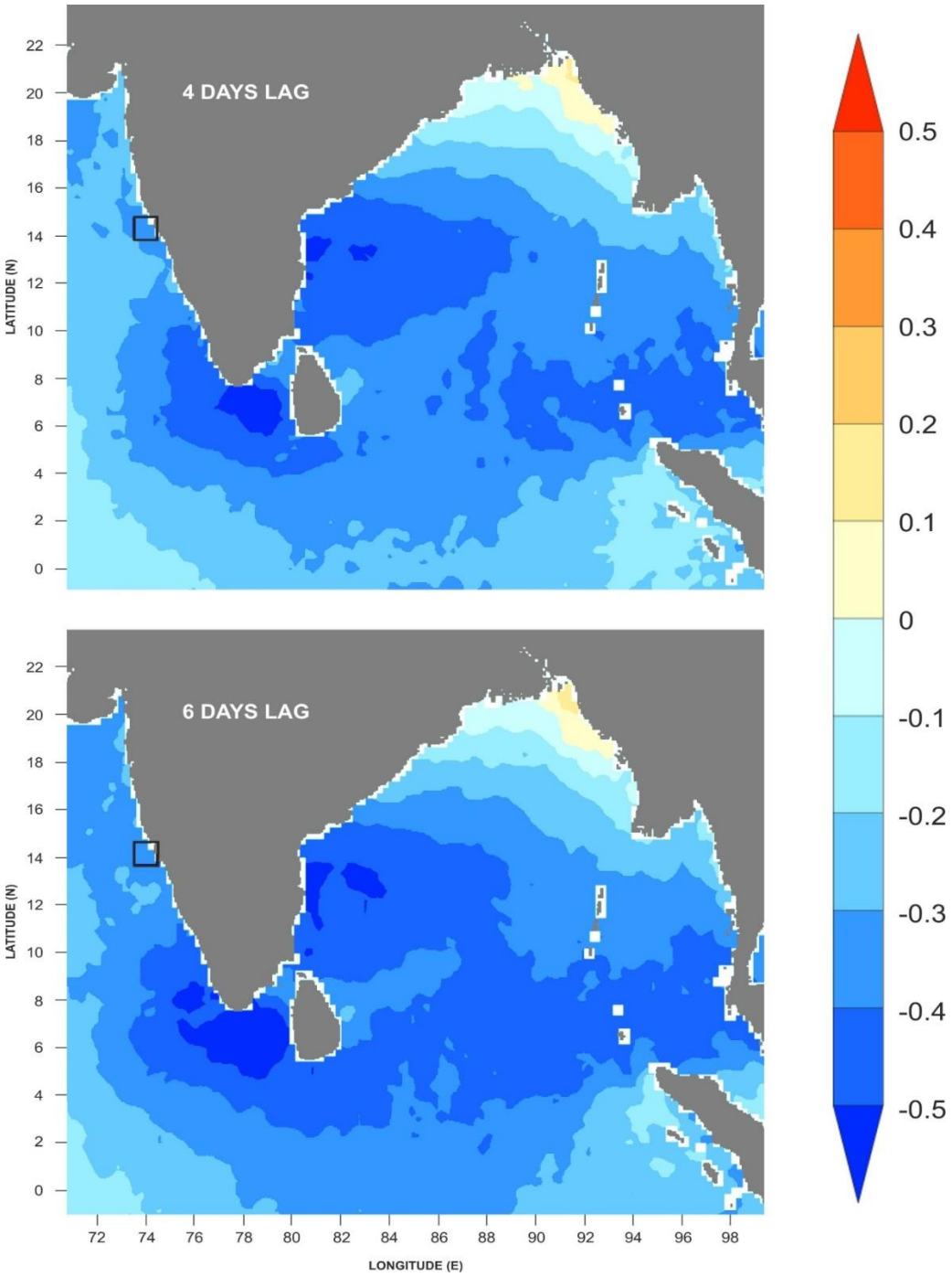

Fig. 3.15(b): Lag correlation (4-6) days between SSHA in the coastal box [14ºN: 15ºN and 73.5ºE: 74.5ºE] and zonal wind over the rest of the basin.

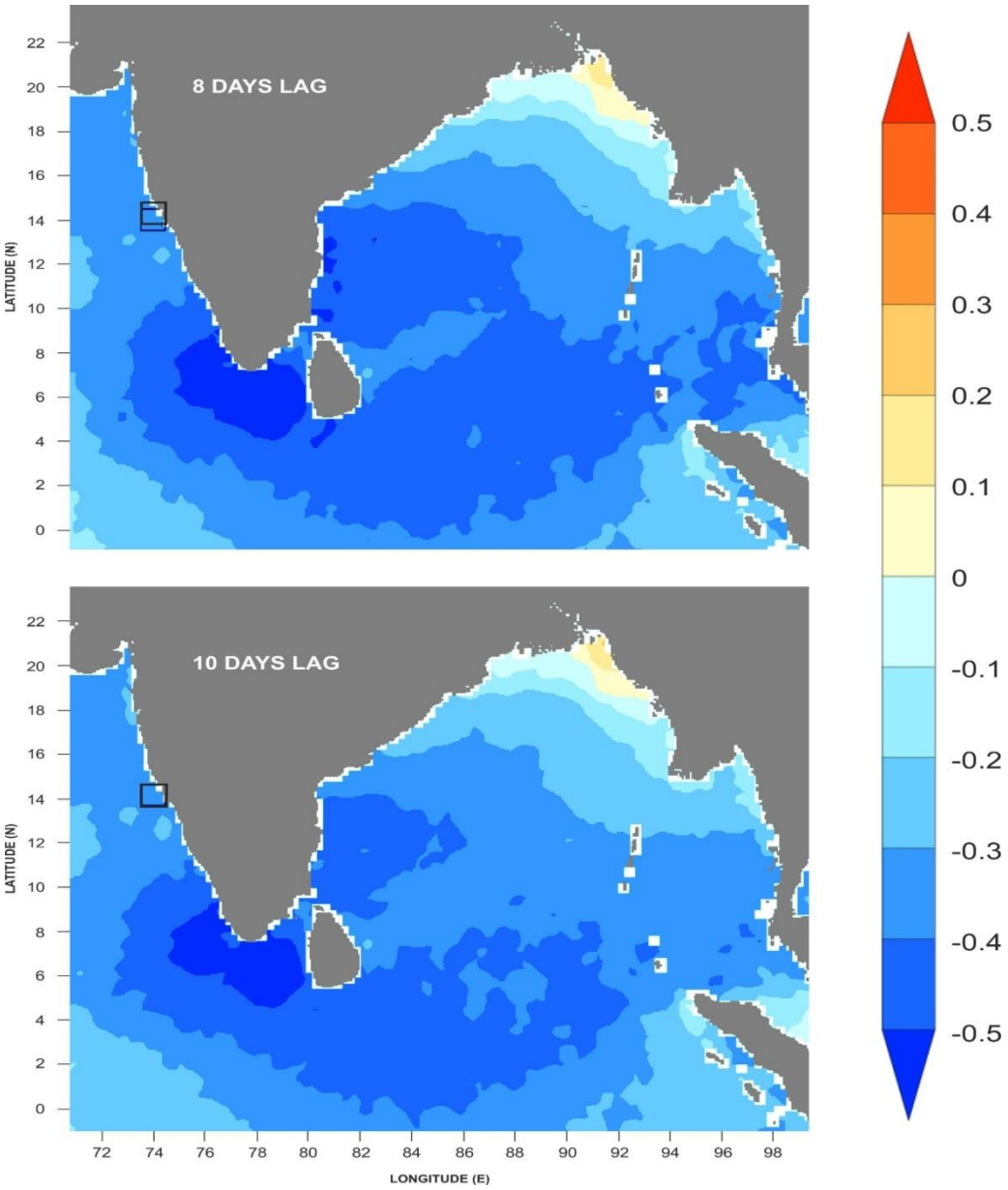

Fig. 3.15(c): Lag correlation (8-10) days between SSHA in the coastal box [14ºN: 15ºN and 73.5ºE: 74.5ºE] and zonal wind over the rest of the basin.

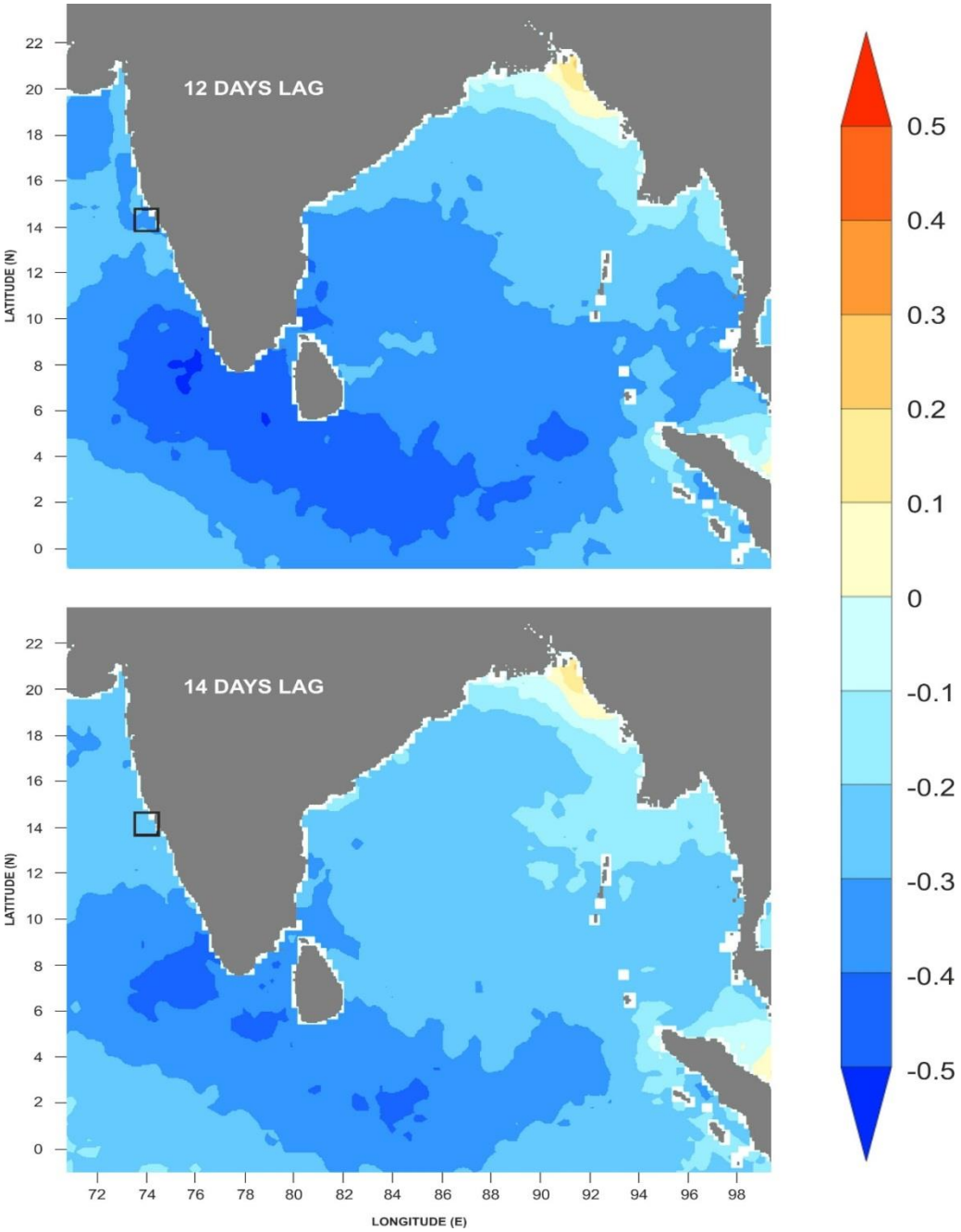

Fig. 3.15(d): Lag correlation (12-14) days between SSHA in the coastal box [14ºN: 15ºN and 73.5ºE: 74.5ºE] and zonal wind over the rest of the basin.

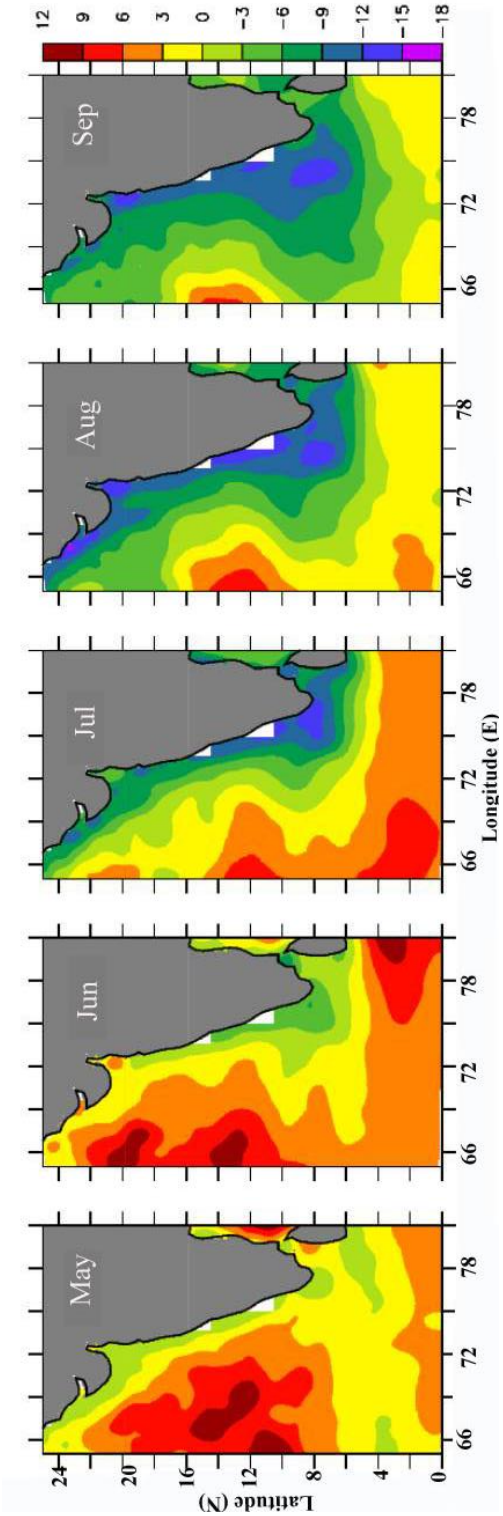

Fig. 3.16: SSHA (cm) over the west coast of India during the summer monsoon [propagation of SSHA from the Gulf of Mannar region to west coast of India is clearly visible].

3.6 Conclusion

From the analysis of wind-induced surface mass transport, wind vectors, surface currents, horizontal divergence and based on the calculations and interpretations on coastally-trapped Kelvin waves, it is concluded that, during May and September the upwelling along the entire west coast of India is due to the wind-induced surface Ekman mass transport and due to the horizontal divergence of current. From June to August, the upwelling along the southwest coast of India is mainly driven by surface Ekman mass transport, horizontal divergence due to the surface currents and coastally-trapped Kelvin waves from the Gulf of Mannar, while upwelling along the northwest coast is completely driven by coastally-trapped Kelvin waves and weak divergence of currents during this period. The downwelling along the entire west coast is completely driven by the convergence due to the surface currents and Kelvin waves from the equator and Bay of Bengal. Along the west coast of India, the downwelling-favorable Kelvin waves come from the equator and upwelling-favorable Kelvin waves come from the southern tip of India and the Gulf of Mannar region.

.....ꕥ.....

Chapter 4

INTER ANNUAL VARIABILITY AND INFLUENCE OF IOD EVENTS ON UPWELLING AND DOWNWELLING

Contents

4.1 Introduction

El-Niño Southern Oscillation (ENSO) and Indian Ocean Dipole (IOD) are the two major climatic phenomena affecting the tropical ocean. Several previous studies have discussed the impact of these climatic events on the atmosphere over the north Indian Ocean, as well as on the ocean dynamics. This chapter deals mainly with the impact of IOD and ENSO on upwelling and downwelling along the west coast of India.

Bakun et al. (2015) revealed that coastal upwelling ecosystem productivity is threatened by climate change around the world ocean. Tim et al. (2015) studied the impact of ENSO on Benguela upwelling system. Even though ENSO is rooted in the tropical Pacific, several studies have shown the influence of ENSO on the interannual variability of surface warming in the Indian Ocean through remote effects (Nicholls, 1989; Tourre and White, 1995; Meyers, 1996; Tourre and White, 1997; Chambers et al., 1999; Behera et al., 2000; Venzke et al., 2000;

Yoo et al., 2010). Based on the expanded satellite database information and from the analysis of Ocean General Circulation Model (OGCM) simulations, Rao et al. (2002) studied the interannual variability of the subsurface tropical Indian Ocean and concluded that in contrast to the ENSO-dominated SST variability, the subsurface variability of the tropical Indian Ocean is governed mainly by the IOD.

The study of Gnanaseelan and Vaid (2010) revealed the influence of IOD on the Indian Ocean warming in the context of planetary wave propagation. Studies on the 1997-1998 IOD events revealed the overcooling and enhanced anomalous state of prevailing atmosphere over the eastern Indian Ocean during the co-occurrence of El-Niño and positive IOD years (Yu and Reinecker, 1999; Webster et al., 1999; Murtugudde et al., 2000). Some observational and modelling studies dealt with the wind and surface current variability over the north Indian Ocean and along the Equator (Webster at al., 1999; Brown et al., 2008; Nagura and McPhaden., 2010). They revealed the reversal of zonal currents along the Equator during IOD events. Rao et al. (2009) reported that during positive IOD years the propagation of downwelling Kelvin waves along the Equator and the coastal wave guides of north Indian Ocean fade out during October to December. It was also revealed that during the positive IOD years, along the Equator, westerly winds are replaced by easterly and vice versa. Various previous studies discussed the modulation of atmospheric meridional circulation and Indian summer monsoon rainfall over the north Indian Ocean during IOD events (Behera et al., 1999; Ashok et al., 2001; Guan et al., 2003; Li et al., 2003; Lau and Nath., 2004; Gadgil et al., 2003, 2004). Ashok et al. 2004 reported the influence of western pole of IOD on the rainfall over the northwest provinces of India. Their study also revealed that during the co-occurring years, IOD significantly reduces the impact of ENSO on Indian

summer monsoon rainfall. Studies of Sumesh and Ramesh Kumar, 2013 revealed that cyclogenesis over the north Indian Ocean is influenced ENSO and IOD.

Previous studies clearly showed the impact of ENSO and IOD on surface and subsurface variability of Indian Ocean. Based on the above baseline information, I focused on the impact of IOD on the coastal dynamics along the west coast of India during the summer and winter monsoons. In this chapter, the main issue is the impact of climatic events on upwelling and downwelling along the west coast of India, especially during IOD years. Inter annual variability of upwelling and downwelling in the last two decades is also discussed.

According to the Japan Agency for Marine-Earth Science and Technology (JAMSTEC), we classify the years during the last two decades as IOD, El Niño and La Niña (Table 4.1).

Table 4.1: IOD, El Niño and La Niña Events during 1991-2008.

Positive IOD events	Negative IOD events	El Niño events	La Niña events
1994	1992	1991-1992	1995-1996
1997	1996	1992-1993	1998-1999**
2006	1998	1994-1995	1999-2000
2007		1997-1998*	2000-2001
2008		2002-2003	2007-2008**
		2004-2005	
		2006-2007	

Note: Bold letters represent significant (strong) positive IOD events; * represents strong El Niño year; **represents strong La Niña year.

From the above table it is evident that the years 1994, 1997 and 2006 are strong positive IOD years. The positive IOD during 1997 and 2006 co-occurred with strong El Niño events. The years 1992, 1996 and 1998 are strong negative IOD years and negative IOD during 1998 co-occurred with La Niña. The positive IOD in 2007 evolved together with La Niña, which is a very rare phenomenon that has happened only once in the available historical record.

4.2 Materials and Methods

Characteristic ocean dynamics of west coast of India during the summer and winter monsoon is dominated by reversal of west India coastal current and upwelling/downwelling phenomena. So far, there has been no integrated attempt to study interannual variability of upwelling and downwelling along west coast of India in a decade with a large number of extreme climatic events. With the advance of satellite oceanography, data available from different sensors have become a useful tool for continuous physical oceanographic analysis over large areas. Extensive use of satellite real time data for wind and SSHA was made in this study. Results of the previous chapter reveal that upwelling along the west coast of India is driven by the surface mass transport resulting from the alongshore component of wind and horizontal divergence due to the surface currents. Hence the European Remote Sensing Satellite (ERS) and QuikSCAT winds were utilized to study inter annual variability of surface mass transport from 1993 to 2008. Horizontal divergence and vertical velocity was derived from SODA currents. Monthly wind data from scatterometers onboard ERS 1 & 2 with a spatial resolution of $1^o \times 1^o$ were obtained from PO.DACC, Jet Propulsion Laboratory, for a period of 8 years from 1992 to 1999. QuikSCAT winds were used for 2000 to 2008. The spatial resolution of QuikSCAT and SODA currents were given in the previous chapter. For this chapter, to study interannual variability of upwelling, the above parameters were

averaged over the summer monsoon months from June to September. An average over the southwest and northwest coast was also made for comparison.

The previous chapter also showed that downwelling along the west coast of India is driven mainly by the propagation of Kelvin waves from equatorial Indian Ocean and its evolution depends greatly on the zonal component of wind along the Equator. The wind data available from the above sources were also used to study interannual variability of zonal component of wind along the Equator and to assess their impact on the observed SSHA variability along the Equator as well as along the west coast of India. The AVISO merged and blended SSHA from APDRC datasets were utilized to characterize the sea surface height variability. To study interannual variability of downwelling along west coast of India, the SSHA and wind were averaged from November to February for the southwest and northwest coast.

SSHA contours were produced for the east coast of Arabian Sea to trace out the Kelvin wave signals and the variability of downwelling along the coast. An average of SSHA and zonal wind component over 1ºS to 1ºN and 70ºE to 90ºE was made for each of the months of October, November and December to know the evolution and propagation of Kevin waves along the Equator (Rao et al., 2009) and colour-filled Hovmoller diagrams were plotted for 1993-2008. SODA temperature was also used to show the impact of IOD on temperature variability over the Arabian Sea.

4.3 Results and Discussion

4.3.1 Interannual variability of Sea Surface Temperature (SST)

Since the last two decades were characterized by many extreme climatic events and since these climatic events peaked during winter, SST was averaged

over the winter period to study the interannual variability and influence of these climatic events on Arabian Sea.

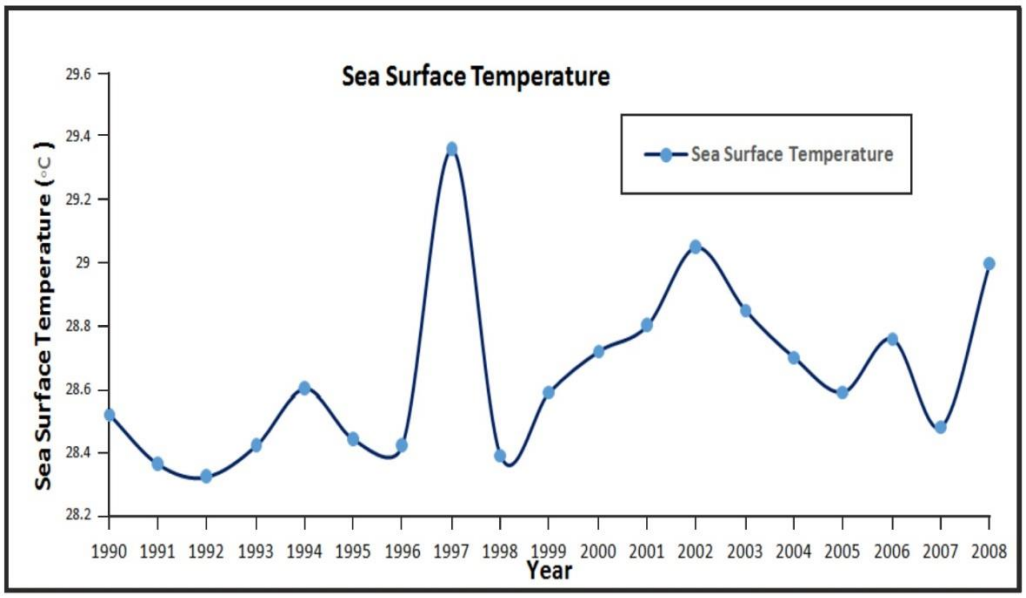

Fig. 4.1: Interannual variability of SST (°c) (averaged from November to February) over the south eastern Arabian Sea.

From Fig. 4.1, it was clear that the SST increased during the positive IOD years 1994, 1997, 2006 and 2008 over the Arabian Sea. During the El-Niño year 2002, an increase in SST was also evident. Peak value of SST was observed during 1997 and it was a strong IOD year that co-occurred with a strong El-Niño. This illustrates the impact of IOD and El-Niño on warming over the eastern Arabian Sea. Unlike the other positive IOD years, the positive IOD year 2007 shows a decrease in SST. This indicates the impact of La-Niña during this year. All the negative IOD years, 1992, 1996 and 1998 showed decreases in SST over the eastern Arabian Sea. Hence from the above analysis it was inferred that years of positive IOD, El-Niño and years with the co-occurrence of positive IOD and El-Niño, are characterized by an increase

in temperature over the eastern Arabian Sea, whereas negative IOD and La-Niña decrease the temperature over the Arabian Sea. This substantiates the results of previous studies that the climatic events IOD and ENSO have specific influence on the temperature variability over the north Indian Ocean.

4.3.2 Inter annual variability of Sea Surface Height Anomaly during summer monsoon

The observed temperature variability over the Arabian Sea during the climatic events hints at the impact of these events on the dynamics as well as on the thermodynamics there. In this chapter we focus on the variability of upwelling and downwelling along the west coast of India. For the study of interannual variability of upwelling following parameters are analysed.

Since the upwelling areas are characterised by lowering of SSHA, variability of SSHA is taken as an index for the study of inter annual variability of upwelling along the west coast of India. From Fig 4.2 and Fig. 4.3 it was obvious that, compared with the positive IOD year 1997, the west coast of India was characterized by a strong reduction in SSHA during the negative IOD year 1998. This suggests that upwelling along the west coast of India diminishes during the positive IOD years. The data on vertical velocity along the west coast of India also substantiate the results from the analysis of SSHA.

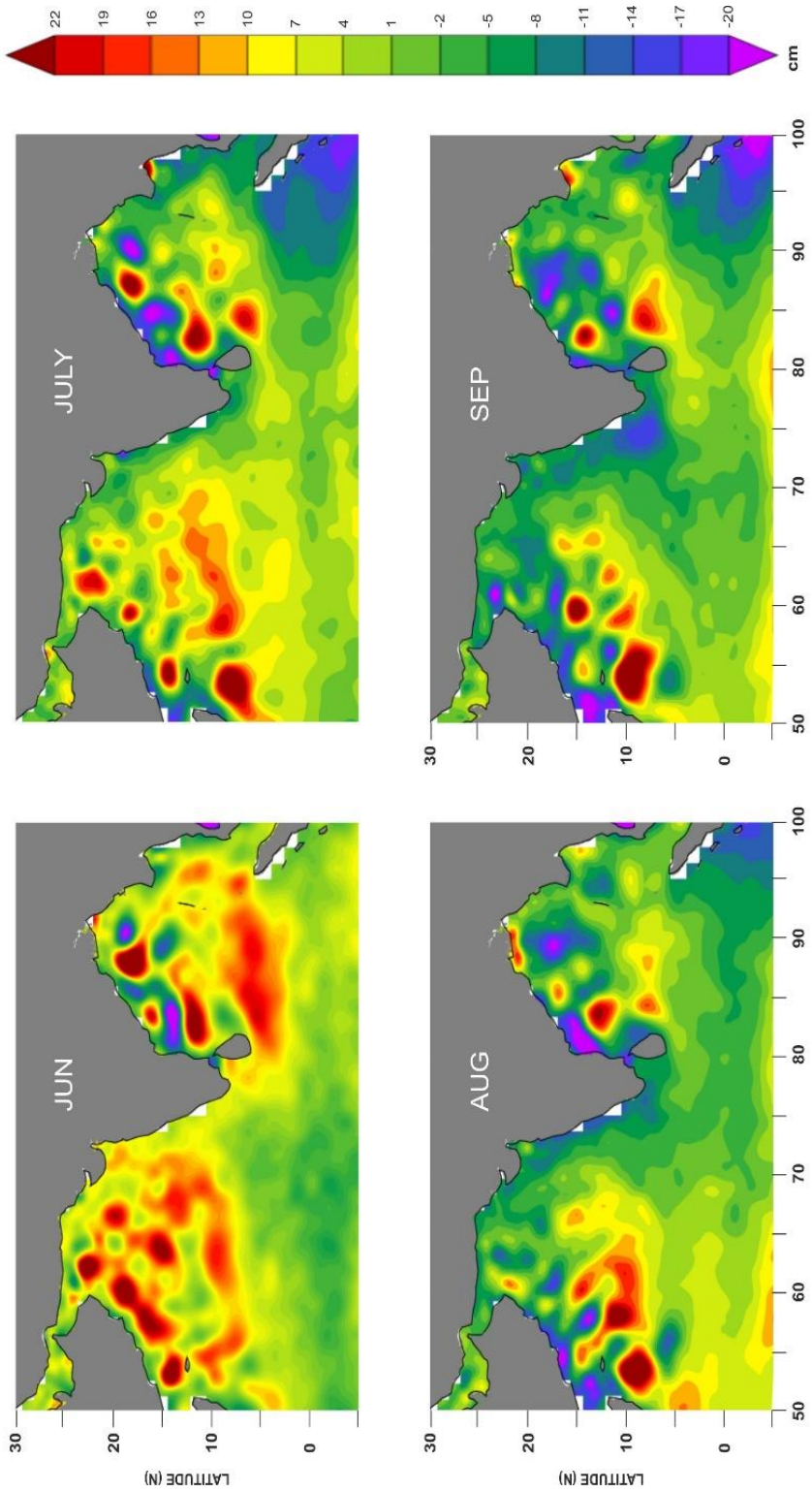

Fig. 4.2: SSHA (cm) of the northern Indian Ocean during the summer monsoon of a strong positive IOD year 1997.

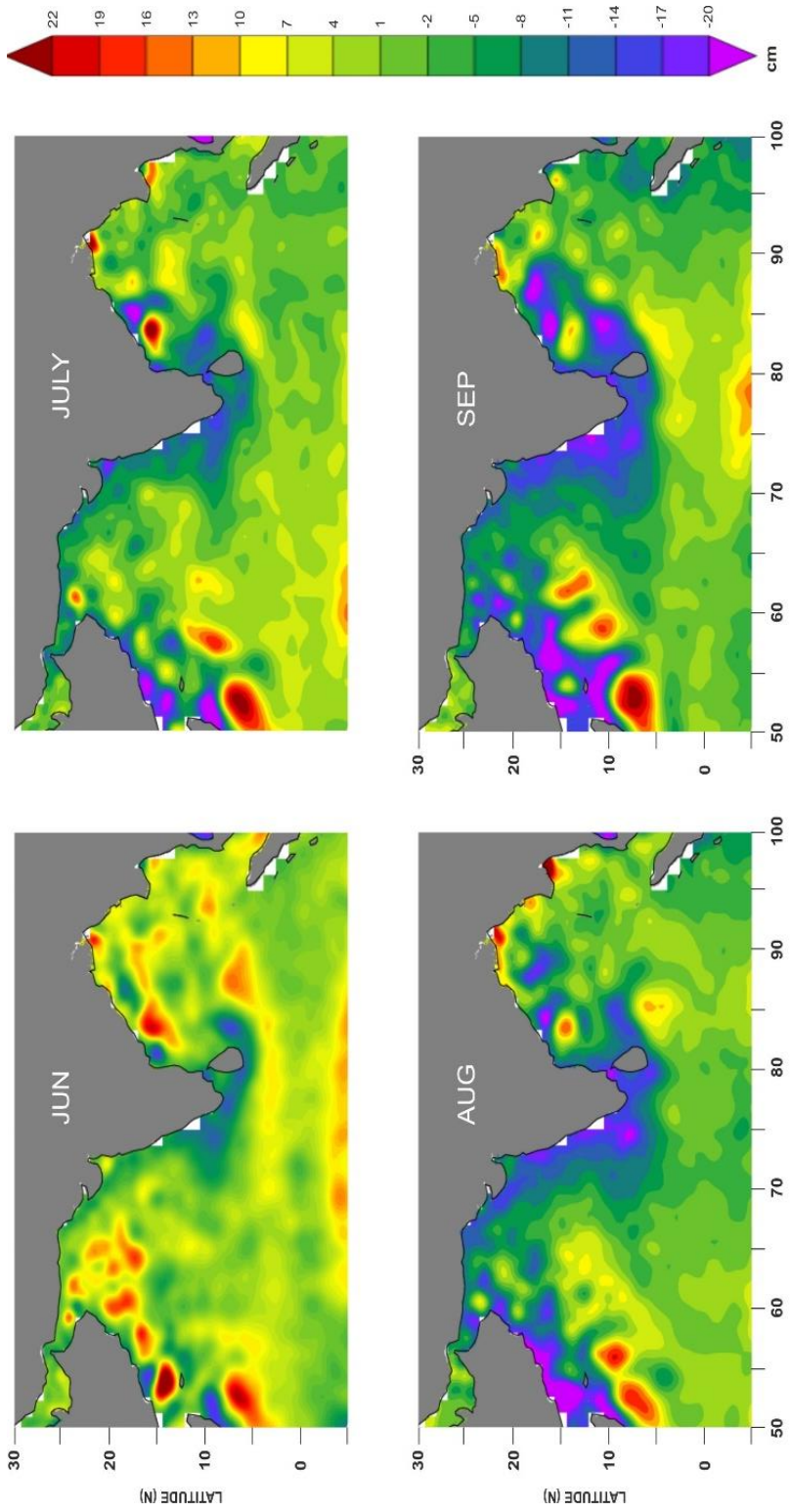

Fig. 4.3: SSHA (cm) of the northern Indian Ocean during the summer monsoon of a negative IOD year 1998.

4.3.3 Interannual variability of vertical velocity during summer monsoon

Interannual variability of vertical velocity along the west coast of India is used as another proxy for the study of variability of upwelling along the west coast of India. Fig. 4.4 represents interannual variability of vertical velocity along the west coast of India during the summer monsoon.

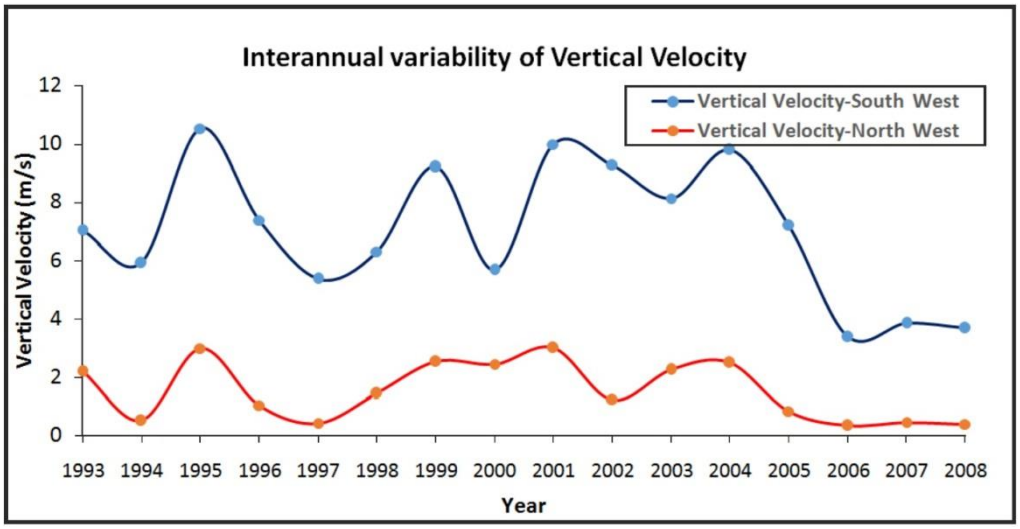

Fig. 4.4: Interannual variability of vertical velocity ($\times 10^{-5}$ m/s) at 100m depth (averaged from June to September) along the southwest and northwest coast of India.

Fig. 4.4 shows that the vertical velocity along the southwest coast of India is about four to five times larger than that observed along the northwest coast. In tune with the observations on SSHA, the positive IOD years (1994, 1997, 2006, 2007, and 2008) show the lowest values of upward vertical velocity along the entire coast. The La-Niña year 2000 also shows a decrease in upwelling along the west coast of India. Compared with the other years, the positive IOD years from 2006 to 2008 show a sharp reduction in upwelling along the west coast of India. This is due to the combined effect of positive IOD and El-Niño/ La-Niña. Here the year 2006 is characterized by co-occurrence of positive IOD

and El-Niño. Year 2007 is also an IOD year that co-occurred with La Niña. The above analysis indicates the impact of positive IOD on the reduction of upwelling along the west coast of India.

4.3.4 Interannual variability of surface offshore mass transport during summer monsoon

The analysis of surface offshore mass transport along the west coast of India reveals that during the summer monsoon, strong offshore mass transport (upwelling-favorable) was limited to the southwest coast of India. Along the northwest coast, weak offshore to moderate onshore transport was observed (Fig. 4.5).

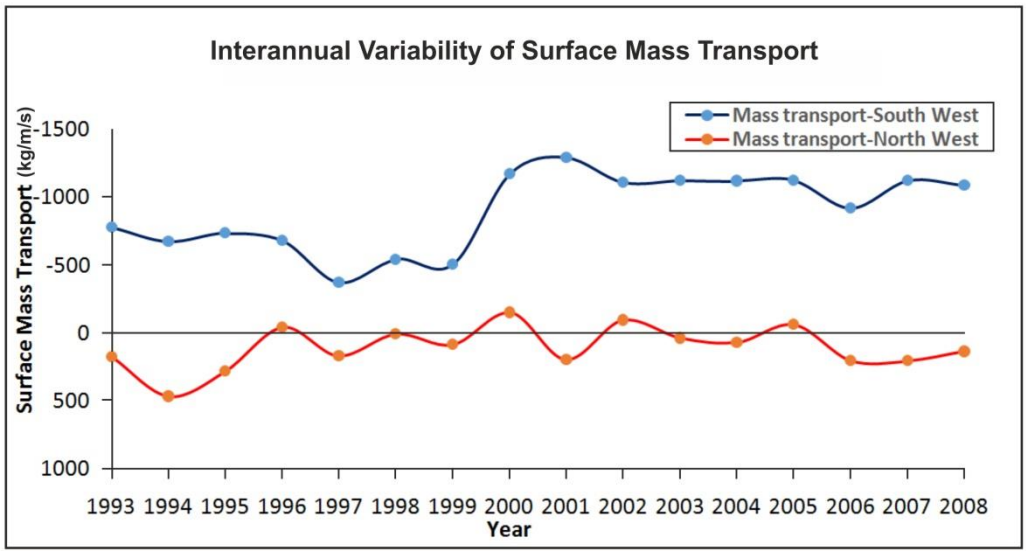

Fig. 4.5: Interannual variability of surface mass transport (kg/m/s) (averaged from June to September) along the southwest and northwest coast of India.

From 1993 to 1999, strength of surface mass transport was substantially less than that during 2000 to 2008. This may have been an artifact of the lower resolution of ERS data sets compared with the QuikSCAT. From 1993 to 1999 the surface mass transport along the southwest coast shows a decrease in offshore transport during the positive IOD years, clearly reflected also in the observations

on vertical velocity. But from 2000 to 2008, even though the offshore transport decreases during the positive IOD year 2006, the other IOD years 2007 and 2008 did not show a strong decrease in the surface offshore transport, while during this decade vertical, velocity along the southwest coast showed a considerable decrease from 2006 to 2008. Hence, the surface mass transport during this decade was not sufficient to explain completely the decrease in vertical velocity and SSHA along the southwest coast. Along the northwest coast, surface mass transport was onshore and was not able to drive any upward motion.

4.3.5 Inter annual variability of horizontal divergence

From the second chapter it was obvious that upwelling along the west coast of India results not only from the wind-induced mass transport but also from horizontal divergence due to the currents that have significant influence on the vertical circulation.

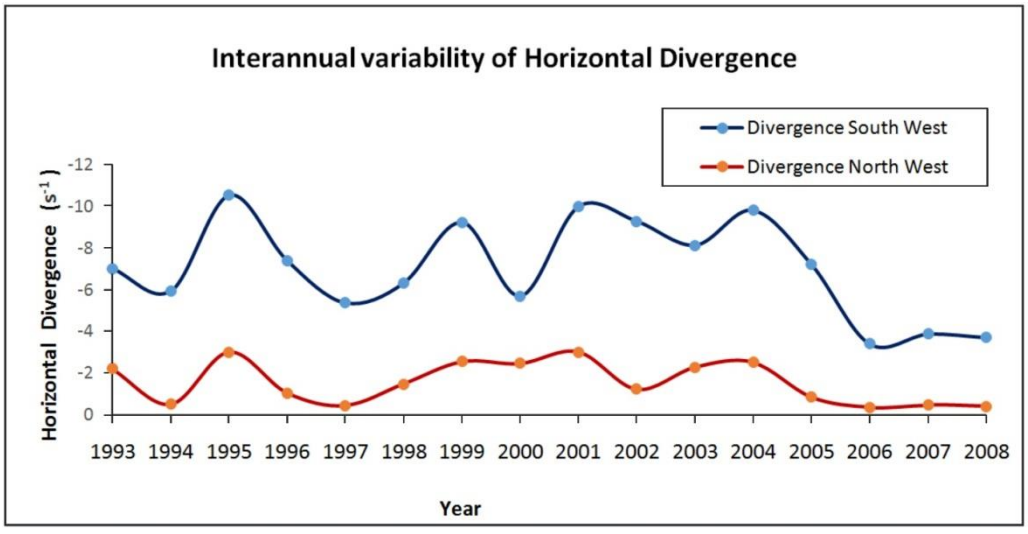

Fig. 4.6: Interannual variability of horizontal divergence ($\times 10^{-7}$ s^{-1}) (averaged from June to September) along the southwest and northwest coast of India.

Analysis of Fig. 4.6 showed that during the summer monsoon, entire west coast of India was characterized by negative values of horizontal divergence. This means that the current field along the entire west coast is divergent during the summer monsoon, inducing an upward vertical circulation. This is the reason for the upward motion observed in the northwest coast of India, even when the wind is not favorable for upwelling during the summer monsoon. Compared with the northwest coast, a strongly-divergent field is observed along the southwest coast of India. Hence the vertical velocity along the southwest coast far exceeds that of the northwest coast.

In tune with the findings of Chapter 2, the divergence along the southwest coast of India is very much stronger than that along the northwest coast. Even though wind does not support upward motion along the northwest coast, this divergence drives upward circulation there. Analysis of Fig. 4.6 reveals that during positive IOD years, the entire west coast of India is characterized by a decrease in horizontal divergence. The IOD years 2006 to 2008 experienced a strong decrease in divergence compared with the IOD years 1994 and 1997. This is the reason for lowest observed values of upward vertical velocity and magnitude of SSHA along the west coast of India during these years. It indicates the combined effect of positive IOD and El Niño/ La Niña on the strength of circulation and divergent field along the west coast of India.

Analysis of SSHA, vertical velocity, surface mass transport and horizontal divergence reveals that upwelling along the west coast of India was considerably decreased during the positive IOD years.

4.3.6 Interannual variability of downwelling along the west coast of India

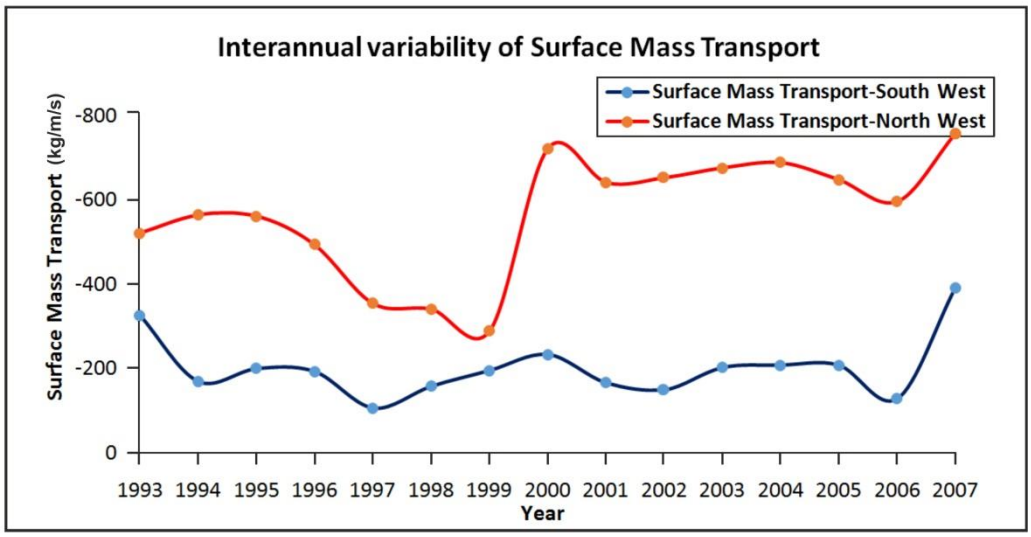

Fig. 4.7: Interannual variability of surface mass transport (kg/m/s) (averaged from November to February) along the southwest and northwest coast of India.

The analysis of surface mass transport due to the along shore component of wind shows weak offshore (upwelling-favorable) transport along the southwest coast to moderate offshore (upwelling-favorable) transport along the northwest coast (Fig. 4.7). This substantiates the results of Chapter 2 that surface mass transport due to the alongshore component of wind along the west coast of India is not favorable for downwelling along the coast during the northeast monsoon and winter.

Since downwelling along the west coast of India is driven mainly by Kelvin waves from equatorial Indian Ocean, scrutiny of interannual variability in these Kelvin waves gives a clear understanding of interannual variability of downwelling along the coast. Variability of SSHA is used as the most appropriate proxy for identification of propagating Kelvin waves and its interannual variability reflects inter annual variability of downwelling.

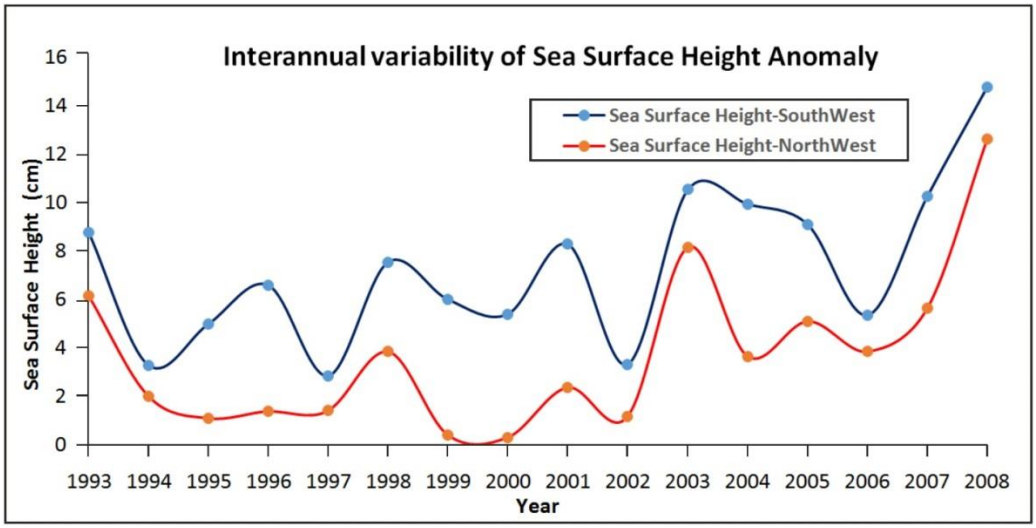

Fig. 4.8: Interannual variability of SSHA (cm) (averaged from November to February) along the southwest and northwest coast of India.

From Fig. 4.8 it was evident that during the northeast monsoon and winter season, the entire west coast of India was characterized by positive SSHA. This was a clear indication of downwelling along the west coast of India during that season. Compared with northwest coast, SSHA values are higher on the southwest coast. This indicates that as with upwelling, downwelling is also stronger on the southwest coast than the northwest.

The observations on inter annual variability of SSHA reveal that during positive IOD years 1994,1997 and 2006, downwelling was considerably reduced along the west coast of India. The same trend was also observed in upwelling during these years, while during positive IOD years 2007 and 2008, an unusual increase in SSHA was observed. This indicates that unlike the case for the other positive IOD years, downwelling was significantly increased during 2007 and 2008. Over the entire study period from 1993 to 2008, years 2007 and 2008 show maximum downwelling along the coast. But upwelling was minimum during these years.

From the spatial correlation of SSHA along the west coast of India and zonal wind over the entire north Indian Ocean basin, Chapter 3 revealed that downwelling along the west coast of India is mainly driven by Kelvin waves from the equatorial Indian Ocean. And these downwelling Kelvin waves are generated when westerly winds blow over the equatorial Indian Ocean. From the climatology of SSHA over the Arabian Sea during northeast monsoon season it was obvious that during December along the southwest coast there was a rapid increase in sea surface height due to the arrival of the Kelvin waves. The similar study of Rao et al. (2009) showed that when westerly winds blow over the Equator, downwelling-favorable equatorially-trapped Kelvin waves radiate into the eastern ocean, deepening the thermocline there, while the easterly winds led to the formation of upwelling-favorable Kelvin waves at the Equator.

4.3.8 Interannual variability of SSHA over the Eastern Arabian Sea

To elucidate the reason for weakened downwelling during the positive IOD years 1994 and 1997, spatial contours of SSHA were made over the entire eastern Arabian Sea during the northeast monsoon from 1993 to 2000. From Fig 4.9(a) and Fig. 4.9(b), it was evident that during October and November, SSHA over the south eastern Arabian Sea in positive IOD years (1994, 1997) was higher than that during negative IOD (1996, 1998) and normal years. But during December, compared with the negative IOD and normal years, SSHA was considerably diminished along the west coast of India in positive IOD years (Fig. 4.9(c)). Since Kelvin waves reach the west coast of India during December, the weakened SSHA in December during the positive IOD years represents the absence or weakening of these Kelvin waves.

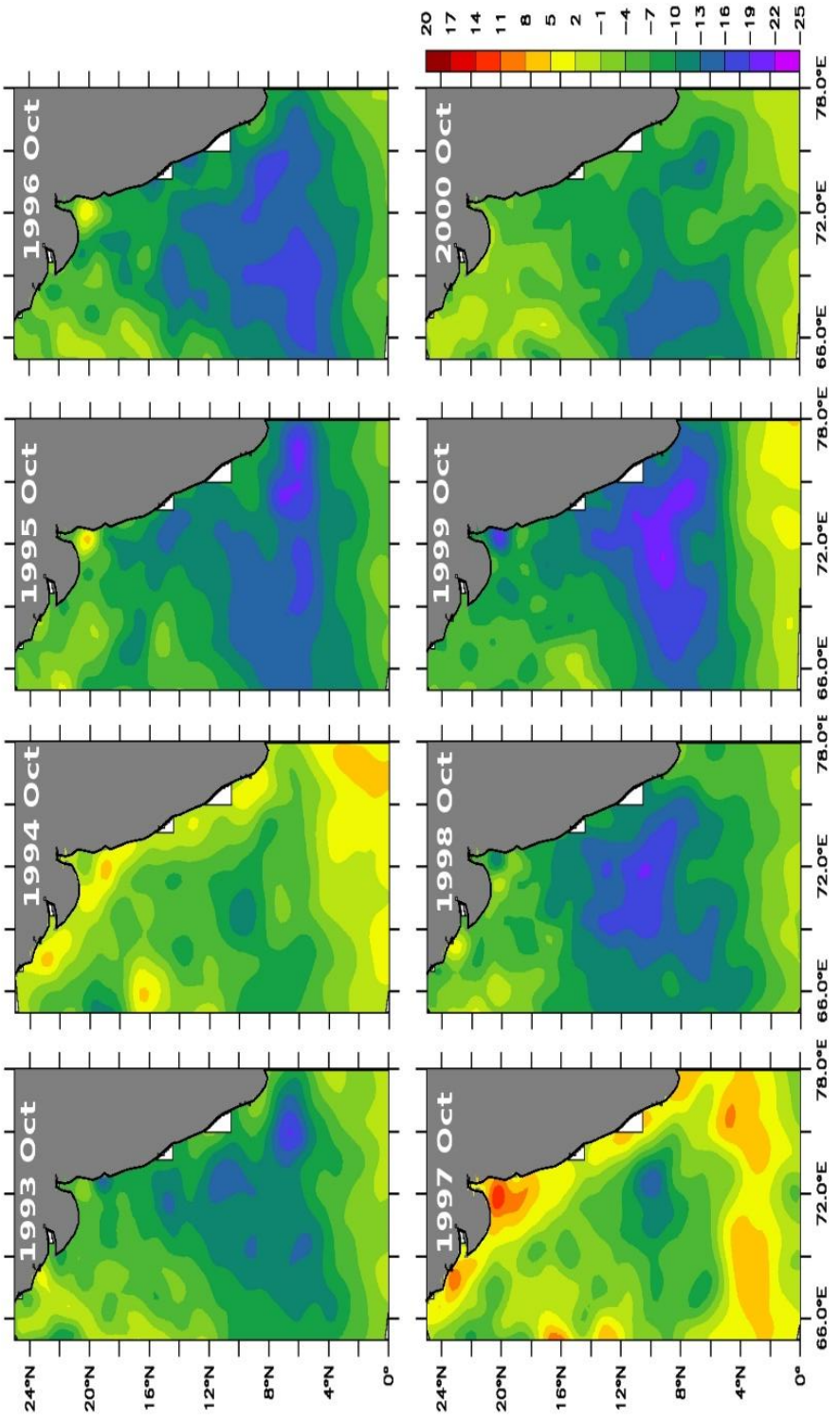

Fig. 4.9(a): Interannual variability of SSHA (cm) during October along the west coast of India from 1993-2000.

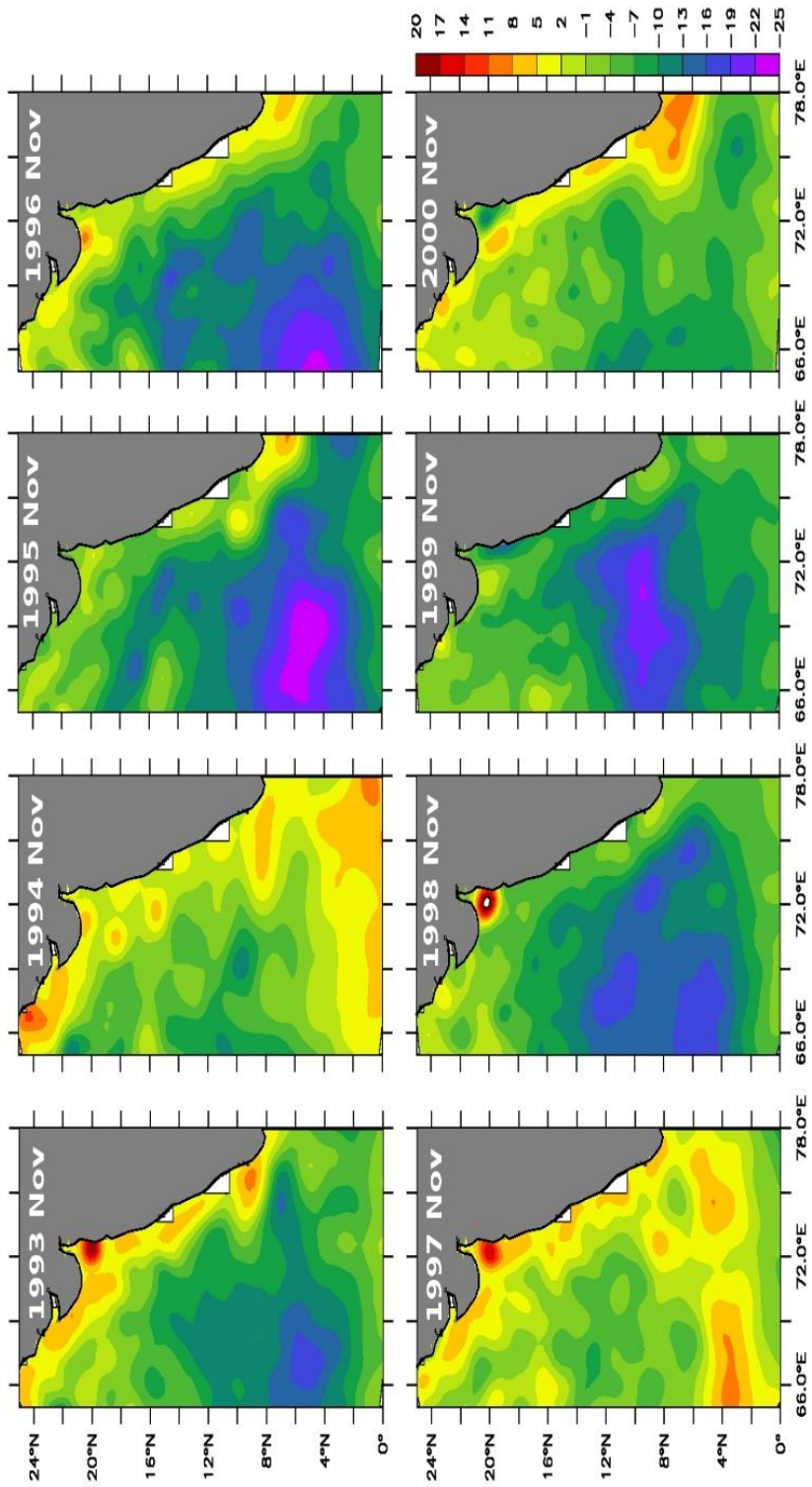

Fig. 4.9(b): Interannual variability of SSHA (cm) during November along the west coast of India from 1993-2000.

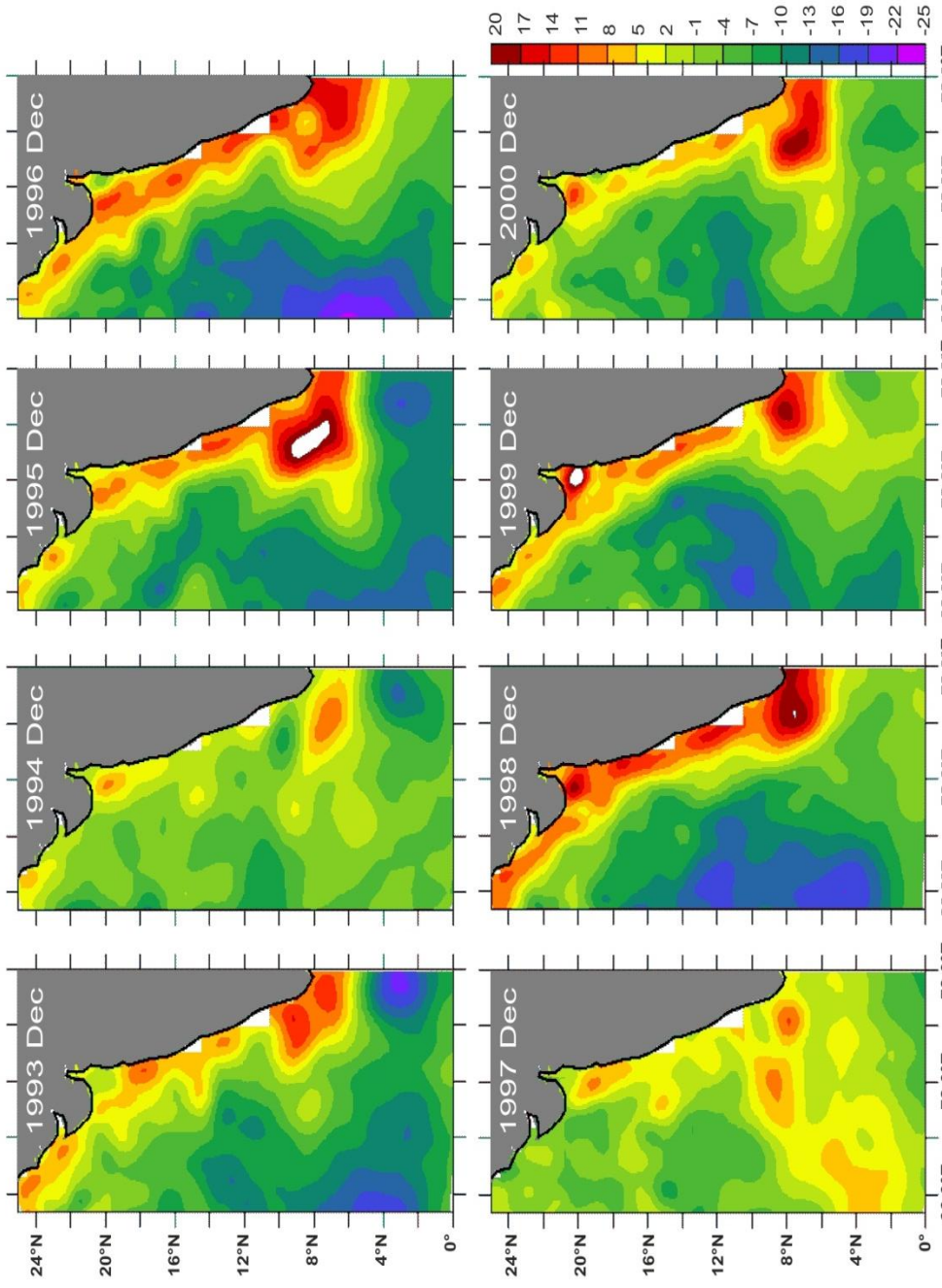

Fig. 4.9(c): Inter annual variability of SSHA (cm) during December along the west coast of India from 1993-2000.

4.3.8 Inter annual variability of SSHA and Wind over the Equator

From the observed climatology of the zonal wind stress, Sengupta et al. (2001) reported that zonal wind stress is mostly westerly throughout the year within the east and central equatorial region. Following the approach of Rao et al. (2009), we analyzed SSHA and wind along a narrow band of equator from 1°S to 1°N. From Fig. 4.10(a) and Fig. 4.10(b) it was evident that, in all the years other than positive IOD years 1994, 1997 and 2006 the winds along the equator are westerly (positive values) during northeast monsoon season and positive values of SSHA are observed over the equator. In these positive IOD years, the westerlies are replaced by easterlies and SSHA values are considerably decreased. This indicates that there were no downwelling-favorable Kelvin waves produced in the Equator during positive IOD years 1994, 1997 and 2006. Fig. 4.11 clearly shows that, during the positive IOD year 1997, downwelling-favorable Kelvin waves are replaced by upwelling-favorable Kelvin waves and did not reach the west coast of India, whereas during the negative IOD year 1998, strong downwelling-favorable Kelvin waves from equator propagated along the wave guides of Bay of Bengal and reached the west coast of India. Unlike the other positive IOD years, the positive IOD co-occurred with strong La Niña year 2007, and year 2008 was characterized by the propagation of strong downwelling-favorable Kelvin waves from the equator that reached the west coast of India (Fig. 4.12 and Fig. 4.13). During these years, strong westerlies blew over the equator during the northeast monsoon and these resulted in the generation of downwelling-favorable Kelvin waves (Fig. 4.10(a) and 4.10(b)).

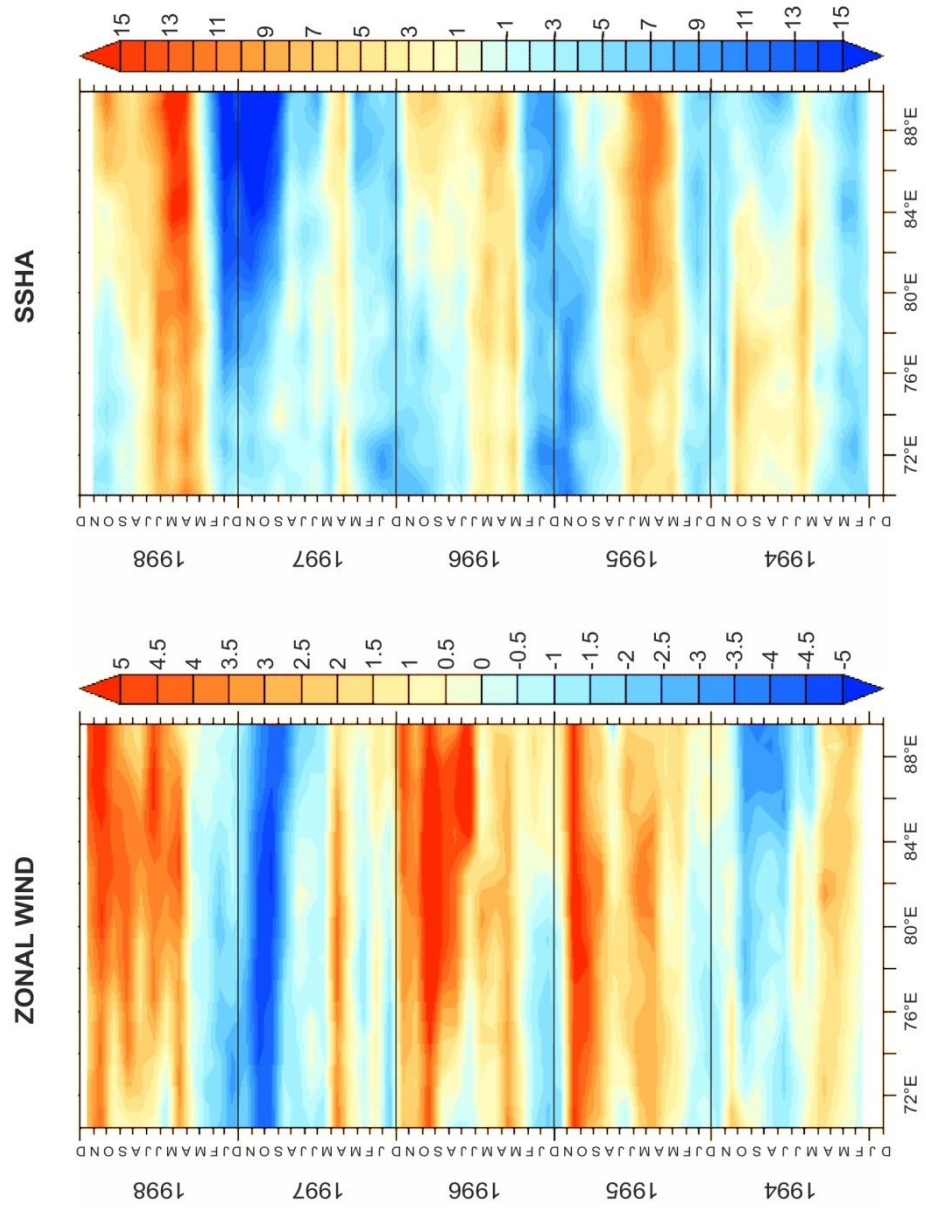

Fig. 4.10(a): Hovmoller diagrams of zonal wind (m/s) and SSHA (cm) over the Equator from 1993-2000.

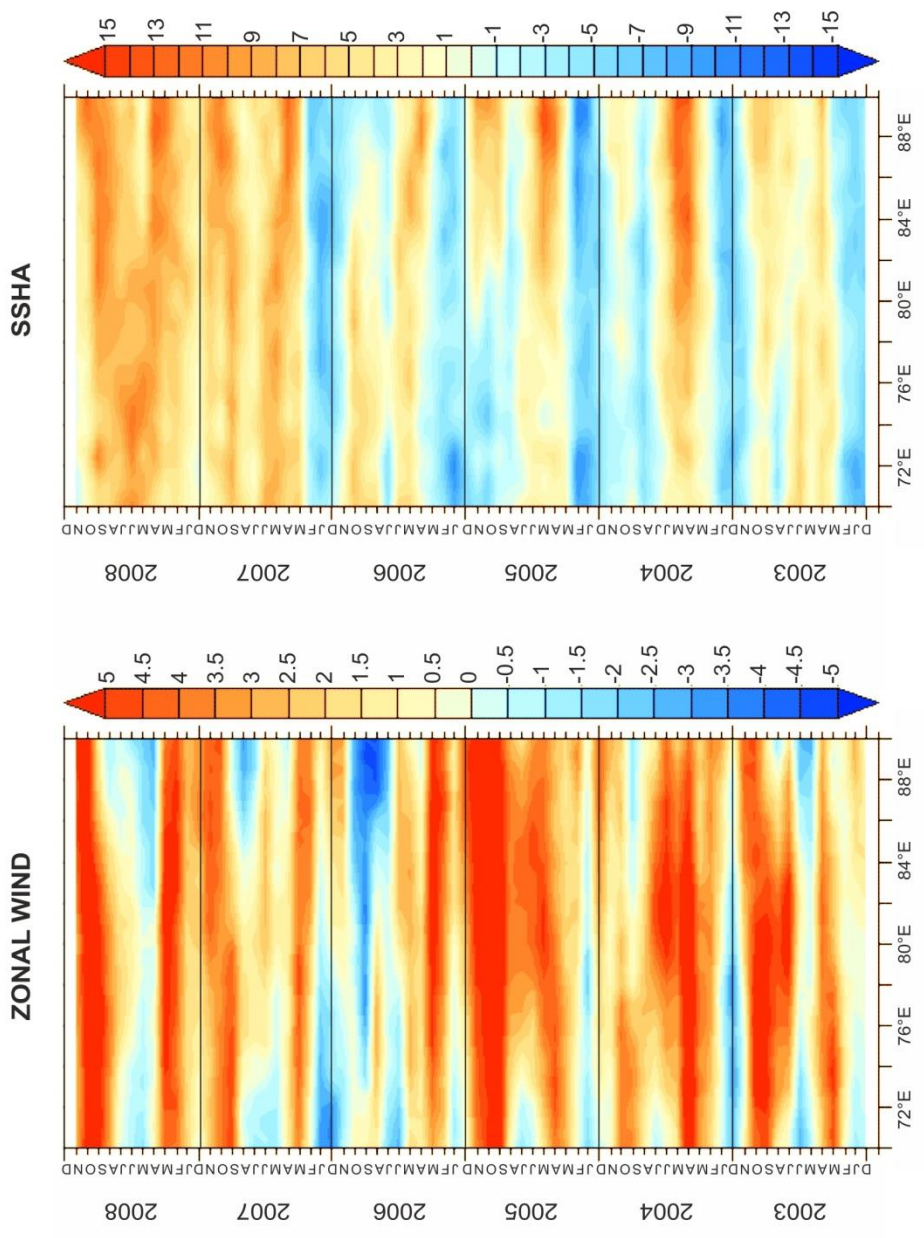

Fig. 4.10(b): Hovmoller diagrams of zonal wind (m/s) and SSHA (cm) over the Equator from 2003-2008.

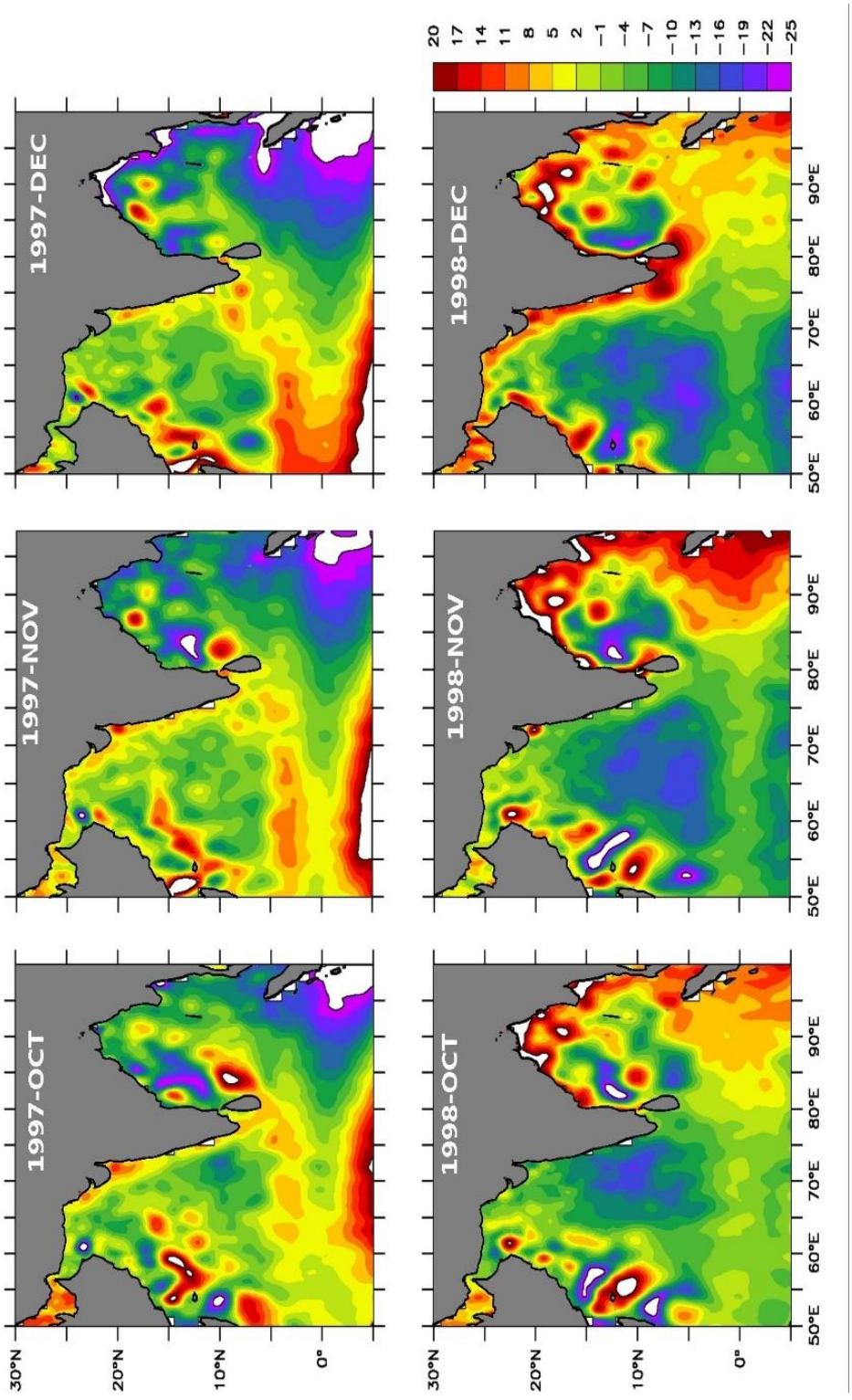

Fig. 4.11: SSHA (cm) over the northern Indian Ocean during northeast monsoon of 1997 and 1998.

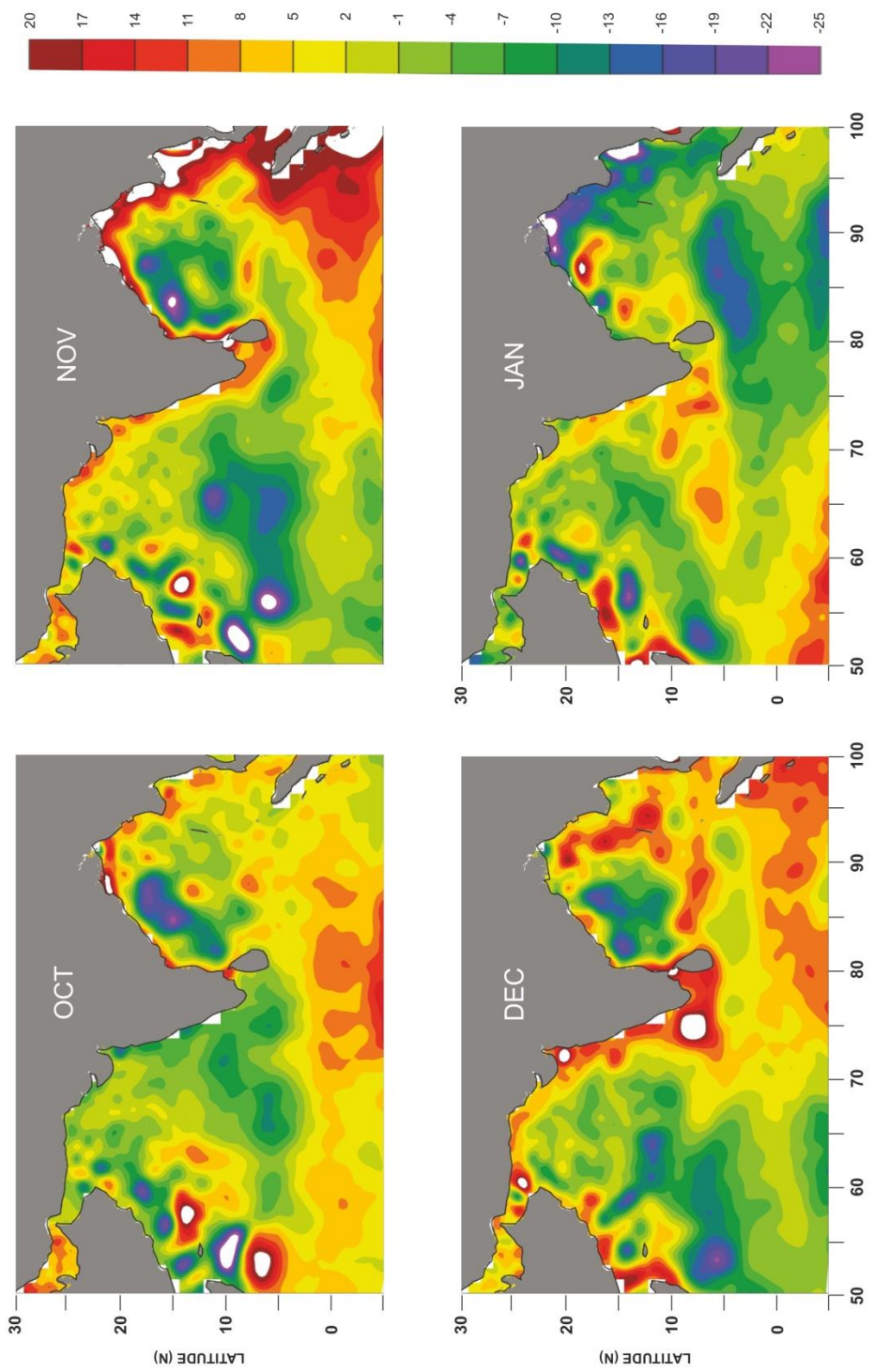

Fig. 4.12: SSHA (cm) over the northern Indian Ocean during northeast monsoon of 2007.

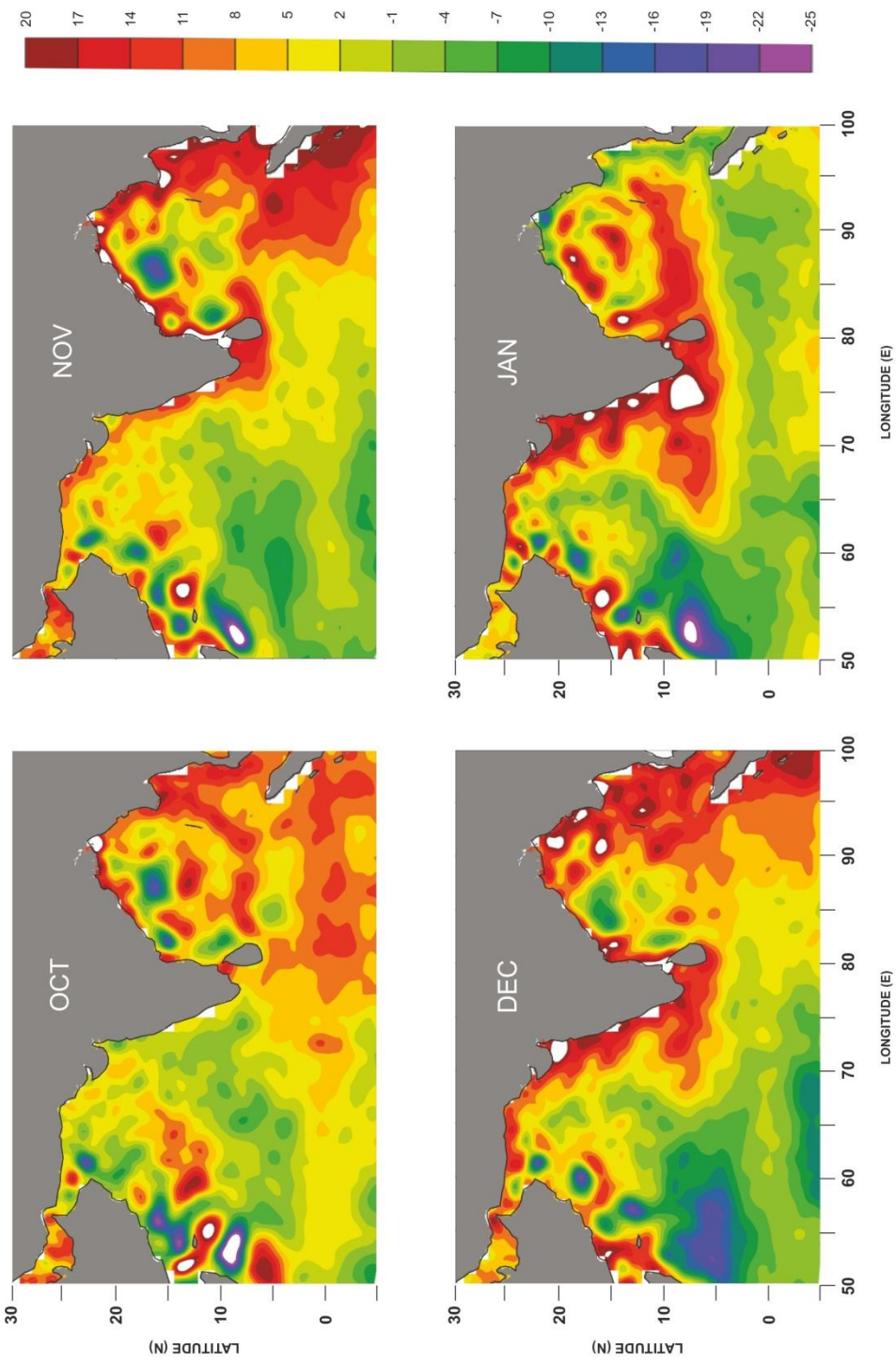

Fig. 4.13: SSHA (cm) over the northern Indian Ocean during northeast monsoon of 2008.

4.4 Conclusion

From the analysis of various physical oceanographic parameters, the present chapter concluded that due to the weakening of horizontal divergence and surface offshore mass transport, upwelling along the west coast of India was considerably decreased during the positive IOD years compared with the other negative IOD and with normal years. Compared with other years, the most intense decrease in upwelling was observed during 2006 to 2008, and these years were characterized by strong reduction of horizontal divergence along the west coast of India. Upwelling Kelvin waves along the west coast of India during July and August were completely absent during positive IOD years. This also led to the weakening of upwelling during the positive IOD years.

Over the west coast of India, downwelling also decreased during the positive IOD years 1994, 1997 and 2006. During these years, westerly winds were replaced by easterlies over the Equator in the northeast monsoon. This resulted in the collapse of propagation of downwelling-favorable Kelvin waves from the Equator, whereas during the positive IOD associated with La Niña, the year 2007 was characterized by a strong propagation of downwelling-favorable Kelvin waves and most intense downwelling was observed during 2007 and 2008.

Chapter 5

SUMMARY AND CONCLUSION

Although several studies have been made on upwelling along the southwest coast of India, earlier work on upwelling along northwest coast and downwelling along the west coast of India has been minimal. The present work reports an integrated attempt, with an extensive use of satellite-derived and in-situ climatologies, to study the upwelling and downwelling along the west coast of India for the entire range from 8ºN to 20ºN. The main objectives was to identify the period and location of upwelling and downwelling along the west coast of India and to seek out the relative importance of difference forcing mechanisms involved in the vertical motion along this coast. From a detailed study analyzing the depth of 26º isotherms, sigma-t, LTA, SSHA, chlorophyll-a concentration and mean vertical velocity calculated over a depth of surface to 100m depth, it is concluded that upwelling along the west coast of India starts during April at 8ºN and propagates northward as the summer monsoon progresses. Most intense upwelling was observed along southwest coast from 8ºN to 15ºN during July-August and along the northwest coast it was observed during August-September, revealing a clear south to north lag in the evolution of upwelling along the west coast of India. Even though surface LTA values

were consistent with those of previous studies from which it was concluded that upwelling was limited to the southern shelf and was less conspicuous towards north, the observations on LTA at 10m to 30m depth levels, depth of 26º isotherms and vertical distribution of sigma-t indicated that upwelling features were also evident on the northwest coast from 15ºN to 20ºN in the subsurface levels. The analysis on SSHA and chlorophyll-a showed sea surface manifestation of upwelling along the northwest coast during the summer monsoon. Vertical velocity calculated along the west coast of India during the summer monsoon was stronger along the southwest coast from May to September. But moderate values of upward vertical velocities are observed also along the northwest coast only during July to September. When comparing the upwelling between south and north along the west coast of India from 8ºN to 20ºN, all the indices used shown stronger manifestation of upwelling along the southwest coast compared with the northwest coast.

Downwelling along the southwest coast of India starts during October and propagates northward as the northeast monsoon progresses. The coast was also characterized by downwelling during the winter that continued to February-March. Along the southwest coast, the most intense upwelling was observed during December and January. Downwelling along the northwest coast was visible first during November and continued to March-April. Intensification of downwelling along the northwest coast was observed during January. Vertical velocity calculated along the west coast of India during northeast monsoon and winter showed stronger values of downward vertical velocities along the southwest coast and moderate values of downward velocity along the northwest coast: as with upwelling, downwelling was also stronger along the southwest coast compared with the northwest coast of India.

Based on several previous studies, the plausible explanation for upwelling and downwelling along the west coast of India was linked to surface Ekman mass transport due to the alongshore and cross shore component of wind. Hence, I analyzed these processes along the west coast of India during both monsoon and transition periods. Analysis of surface mass transport due to the alongshore wind revealed that throughout the year, entire west coast of India experienced weak-to-moderate offshore transport except during the peak summer monsoon months June, July and August. During the peak summer monsoon, moderate onshore transport was observed along the northwest coast, and strong offshore transport was noticed along the southwest coast. The surface mass transport due to the cross shore component of wind also followed the same trend of surface mass transports due to the alongshore wind component, except during the peak summer monsoon. During summer monsoon, the mass transport due to the alongshore component of wind was upwelling-favorable along the southwest coast of India, whereas the mass transport due to the cross shore component was downwelling-favorable.

Synthesizing the observations on area and period of upwelling and downwelling along the west coast of India and on the surface Ekman mass transport due to both components of wind, I have concluded that even though surface offshore Ekman mass transport was limited to the southwest coast of India during the peak summer monsoon months June, July and August, the entire west coast of India was nevertheless characterized by upwelling. This indicates that along the southwest coast of India, wind-induced surface offshore mass transport played a significant role in upwelling, but that along the northwest coast upwelling was driven by some other forcing mechanism: upwelling along the west cost of India is not only driven by wind but some

other forcing mechanisms are also involved. During May and September, wind is favorable for upwelling along the entire west coast and it is well correlated with the surface manifestation of upwelling along the west coast.

Analysis of surface Ekman mass transport during the northeast monsoon and winter revealed that even though the surface mass transport due to the wind stress is towards offshore and does not favour downwelling along the coast during this period, the entire west coast of India was characterized by downwelling: downwelling along the west cost of India is not driven by wind.

Hence, the horizontal divergence due to the currents along the west coast of India was analyzed throughout the year. The analysis revealed that during the summer monsoon, the southwest coast of India was characterized by strong horizontal divergence from May to September. During June, intensification of horizontal divergence was observed over the west coast from 8ºN to 18ºN, but the strength of upwelling was comparatively higher in the southern latitudes compared with the northern ones. During July, August and September, higher values of horizontal divergence were observed over the southwest coast and moderate horizontal divergence was observed over the northwest coast. Even though strong horizontal divergence was limited to the southwest coast, northern latitudes also showed considerable horizontal divergence during the peak summer monsoon.

Hence, strong upwelling along the southwest coast of India during the peak summer monsoon is due to the combined effect of current-induced, horizontal divergence and wind-induced surface offshore mass transport. Along the northwest coast, upwelling during the peak summer monsoon month is due to the effect of this moderate horizontal divergence. But the strong onshore surface mass transport due to the wind stress inhibits the excursion of upwelled

water to the surface level during this period, along the northwest coast. This is the explanation for the vertical ceiling of upwelling along the northwest coast compared with the southwest.

During the northeast monsoon and winter, the west coast of India was characterized by moderate-to-strong convergence. During December and January, strong convergence was observed along the southwest coast from 8ºN to 14ºN, and along the northwest coast, moderate convergence was observed. The months November, February and March showed moderate convergence along the entire west coast of India. Compared with the northwest coast, the magnitude of convergence was stronger over the southwest coast. Even though the wind-induced surface mass transport did not favour downwelling along the west coast of India during the winter season, the convergence due to the surface currents did induce downwelling. This is the basis for downwelling along the west coast of India.

Analysis of surface current, wind and horizontal divergence along the west coast of India revealed that during the summer monsoon, the wind and surface currents were in the same (equatorward) direction along southwest coast of India. But along the northwest coast, their directions did not correlate well. During the northeast monsoon and winter, the entire west coast of India was characterized by poleward currents but winds were blowing against them. Even though wind does not support convergence during this period, the coast was characterized by strong convergence, indicating the influence of remote forcing on both horizontal and vertical circulation along the west coast of India.

Calculations and interpretation of baroclinic radius, baroclinic velocity and critical period of coastally-trapped waves along the continental shelf waters

of west coast of India showed that the baroclinic radius of deformation along the west coast of India decreases from 116 km at 8ºN to 50 km at 20ºN, whereas the critical period shows an increasing trend from south to north. The values of critical period range between 49 days at 8ºN to 123 days at 20ºN. Based on the information on critical period along the west coast of India, the frequency-filtered daily data sets of SSHA and zonal component of wind were used for the spatial correlation of SSHA over the west coast of India and zonal wind over the entire north Indian Ocean domain. This revealed the influence of zonal winds blowing over the eastern equatorial Indian Ocean on the downwelling along west coast of India by the propagation of equatorially-generated downwelling Kelvin waves. The influence of remote forcing from the Gulf of Mannar on the upwelling along the west coast of India was also brought to light.

In this thesis, the influence of IOD events on upwelling and downwelling along the west coast of India was also demonstrated. It was concluded that due to the weakening of horizontal divergence and surface offshore mass transport, upwelling along the west coast of India was considerably decreased during the positive IOD years compared with the other negative IOD and with normal years. Compared with other years, the most intense decrease in upwelling was observed during 2006 to 2008, and these years were characterized by strong reduction of horizontal divergence along the west coast of India. Over the west coast of India, downwelling also decreased during the positive IOD years 1994, 1997 and 2006 due to the collapse of propagation of downwelling-favorable Kelvin waves from the Equator, whereas during the positive IOD associated with La Niña, the year 2007 was characterized by a strong propagation of downwelling-favorable Kelvin waves and most intense downwelling was observed during 2007 and 2008.

Even though the thesis enhances our understanding on the origins and role of upwelling and downwelling processes along the west coast of India, more fine-resolution in-situ data sets and application of models would definitely provide even more insights on this topic.

.....ൠ.....

Bibliography

Antony, M.K., Narayana, S.G. and Somayajulu, Y.K., 2002: Offshore limit of coastal ocean variability identified from hydrography and altimeter data in the eastern Arabian Sea, *Cont. Shelf Res*, **22,** 525–2536.

Ashok, K., Guan, Z. and Yamagata, T., 2001: Impact of the Indian Ocean Dipole on the relationship between the Indian Monsoon rainfall and ENSO, *Geophys. Res. Lett.*, **28**, 4499-4502.

Ashok, K., Guan, Z., Saji, N.H. and Yamagata, T., 2004: Individual and combined influences of ENSO and the Indian Ocean Dipole on the Indian Summer Monsoon, *J. Climate*, **17**, 3141 – 3155.

Bakun, A., B. A. Black, S. J. Bograd, M. García-Reyes, A. J. Miller, R. R. Rykaczewski and W. J. Sydeman, 2015: Anticipated Effects of Climate Change on Coastal Upwelling Ecosystems, Curr. Clim. Change Rep., **1,** 85–93, DOI: 10. 1007/ s40641-015-0008-4.

Banse, K., 1959: On upwelling and bottom trawling off the southwest coast of India, *J.Mar. Biol. Assoc. India*, **1**, 33 – 49.

Banse, K., 1968: Hydrography of the Arabian Sea shelf of India and Pakistan and effects on demersal fishes, Deep Sea Res 15:45-79.

Barth, J. A., B. A. Menge, J. Lubchenco, F. Chan, J. M. Bane, A. R. Kirincich, M. A. McManus, K. J. Nielsen, S. D. Pierce, and L. Washburn, 2007: Delayed upwelling alters nearshore coastal ocean ecosystems in the Northern California Current, Proc. Natl. Acad. Sci. U. S. A., **104(10)**, 3719–3724, doi:10.1073/pnas.0700462104.

Bauer, S., Hitchcock, G. L., and Olson, D. B., 1992: Response of the Arabian Sea surface layer to monsoon forcing, In Desai, B. N., (Ed.), Oceanography of the Indian Ocean New Delhi, Oxford & IBH. Pp: 659 – 672.

Behera, S. K., Salvekar, P. S. and Yamagata, T., 2000: Simulation of interannual SST variability in the tropical Indian Ocean, *J. Climate,* **13**, 3487-3489.

Behera, S.K., Krishnan, R. and Yamagata, T., 1999: Unusual Ocean-Atmosphere conditions in the tropical Indian Ocean during 1994, *Geophys. Res. Lett.,* **26**, 3001-3004.

Botsford, L. W., C. A. Lawrence, E. P. Dever, A. Hastings, and J. Largier, 2006: Effects of variable winds on biological productivity on continentalshelves in coastal upwelling systems, Deep Sea Res. II, **53**, 3116–3140, DOI:10.1016/j.dsr2.2006.07.011.

Brown, J., Clayson, C. A., Kantha, L. and Rojsiraphisal, T., 2008: North Indian Ocean variability during the Indian Ocean Dipole, *Ocean Sci. Discuss.*, **5**, 1 – 41.

Chambers, D.P., Tapley, B.D. and Stewart, R.H., 1999: Anomalous warming in the Indian Ocean coincident with El Niño, *J. Geophys. Res.,* **104**, 3035 – 3047.

Chatterjee, A., Shankar, D., Shenoi, S.S.C., Reddy, G.V., Michael, G.S., Ravichandran, M., Gopalkrishna, V.V., Rama Rao, E.P., Udaya Bhaskar, T.V.S., and Sanjeevan, V.N., 2012: A new atlas of temperature and salinity for the North Indian Ocean, Journal of Earth System Science, 121(3), 559–593.

Chelton, D. B., R. A. DeSzoeke, M. Schlax, K. El Naggar, and N. Siwertz, 1998: Geographical variability of the first baroclinic Rossby radius of deformation, J. Phys. Oceanogr., **28**, 433–460, DOI:10.1175/1520-0485028<0433: GVOTFB>2.0.CO;2.

Clarke, A. J., 1983: The reflection of equatorial waves from oceanic boundaries, J. Phys. Oceanogr., 13, 1193– 1207.

Cutler, A. N. and Swallow, J. C., 1984: Surface currents of the : Compiled from historical data archived by the meteorological office, Bracknell, U. K. Institute of Oceanographic Sciences, Report No. 187, 88 p. and 36 charts.

Darbyshire, M., 1967: The surface waters off the Coast of Kerala, southwest India, Deep Sea Res. 14:295-320.

Gadgil, S., Vinayachandran, P.N. and Francis, P.A., 2003: Droughts of Indian summer monsoon: role of clouds over the Ocean, *Curr. Sci.,* **85,** 1713–1719.

Gadgil, S., Vinayachandran, P.N. and Francis, P.A., 2004: Extremes of the Indian summer monsoon rainfall, ENSO, and equatorial Indian Ocean oscillation, *Geophys. Res. Lett.,* **31**, 1821 pp., DOI 10.1029/2004GL019733.

Gnanaseelan, C. and Vaid, B. H., 2010: Interannual variability in the Biannual Rossby waves in the tropical Indian Ocean and its relation to Indian Ocean Dipole and El Niño forcing, *Ocean Dyn.*, **60**, 27 – 40, DOI 10.1007/s10236-009-0236-z.

Gopalakrishna, V.V.; Rao, R.R.; Nisha, K.; Girish Kumar, M.S.; Pankajackshan, T.; Ravichandran, M.; Johnson, Z.; Girish, K.; Aneeshkumar, N.; Srinath, M.; Rajesh, S., and Rajan, C.K., 2008: Observed anomalous upwelling in the Lakshadweep Sea during the summer monsoon season of 2005, Journal of Geophysical Research, **113(C5)**, 1–12.

Guan, Z., Ashok, K. and Yamagata, T., 2003: The summertime response of the tropical atmosphere to the Indian Ocean sea surface temperature anomalies, *J. Meteor. Soc. Japan*, **81**, 533–561.

Hickey, B. M., and N. S. Banas, 2008: Why is the north end of the California Current System so productive?, Oceanography, **21(4)**, 90–107.

Ianson, D., R. A. Feely, C. L. Sabine, and L. W. Juranek, 2009: Features of coastal upwelling regions that determine net air-sea CO2 flux, J. Oceanogr., **65**, 677–687.

Jayaram, C., Neethu, C., Ajith Joseph, K. and Balchand, A. N., 2010: Interannual variability of upwelling indices in the Southeastern Arabian Sea: A satellite based study, *Ocean Sci. J.*, **45(1)**, 27 – 40, DOI 10.1007/ s12601-010-0003-6.

Johannessen, O.M., Subbaraju, G., Blindheim, J., 1987: Seasonal variation of oceanographic conditions off the southwest coast of India during 1971-1975. Fisk. Dir. Skr. Ser. Hav Unders. **18**:247-261.

Koracin, D.; Dorman C.E., and Dever E.P., 2004. Coastal perturbations of marine-layer winds, wind stress, wind stress curl along California and Baja California in June 1999, Journal of Physical Oceanography, **34(5)**, 1152–1173.

Large, W.G. and Pond, S., 1981. Open ocean momentum flux measurements in moderate to strong winds. Journal of Physical Oceanography, **11(3)**, 324–336.

Lau, N.C. and Nath, M.J, 2004: Coupled GCM simulation of atmospheric-ocean variability associated with zonally asymmetric SST changes in the tropical Indian Ocean, *J. Climate*, **17**, 245 – 265.

Li, T., Wang, B., Chang, C-P, Zhang, Y., 2003: A theory for the Indian Ocean dipole-zonal mode, *J. Atmos. Sci.* **60,** 2119–2135.

Luis, A. J. and Kawamura, H., 2004: Air-sea interaction, coastal circulation and biological production in the eastern Arabian Sea: A review, *J. Oceanogr*., **60**, 205 – 218.

Mackas, D. L., R. R. Thomson, and M. G Albraith, 2001: Changes in the zooplankton community of the british columbia continental margin, 1985–1999, and their covariation with oceanographic conditions, Can. J. Fish. Aquat. Sci. **58,** 685–702.

Mackas, D. L., W. T. Peterson, M. D. Ohman, and B. E. Lavaniegos, 2006: Zooplankton anomalies in the California Current system before and during the warm ocean conditions of 2005, Geophys. Res. Lett., **33**, L22S07, DOI: 10. 1029/ 2006 GL027930.

Madhupratap, M., Nair, K.N.V., Gopalakrishnan, T.C., Haridas, P., Nair, K.K.C., Venugopal, P. and Mangesh Gauns, 2001: Arabian Sea oceanography and fisheries of the west coast of India, *Curr. Sci.*, **81** (4), 355 – 361.

Madhupratap, M., Prasannakumar, S., Bhattathiri, P.M.A., 1996: Mechanism of the biological response to winter cooling in the northeastern Arabian Sea, *Nature*, **384**, 549 – 552.

Madhupratap, M., Shetye, S.R., Nair, K.N.V. and Sreekumaran Nair, S.R., 1994: Oil sardine and Indian mackerel: their fishery, problems and coastal oceanography, *Curr. Sci.*, **66** (5), 340 – 348.

McCreary, J. P., Han, W., Shankar, D., and Shetye, S. R., 1996: Dynamics of the East India Coastal Current: 2. Numerical solutions, J. Geophys. Res. **101,** 13993–14010.

McCreary, J. P., Kundu, P. K. and Molinary, R., 1993: A numerical investigation of dynamics, thermodynamics and mixed-layer processes in the Indian Ocean, *Prog. Oceanogr*., **31,** 181 – 244.

McCreary, J.P. and Chao, S.Y., 1985: Three dimensional shelf circulation along an eastern ocean boundary, Journal of Marine Research, **43(1)**, 13–36.

Meyers, G., 1996: Variations of Indonesian throughflow and the El Nino-Southern Oscillation, *J. Geophys. Res.*, **101**, 12255-12263.

Michael A. Spall, 2008: Buoyancy - Forced Downwelling in Boundary Currents, J. Phys. Oceanogr., **38**, 2704–2721, DOI: 10.1175/2008jpo3993.1

Muraleedharan, P.M. and Prasanna Kumar, S., 1996: Arabian Sea upwelling a comparison between coastal and open ocean regions, Current Science, **71(11)**, 842–846.

Murtugudde, R., McCreary, J.P. and Busalacchi, A., 2000: Oceanic processes associated with anomalous events in the Indian Ocean with relevance to 1997–1998, *J. Geophys. Res*., **105**, 3295–3306.

Nagura, M. and McPhaden, M. J., 2010: Dynamics of zonal current variations associated with the Indian Ocean Dipole, *J. Geophys. Res.*, **115**, C11026, DOI: 10.1029/2010JC006423.

Naidu, D.P., Ramesh Kumar, M.R. and Ramesh Babu, V., 1999: Time and space variations of monsoonal upwelling along the west and east coast of India, Continental Shelf Research, **19(4)**, 559–572.

Nicholls, N., 1989: Sea Surface temperatures and Australian winter rainfall, *J. Climate*, **2**, 965–973.

Ocean Circulation: Angela Colling, Open University. Oceanography Course Team Butterworth-Heinemann, 2001 - Science - 286 pages ISBN: 978-0-7506-5278-0.

Pankajakshan, T., Pattnaik, J. and Ghosh, A.K., 1997: An Atlas of Upwelling Indices along East and West Coast of India. Goa, India: Indian National Oceanographic Data Center, National Institute of Oceanography, 55p.

Potemra, J.T., M.E. Luther, and J.J.O'Brien, 1991: The seasonal circulation of the upper ocean in the Bay of Bengal, J. Geophysical Research, **96**, 12667-12683.

Rao A.D., Joshi M. and Ravichandran M., 2008: Oceanic upwelling and downwelling in the waters off west coast of India, Ocean Dyn. **58**, 213-226, DOI 10.1007/s10236-008-0147-4

Rao, R. R. and Sivakumar, R., 2002: Seasonal variability of sea surface salinity and salt budget of the mixed layer of the north Indian Ocean, *J. Geophys. Res.*, **107,** DOI: 10.1029/2001JC00907.

Rao, R. R., Girish Kumar, M. S., Ravichandran, M., Rao, A. R., Gopalakrishna, V. V. and Thadathil, P., 2009: Interannual variability of Kelvin wave propagation in the wave guides of the equatorial Indian Ocean, the coastal Bay of Bengal and the southeastern Arabian Sea during 1993-2006, *Deep Sea Res. I*, **57**, 1 - 13.

Rao, S.A., Behera, S.K., Masumoto, Y., Yamagata T., 2002: Interannual variability in the subsurface Indian Ocean with special emphasis on the Indian Ocean dipole, Deep Sea Res. II **49**,1549–1572.

Saji, N.H., Goswami, B.N., Vinayachandran, P.N. and Yamagata, T., 1999: A dipole mode in the tropical Indian Ocean, *Nature*, **401**, 360 - 363.

Sanilkumar, K.V., V.K. Unni and V.V. James, 2004: Upwelling characteristics of the southwest coast of India during 2003, Proceedings, METOC-2004.

Sanjeevan, V.N., Jasmine, P., Smitha, B.R., Ganesh, T., Sabu, P. and Shunmugaraj, T., 2009: Eastern Arabian Sea Marine Ecosystems. Proceedings of the symposium on Marine Ecosystems: Challenges and Opportunities, MECOS-2009, Kochi.

Schott, F. and McCreary, J. P., 2001: The monsoon circulation of the Indian Ocean, *Prog. Oceanogr.*, **51**, 1–123.

Sengupta, D., Goswami, B.N. and Senan, R., 2001: Coherent intraseasonal oscillations of ocean and atmosphere during the Asian Summer Monsoon, Geophysical Research Letters **28**: DOI: 10.1029/2001GL013587.

Shah, P., Sajeev, R. and Gopika, N., 2015: Study of upwelling along the West Coast of India-A climatological Approach, Journal of Coastal Research, **31(5)**, 1151 – 1158. Coconut Creek (Florida), ISSN 0749-0208.

Shankar, D. and Shetye, S. R., 1997: On the dynamics of the Lakshadweep High and Low in the southeastern Arabian Sea, *J. Geophys. Res.*, **102 (C6),** 12551-12562.

Shankar, D., Shenoi, S.S.C., Nayak, R.K., Vinayachandran, P.N., Nampoothiri, G., Almeida, A.M., Michael, G.S., Rameshkumar, M.R., Sundar, D., and Sreejith, O.P., 2005: Hydrography of the eastern Arabian Sea during summer monsoon 2002, Journal of Earth System Science, **114(5)**, 459–474.

Shankar, D., Vinayachandran, P. N. and Unnikrishnan, A. S., 2002: The monsoon currents in the north Indian Ocean, *Prog. Oceanogr.*, **52(1)**, 63-120.

Sharma, G.S., 1978: Upwelling of the southwest coast of India, Indian J. of Mar. Sci. 7, 209-218.

Shetye, S. R. and A.D. Gouveia, 1998: Coastal circulation in the north Indian Ocean, Coastal Segment (14, S-W), The Sea, **11**, 523-556.

Shetye, S. R. and Shenoi, S. S. C., 1988: Seasonal cycle of surface circulation in the coastal North Indian Ocean, *Proc. Indian Acad. Sci. (Earth Planet. Sci.)*, **97**, 53-62.

Shetye, S. R., Gouveia, A. D., Shenoi, S. S. C., Sundar, D., Michael, G. S., Almeida, A. M. and Santanam, K., 1990: Hydrography and the circulation off the west coast of India during southwest monsoon 1987, *J. Mar. Res*., **48**, 359-378.

Shetye, S.R., Shenoi, S.S.C., Antony, M.K. and Krishna Kumar, V., 1985: Monthly mean wind stress along the coast of the north Indian Ocean. Proceedings of the Indian Academy of Science (Earth and Planetary Science), **94(2)**, 129–137.

Smith, R. L., 1964: An investigation of upwelling along the Oregon Coast, Ph.D. thesis, Oregon State University. Corvallis.

Smitha, B. R., Sanjeevan, V. N., Vimalkumar, K. G. and Revichandran, C., 2008: On the upwelling off the southern tip and along the west coast of India, *J. Coast. Res.*, **24 (3)**, 95-102.

Thomson, R. E., and D. M. Ware, 1996: A current velocity index of ocean variability, J. Geophys. Res., 101(C6) **14**,297–14,310.

Tim, N., E. Zorita, and B. Hünicke, Decadal variability and trends of the Benguela upwelling system as simulated in a high-resolution ocean simulation, Ocean Sci., **11**, 483–502, DOI:10.5194/os-11-483-2015.

Tourre, Y. M., *and* W. B. White, 1995: ENSO signals in global upper-ocean temperature, J. Phys. Oceanogr., 25, 1317–1332.

Tourre, Y. M., and W. B. White, 1997: Evolution of the ENSO signal over the Indo-Pacific domain, J. Phys. Oceanogr., **27**, 683–696.

Varadachari, V. V. R. and Sharma, G. S., 1967: Circulation of the surface waters in the North Indian Ocean, *J. Indian. Geophys. Uni.*, **4** (2), 61-73.

Venzke, S., Latif, M. and Villwock, A., 2000: The coupled GCM ECHO-2. Part II: Indian Ocean response to ENSO, *J. Climate*, **13**, 1371-1383.

Vialard, J., S. S. C. Shenoi, J. P., McCreary, D. Shankar, F. Durand, V. Fernando, and S. R. Shetye., 2009: Intraseasonal response of the northern Indian Ocean coastal waveguide to the Madden-Julian Oscillation, Geophysical Research Letters, Vol.**36**, DOI: 10. 1029/2009GL038450.

Vinayachandran, P. N., Francis, P. A. and Rao, S. A., 2009: Indian Ocean Dipole: Processes and Impacts, *Current trends in science*, Indian Academy of sciences platinum jubilee special edition, 569-589.

Vinayachandran, P. N., S. Iizuka, and T. Yamagata, 2002: Indian Ocean Dipole mode events in an ocean general circulation model, *Deep- Sea Res., II, **49**, 1573-1596.*

Wang, B., 2002: Kelvin Waves, Copyright 2002 Elsevier Science Ltd., DOI: 10.1006 /rw as.2002.0191.

Ware, D. M., and R. E. Thomson, 1991: Link between long-term variability in upwelling and fish production in the Northeast Pacific Ocean, Can.J. Fish. Aquat. Sci, **48**, 2296–2306.

Webster, P.J., Moore, A.M., Loschnigg, J.P. and Leben, R.R., 1999: Coupled ocean-atmosphere dynamics in the Indian Ocean during 1997-1998, *Nature*, **401**, 356-360.

Wooster, W. S. A., Bakun, A. and McLain, D. R., 1976: The seasonal upwelling cycle along the eastern boundary of the North Atlantic, *J. Mar. Sci.*, **34**, 131-141.

Wyrtki, K., 1973: An equatorial jet in the Indian Ocean. *Science*, **181**, 262–264.

Yoo, S.-H., Fasullo, J., Yang, S. and Ho, C.-H., 2010: On the relationship between Indian Ocean sea surface temperature and the transition from El Nino to La Nina, *J. Geophys. Res.*, **115**, D15114, DOI:10.1029/2009JD012978.

Yu, L. and Reinecker, M.M., 1999: Mechanisms for the Indian Ocean warming during 1997-1998 El Nino, *Geophys. Res. Lett.* **26**, 735-738.

Yu, L., J.J.O'brien, and J. Yang, 1991: On the remote forcing of the circulation in the Bay of Bengal, J. Geophys. Res., **96**, 20449-20454.

…..ஜ۞ஜ…..

List of Publication

[1] **Phiros Shah**, R. Sajeev and N. Gopika., 2015. Study of upwelling along the West Coast of India-A climatological Approach. **Journal of Coastal Research**, 31(5), 1151 – 1158. Coconut Creek (Florida), ISSN 0749-0208.

[2] **Phiros Shah** and Sajeev R. Influence of IOD events on coastal dynamics along the south - west coast of India -– Paper Presented in PORSEC-2012.

[3] **Phiros Shah**, Sajeev R and Thara K.J., Impacts of Indian Ocean dipole on major pelagic fish species of south-west coast of India -. Paper presented in the International Symposium "SAFARI", February 2010. Cochin.

[4] Thara K.J, **Phiros Shah** and **R.Sajeev**, Response of oil sardine of Kerala with special reference to extreme oceanographic events. Paper presented in the International Symposium "Marine Ecosystems Challenges and Opportunities" (MECOS 09) 9-12 February 2009 Cochin, India.

[5] **Phiros Shah**, Sajeev R and Thara K.J., 2009. An upwelling Front along the north Malabar zone (south-west coast of India) during July 1995 - India - Paper presented in the National Conference of Ocean Society of India – OSICON '09. Recent developments in Ocean science, Engineering and Technology. March 19-21, 2009 Andhra University, Visakhapatnam. Published in OSICON -09 Special proceedings.

…..ꕥ…..